GROSS, JOHN LEWIS, III

DESIGN FOR THE PREVENTION OF PROGRESSIVE COLLAPSE USING INTERACTIVE COMPUTER GRAPHICS

Cornell University PH.D. 1980

DESIGN FOR THE PREVENTION OF PROGRESSIVE COLLAPSE USING INTERACTIVE COMPUTER GRAPHICS

A Thesis

Presented to the Faculty of the Graduate School

of Cornell University

in Partial Fulfillment for the Degree of

Doctor of Philosophy

by

John Lewis Gross III

May, 1980

BIOGRAPHICAL SKETCH

The author was born in Philadelphia, Pennsylvania, on August 9, 1947. After graduating from Springfield Township Senior High School he enrolled at Cornell University. He completed the Bachelor of Science degree in 1969, and Master of Engineering (Civil) in 1970. He then worked as a design engineer for Pittsburgh-Des Moines Steel Company in Pittsburgh, Pennsylvania, for a period of five years.

In 1975, the author returned to Cornell University to continue graduate study toward the degree of Doctor of Philosophy. Completing his dissertation in 1979, he joined the structural engineering faculty at the University of Colorado at Boulder.

The author is a member of Phi Kappa Phi and Sigma Xi and is a Registered Professional Engineer in the Commonwealth of Pennsylvania. He served in the Pennsylvania Air National Guard and the United States Army Reserve and received an honorable discharge in 1976.

DEDICATION

to

Phyllis

ACKNOWLEDGEMENTS

There are many to whom I owe my sincerest thanks for their part in making my graduate education at Cornell both enjoyable and rewarding.

Foremost, I would like to thank Professor William McGuire, chairman of my special committee, for his supervision, guidance, and advice throughout my graduate studies. To him I owe my deepest gratitude. I would also like to acknowledge the help and support of Professors John F. Abel, H. D. Conway, Richard H. Gallagher, and Donald P. Greenberg.

I am especially grateful to Tom Mutryn for his cooperation and hard work in writing many of the graphics programs used in this research.

Thanks also go to my fellow graduate students, Mark Shephard, Sheng-Chuan Wu, Bob Haber, and George Blandford for their inspiring companionship.

In addition, I would like to express my appreciation for all the help provided by the many people associated with the Laboratory of Computer Graphics. Special thanks go to Ted Crane and Mark Levoy.

I would also like to thank Mark Spitzer for taking the photographs, Dave Nelson for preparing the drawings, and Marie Kindgren for typing this thesis.

The support of this research by the National Science Foundation is gratefully acknowledged.

Finally, I would like to express my deepest gratitude to my wife Phyllis, for her understanding and encouragement, and to my parents for all the love and support they have given me.

PREFACE

Many of the figures in this thesis are photographic reductions of computer-generated images. In some cases the small lettering in the figures is not legible. In each of these instances, no pertinent information is contained in the illegible lettering. The figures are included primarily to illustrate the nature of computer graphics displays.

TABLE OF CONTENTS

LIST OF TABLES

LIST OF FIGURES

1. INTRODUCTION

Since the collapse of the Ronan Point apartment building in 1968 [1]*, considerable attention has been focused on the phenomenon of progressive collapse. A progressive collapse is characterized by the loss of load carrying capacity of a small portion of a structure due to an abnormal load which, in turn, triggers a cascade of failure affecting a major portion of the structure. The Ronan Point incident pointed out most dramatically that there exists a need for considering the resistance to progressive collapse in design. Several buildings have collapsed in this manner in recent years (see Reference [2]) and the possibility of progressive collapse is a source of continuing concern.

Several approaches have been proposed for including progressive collapse resistance in the design of building structures. The direct design approach explicitly considers resistance to progressive collapse and the ability of a structure to absorb localized damage. Indirect design refers to consideration of resistance to progressive collapse by providing minimum levels of strength, continuity, and ductility. The intent of either approach is to assure that, in the event of an abnormal load, damage will be restricted to a localized area and will not propagate through the remaining structure causing widespread failure and possible collapse.

To investigate whether or not a local failure will spread, the structural analyst needs procedures that account for the sequential nature of the phenomenon wherein progressive failure of portions of the structure

*Numbers in square brackets refer to references at the end of the Thesis.

continually modifies the structural system under analysis. The procedure must be capable of tracing the behavior of the structure not only to the point of incipient damage, but beyond the initial damage stage into a true limit state in which the badly damaged structure is called upon to resist imposed loadings.

1.1. Objectives of Research

The research reported herein is directed towards the goal of developing accurate analytical techniques for simulating the actual behavior of structures up to, and through, collapse. Initial work has focused on the nonlinear analysis of elasto-plastic planar steel frame structures subjected to non-proportional static joint loads. A computer program has been developed for the analysis of frame structures including beam-column action and the effects of shear walls and beam-to-column connections. Both geometric and material nonlinear behavior may be modeled. Of particular note is the capability to remove selectively one or more structural members during the course of analysis to simulate the loss, through accident, of load carrying capacity. Computer graphics capabilities permit the rapid generation of structural data and facilitate the review of the large amount of data resulting from nonlinear analyses.

This analysis capability may be employed in several ways to implement the various progressive collapse design strategies. For example, it can be used to determine if a structure is able to develop alternate load paths upon the removal of one or more load carrying members. Alternatively, results from an analysis may be used to assist in evaluating requirements for the application of the indirect design method such as ductility or

joint forces. It is intended that this capability will provide the foundation for the analysis and design of complex building structures to insure against progressive collapse.

To date there has been very little research specifically directed toward the development of analysis techniques for the resistance of building structures to progressive collapse. McGuire and Leyendecker [3] studied several examples of contemporary masonry building construction to determine the resistance of actual buildings to abnormal loads. In their work, a combination of hand calculations and existing computer analysis techniques were used to determine the strength of component members. Clough and Petersson [4] analyzed several structures as part of an investigation of progressive collapse in prefabricated large panel concrete building systems. The studies included linear static, nonlinear static, and both linear and nonlinear dynamic analyses of the damaged building. Again, conventional computer analysis techniques were employed.

1.2. Scope of Investigation

The basic concepts and definitions of abnormal loading and progressive collapse are presented in Chapter 2. Here, the occurrence of abnormal loads and the associated risk of structural failure are discussed. Various design strategies to prevent progressive collapse are presented and the implementation of direct design strategies is described. Finally, the application of the analysis capability developed herein is discussed in relation to design for the prevention of progressive collapse.

The analysis of structures to account for material and geometric nonlinear behavior is discussed in Chapter 3. The direct stiffness method is first reviewed. Several nonlinear solution techniques including incremental, iterative, and mixed procedures are discussed next. Then the incremental form of the beam-column stiffness matrix is developed from the principal of stationary potential energy. The simple-step and predictor-corrector incremental procedures used in the current study are described. Several program features such as the incremental-step termination criteria, load-step tolerance, and post-collapse behavior are also discussed.

In Chapter 4 the various structural elements which constitute the present capability are described. These elements include a beam-column, shear infill panel, and semi-rigid connection. Since the intent of the analysis program is to evaluate building structures at or near collapse, the elements presented here must be capable of accurately representing the behavior of structural components as damage is incurred. Considerable attention is devoted to the inelastic and nonlinear behavior of these elements.

Chapter 5 presents a description of the progressive collapse analysis system. Interactive computer graphics is first described as it relates to the present study. The four basic system functions are next described: problem definition, analysis control, member removal, and result interpretation. Photographs of both black and white and color graphic displays are used to illustrate the program capabilities and interactive environment. Finally, the program file structure and data flow are presented.

Several examples which illustrate the use of the progressive collapse analysis system are presented in Chapter 6. The examples include verification of analysis results by comparison with test data and known solutions. In addition, several applications are presented which demonstrate the member removal capability and the subsequent analysis to determine the collapse resistance of the structure under consideration. Photographs of the various computer-generated displays illustrate the use of computer graphics in both the definition of the example problems and the interpretation of the analysis results.

In Chapter 7 a summary of the results of the current study is presented. Some conclusions are drawn and areas for future work are outlined.

2. PROGRESSIVE COLLAPSE AND ABNORMAL LOADS

It has long been recognized that absolute safety against all possible conditions and hazards can never be achieved [5]. Safety is related to both the risk of an accident and the structural consequence of a particular accident. Past experience has shown that this combination has been adequately dealt with since there have been relatively few serious building failures. Structures designed to withstand normal load conditions have usually been capable of tolerating abnormal load conditions. This is due, in part, to the inherent strength and continuity of most older forms of construction. Recent developments in the efficient use of building materials as well as refinements in analysis techniques have resulted in structures which are constructed with a considerably smaller true margin of safety. Such structures may have little reserve capacity to accommodate abnormal load conditions. Further, some may not have the continuity or ductility needed to redistribute resistance following a local failure. It is clearly no longer sufficient to assume that a structure designed for normal conditions will react satisfactorily to the abnormal or accidental condition [5].

Since 1968, there has been concern that buildings, most notably multi-story buildings, are being designed and built without explicit consideration for abnormal loads. In May of that year, the Ronan Point apartment building in London, England suffered one of the world's worst structural collapses [1]. In this incident, an explosion resulting from a gas leak blew out an exterior wall on the eighteenth floor of the twenty two story precast concrete panel building. The resulting loss of support to the nineteenth floor caused it, in turn, to collapse. This loss-of-support

failure propagated to the roof. The debris from the collapsing floors above fell onto the eighteenth floor which caused it to fail also. This failure due to debris loading cascaded down to the podium level leaving in ruin one quadrant of the twenty two story building. A failure such as this is termed a progressive collapse.

In the United States, the frequency and severity with which abnormal loadings occur is relatively significant [6]. Allen and Schriever [2] conducted a survey to determine the frequency of occurrence of progressive collapse. Two news sources, Engineering News Record and the Canadian Press newspaper, were used. The results of the survey are shown in Table 2.1. Coverage of Canadian collapses spans a longer period which accounts for the greater number shown for Canada. Results of the ENR data indicate an average of 5.5 progressive collapses per year over a four year period. The survey of Canadian news clippings, spanning a ten year period, indicates a higher estimate of 7.5 collapses per year. The total number of progressive collapses in both cases is considerable. This survey concludes that progressive collapse constitutes about 15 to 20 percent of the total number of collapses. This data no doubt represents a lower bound estimate of the frequency of occurrence of progressive collapse since it is unlikely that all incidents were reported in these two data sources.

It is clear that buildings should not be designed and constructed so as to be susceptible to progressive collapse. This is not to say that they should be built to withstand damage due to an abnormal load by having excessive strength. Rather, a building should be able to tolerate local damage, regardless of the cause, without suffering progressive collapse [7].

Collapse Designation	Engineering News Record (4 years)	Canada (10 years)
During Construction		
Due to impact, explosion	2	1
Formwork, bracing or erection error	10	35
Design error	1	0
During Service Life		
Due to explosion	1	0
Due to impact	4	8
Design, manufacture or construction error	3	22
During Demolition, Adjacent Excavation	1	6
TOTAL	22	75
Total News Incidents Involving All Types of Collapse	110	495

Table 2.1 News Incidents Involving Progressive Collapse (Reference 2)

2.1 Basic Concepts and Definitions

A progressive collapse is described as a chain reaction of failures following damage to a relatively small portion of a structure [8]. The damage which results characteristically is out of proportion to the damage which initiated the collapse. Three components may be defined which are necessary for a progressive collapse. They are: (1) the occurrence of an abnormal load event, (2) the failure of one or more structural elements as a result of the abnormal load, and (3) a propagation of failure affecting a major portion of the structure. The sequence of events that occurs during structural collapse [9] is shown schematically in Figure 2.1. This diagram serves to facilitate the evaluation of a structureal collapse to determine whether or not it constitutes a progressive collapse.

An abnormal loading may be defined as a condition of loading which a designer, following established practice, does not include in the normal course of design of a particular structure. It is a loading condition of sufficient severity and probability of occurrence to be a cause for concern, but still of such a relatively rare nature as to be outside of normal design-life expectancy [8]. Since it is not possible to design for absolute safety, the designer must consider only those abnormal events which have a reasonable probability of occurrence. In the next section the sources of abnormal loads, the probability of their occurrence, and the risk of structural failure are discussed.

2.2 Abnormal Loads and the Risk of Structural Failure

In this section, the various abnormal loads which have a reasonable probability of occurrence and which have a sufficient magnitude to cause

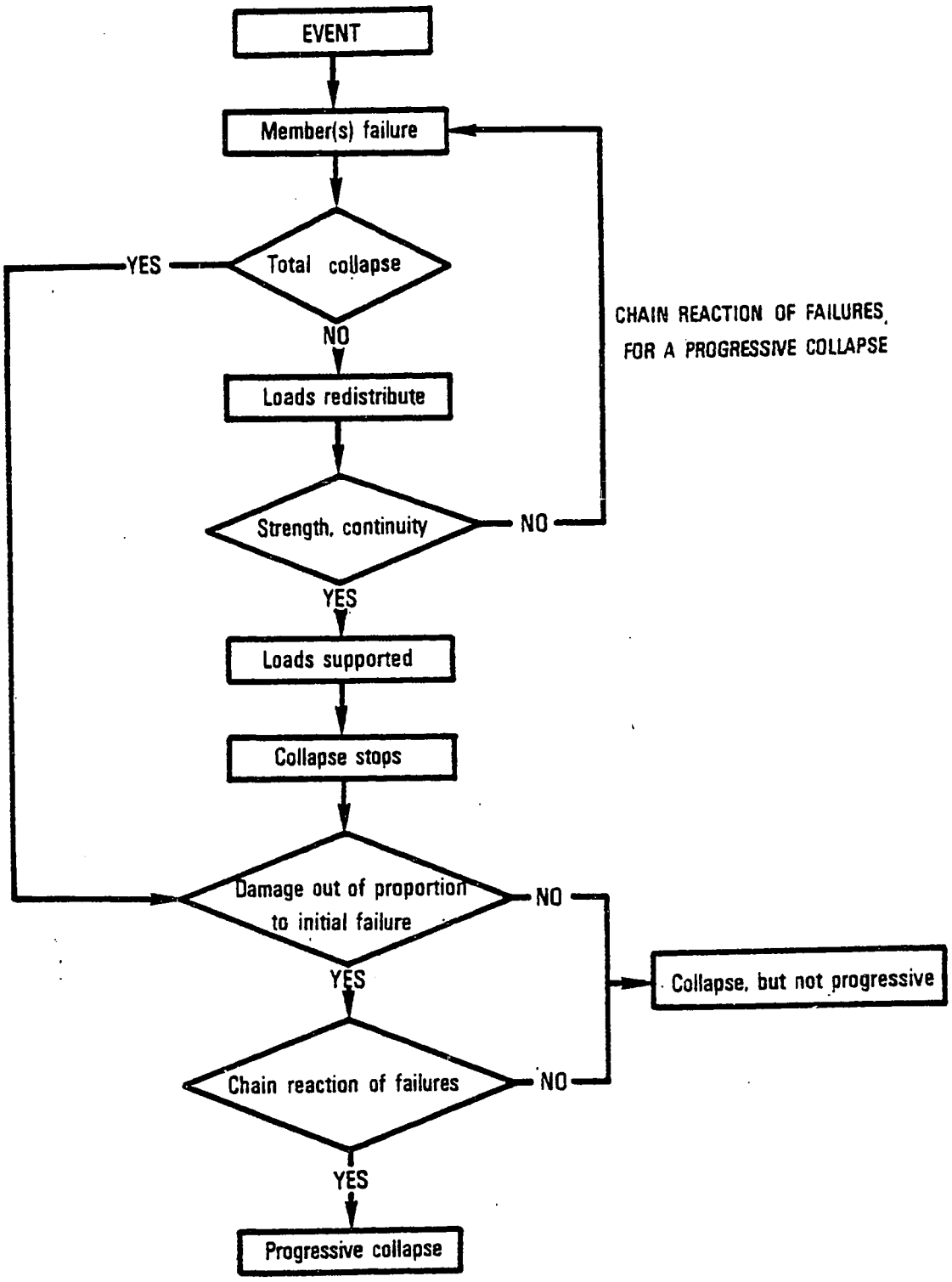

Figure 2.1 Sequence of Events During Structural Collapse (Reference 9)

structural damage are identified. Next, the probability of the occurrence of abnormal loads and the consequent risk of structural failure are addressed.

2.2.1 Classification

Somes [8] has identified and classified various abnormal loadings for which the probability of occurrence seems significant. They are as follows:

(1) Violent change in air pressure
- Sabotage bombings
- Service system explosions
- Other explosions within the building
- Explosions external to the building

(2) Accidental impact
- Highway vehicles
- Construction equipment
- Aircraft

(3) Faulty practice
- Design error
- Construction error
- Misuse or abuse by the occupant

(4) Foundation failure
- Unforeseen settlement
- Foundation wall failure
- Scouring action of floods on foundations
- Adjacent excavation

This system for classification of abnormal loads is quite complete. Two points are worth noting, however. First, not all loads which have a reasonably high probability of occurrence actually constitute a significant risk of structure failure. And, second, data on all of the above abnormal loads is not readily available and is often incomplete when it is available. In the next section, the risk of occurrence of some of these loading conditions and the associated risk of collapse are discussed.

2.2.2 Probability of Occurrence of Abnormal Loads

In a report on the incidence of abnormal loading in residential buildings, Leyendecker and Burnett [10] assess abnormal loadings to determine whether or not they can continue to be neglected in design. In their report they discuss sources of abnormal loads and estimate the risk of such loading in residential building design. The loadings considered are as follows:

(1) Gas-Related Explosions

(2) Bomb Explosions

(3) Motor Vehicle Collision with Buildings

(4) Sonic Boom

(5) Aircraft Collision with Buildings

(6) Explosion of Hazardous Materials.

These loadings fall into the first two categories defined by Somes. The authors point out that the loadings do not constitute a complete list of the abnormal loadings that may occur. Rather these loads represent plausible potential sources of the initial failure which may lead to progressive collapse. It was concluded [10] that only the gas-related

explosion, bomb explosion, and motor vehicle collision with buildings constitute a realistic problem for buildings. To compare the data for these loadings, the following definitions of terms were adopted:

(1) Total Incidents - All incidents involving a particular abnormal load.

(2) Intermediate or greater damage - Damage in excess of $1000 for gas explosions; $1000 for vehicle collision, or described as intermediate or greater for bomb explosions. This level implies fairly extensive damage such as walls blown down.

(3) Severe damage - Damage in excess of $10,000 for gas explosions; $5,000 for vehicle collision, or described as severe for bomb explosions. This level implies extensive damage, such as unit destroyed.

The annual frequency of occurrence of the gas explosion, bomb explosion, and vehicle collision is summarized in Figure 2.2.

Leyendecker and Burnett used this data to compute the probability of structural failure given the occurrence of an abnormal load. Let F indicate failure and AB the occurrence of an abnormal load event. The probability of failure due to abnormal loads, $P(F)$ may be stated as

$$P(F) = P(F|AB) \times P(AB) \tag{2.1}$$

in which $P(F|AB)$ is the probability of failure given an abnormal load event, and $P(AB)$ is the probability of occurrence of an abnormal load event. Since data for the probability of failure, $P(F)$ are not readily available, data were presented in the form of the probability of damage above a specified level. If D_p is defined as the damage at the

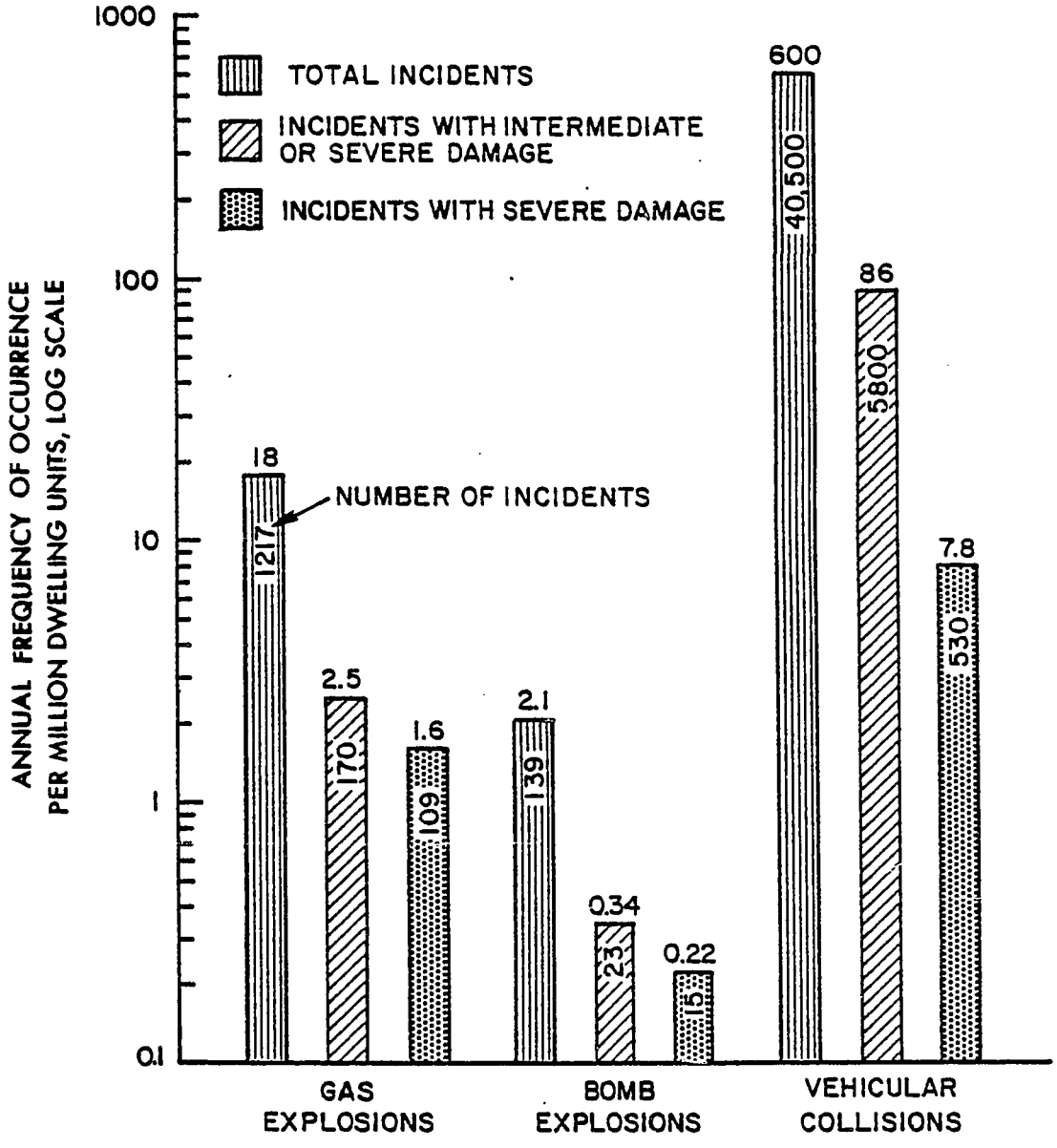

Figure 2.2 Summary of Annual Probabilities of Abnormal Loadings for 1970 (Reference 10)

specified level p, the probability of damage above a certain level may be written as

$$P(D_p) = P(D_p|AB) \times P(AB) \tag{2.2}$$

in which $P(D_p|AB)$ is the probability of damage above a prescribed level given an abnormal load event, $P(AB)$ is the probability of occurrence of an abnormal load event, and the subscript p indicates the prescribed damage level, e.g. intermediate or severe. Thus, the probability of damage above a specified level given an abnormal load event, $P(D_p|AB)$, is computed as

$$P(D_p|AB) = P(D_p)/P(AB) \tag{2.3}$$

Both $P(D_p)$ and $P(AB)$ are obtained from the data in Figure 2.2. The calculated estimates of $P(D_p|AB)$ are given in Table 2.2.

Leyendecker and Burnett make the assumption that severe damage is equivalent to structural failure. Based on this assumption they draw the following conclusions:

(1) Gas explosions occur with an annual frequency of 18 events per million dwelling units with an annual frequency of 1.6 events per million dwelling units causing structural failure. This represents a 9 percent probability of structural failure--given that the event occurs.

(2) Bomb explosions occur with an annual frequency of 2.1 events per million dwelling units with an annual frequency of 0.22 events per million dwelling units causing structural failure. This represents an 11 percent probability of structural failure--given that the event occurs.

Abnormal Loading	P(AB)	$P(D_p)$ Based On Int. Damage	$P(D_p)$ Based On Severe Damage	Calculated $P(D_p \mid AB)$ Based On Int. Damage	Calculated $P(D_p \mid AB)$ Based On Severe Damage
Gas Expl.	18×10^{-6}	2.5×10^{-6}	1.6×10^{-6}	0.14	0.089
Bomb Expl.	2.1×10^{-6}	0.34×10^{-6}	0.22×10^{-6}	0.16	0.11
Veh. Coll.	600×10^{-6}	86.0×10^{-6}	7.8×10^{-6}	0.14	0.013

NOTE: The probabilities listed are per dwelling unit.

Table 2.2 Calculated Estimates of the Probability of Damage Given the Occurrence of an Abnormal Load Event (Reference 10)

(3) Vehicle collisions occur with an annual frequency of 600 events per million dwelling units with an annual frequency of 6.8 events per million dwelling units causing structural failure. This represents a 1 percent probability of structural failure--given that the event occurs.

The probability of failure (or severe damage), as expressed in equation 2.1, consists of the probability of occurrence of an abnormal load event, P(AB), as well as the probability of failure given that the abnormal event occurs, P(F|AB). To reduce the probability of failure, the structural designer must reduce either P(AB), P(F|AB) or a combination of the two. The first of these is certainly more difficult to accomplish as many abnormal loadings are beyond the control of the designer. The more obvious solution is to design a structure so that the probability of failure, given the occurrence of an event, is acceptably small. These alternatives are discussed in more detail in the next section.

2.3 Design to Prevent Progressive Collapse

The approaches for reducing the risk of progressive or chain reaction type of failure may be categorized as follows [11]:

(1) Event control

(2) Indirect design, and

(3) Direct design.

Each of these approaches is discussed in the following sections.

2.3.1 Event Control

Event control refers to reducing the risk of progressive collapse by such means as [9]:

(1) Eliminating the event

(2) Protecting against the event

(3) Reducing the effect of the event.

To reduce the risk of a gas explosion, for example, the use of gas in an apartment or residence could be prevented. The effect of a gas explosion could be reduced by providing explosion venting to reduce the pressure buildup. Motor vehicle impact on buildings could be minimized by either locating the building a distance from roads and highways or by providing barricades to prevent vehicle collision.

In the case of event control it is necessary that all reasonably foreseeable abnormal load events be identified. This approach does not increase the resistance of a structure to progressive collapse. Furthermore, event control is dependent on factors that are outside the control of the designer. Event control, therefore, is not considered a practical means for reducing the risk of progressive collapse [9]. The remaining two approaches are more easily implemented since they are both within the control of the designer.

2.3.2 Indirect Design

Indirect design refers to consideration of resistance to progressive collapse by specifying minimum levels of strength, continuity, and ductility [9]. McGuire [12] uses the term general structural integrity to describe this approach. This method, by itself, does not guarantee that

an alternate load path exists in the event of a localized failure. In addition, Ellingwood and Leyendecker [11] point out that unless the reasons for the minimum code requirements are apparent, a designer of an unusual structure may overlook the need for considering progressive collapse. Also, minimum requirements would have to be established for different types of construction and would have to be revised as practices change. The development of minimum levels of strength, continuity, and ductility to be included in building codes requires additional investigation. This point will be discussed later with regard to the current study.

2.3.3 Direct Design

The direct design approach explicitly considers resistance to progressive collapse and the ability of a structure to absorb localized damage [11]. Two basic means of direct design are:

(1) The specific local resistance method and

(2) The alternate load path method.

The intent of the specific local resistance method is to provide sufficient strength to resist an abnormal load. That is, the load bearing structural elements must be able to remain standing under the extreme load. For example, the Ronan Point collapse would probably not have occurred had the external load-bearing walls been designed to withstand the pressure load of a gas explosion. One drawback of this approach is, however, that a specific collapse-initiating event must be identified so that the local resistance can be referenced to a specific limit state [11].

The alternate load path method, in contrast, permits local damage to occur but provides alternate paths around the damaged area so that

the structure is able to absorb the abnormal load without collapse. In the event of the loss of load carrying capacity of a structural member, the forces in adjacent members redistribute and the loss of support is accommodated by bridging over the damaged area. For the alternate load path method the abnormal load need not be specifically identified.

The above definitions are useful in providing a basis for considering strategies for reducing the risk of progressive collapse. These alternatives are not, however, mutually exclusive. The resistance of a structure to progressive collapse may be evaluated by analyzing it to determine whether alternate load paths around the damaged area can be developed. Alternatively, alternate path studies may be used as guides for developing rules for the minimum levels of strength, ductility, and continuity required to assure general structural integrity. For some buildings, it may not be possible to develop alternate load paths as the structures were originally designed. When this occurs, it may be desirable to redesign critical elements for specific local resistance so that the structure is then able to develop alternate load paths. In this manner the various approaches may be combined to provide a collapse resistant design. Guidelines for the implementation of the direct design methods are presented in the next section.

2.4 Implementation of Direct Design Strategies

Specific criteria for checking the ability of a structure to tolerate damage and resist abnormal loads are given by Ellingwood and Leyendecker [11]. Design equations are presented for both the specific local resistance method and the alternate load path method. They are written in terms of factored nominal resistance and factored loads. This is desirable

because of the uncertainties that arise from statistical variability in the structural resistance and the applied loads. In addition, abnormal load events occur infrequently and randomly in time. Design criteria should reflect this. Load factors that are commensurate with the level of design uncertainty and a corresponding small acceptable failure probability should be selected using probabilistic methods. The resistance factor depends on the construction material.

2.4.1 Specific Local Resistance Method

The specific local resistance method requires that a specific abnormal loading be identified and assessed as to its magnitude and direction. A reliability analysis based design equation for specific local resistance proposed by Ellingwood and Leyendecker [11] is

$$\phi R' \geq D + 0.4L_{ANSI} + 1.3A' \tag{2.4}$$

in which ϕ is the resistance factor, R' is the nominal resistance, D is the dead load, L is the short-term live load*, and A' is the specified abnormal load. Note that wind load has been omitted since it is reasoned that the probability of a joint occurrence of strong wind and abnormal load is negligible.

2.4.2 Alternate Load Path Method

A structure may also be evaluated for resistance to progressive collapse using the alternate path method. Such a determination is made

*ANSI refers to American National Standard, ANSI A58.1 [13]

by assuming that the primary structural elements are incapable of carrying load, one element at a time, and evaluating the resulting structural behavior. When a primary structural element is removed, the remaining structure must continue to support its existing loads for a sufficient period of time to safely evacuate the building. Primary structural elements as defined by Leyendecker and Ellingwood are:

(1) Major load carrying beams

(2) Floor slabs between supports

(3) Columns

(4) Bearing wall panels.

The design equation for applying the alternate load path concept is

$$\phi R' \geq D + 0.45L_{ANSI} + 0.20W \tag{2.5}$$

in which ϕ is the resistance factor, R' is the nominal resistance, D is the dead load, L is the short-term live load, and W is the monthly maximum wind. The effect of wind is included in this case since the damaged building must be able to function for an extended period of time.

2.5 Analysis and Behavior of Damaged Structures

Development of design and construction procedures to minimize the risk of progressive collapse requires analytical capabilities which go well beyond those used in conventional design. To investigate whether or not a local failure will spread, the analyst needs procedures that account for the sequential nature of the phenomenon wherein progressive failure of portions of the structure continually modifies the structural system under analysis. The procedures must be capable of tracing the behavior not only

to the point of incipient damage, but beyond the initial damage stage into a true limit state in which the badly damaged structure is called upon to resist imposed loadings.

The analysis of structures in the damaged state is extremely complex. While a number of researchers have considered force redistribution in limit design studies, these have generally involved flexural capacity only and do not consider the large deformations and drastic changes in force paths that occur in the damaged state [14]. A particularly important area of study with respect to collapse analysis is the behavior of joints. The force-displacement relationships of joints, including nonlinear behavior as well as slip characteristics, must be included in any realistic analysis.

A recent workshop on progressive collapse [14] identified the development of such analysis capability as a major research need. It was concluded that there is an immediate need to begin development of accurate analytical techniques for simulating the actual behavior of structures up to, and through, collapse. These methods should be adaptive in character, that is, they should be capable of detecting changes in the behavior of the structure as loads increase and of permitting interactive accommodation to these changes in subsequent stages of the analysis.

The research reported herein is directed towards the goal of developing a highly accurate and generalized computer program for the analysis of structures for progressive collapse. The more tractable problem of planar frame structures has been undertaken. The program is based on the finite element method and is modular in character. That is, it readily permits the addition of structural members or elements. At present three elements are included for the representation of framed

building structures; beam-column, shear wall, and connection. The analysis takes into consideration both material and geometric nonlinearities. Inelastic nonlinear behavior of the various component members is handled in a consistent fashion. One of the unique features of the analysis capability is that it permits the removal of one or more load carrying members during the course of analysis. The theory, formulation, and implementation of this computer program is extensively covered in the remaining sections of this thesis.

The computer program described herein is directly suited for the analysis of structures for resistance to progressive collapse. It can be employed in any of several ways to implement the strategies previously described. Three alternative ways in which such an analysis capability can be used are:

(1) To determine if alternate paths may be developed upon the removal of one or more load carrying members. This is a direct application of the alternate load path method.

(2) To identify those elements which, if removed, would precipitate a collapse. These elements could then be designed to resist failure in the event of an abnormal load using the specific local resistance design strategy.

(3) To assist in evaluating requirements for general structural integrity such as ductility, tie forces, joint resistance, and continuity.

Examples demonstrating the application of these techniques to evaluate the resistance of framed building structures to progressive collapse are presented in Chapter 6.

3. NONLINEAR STRUCTURAL ANALYSIS

The assumption of linear structural behavior is often made in the analysis of practical frame building structures. For structures subjected to extreme loads, however, the assumption of linear behavior cannot, in general, be justified. Failure or yielding of portions of the structure and excessive deflections characterize the behavior of buildings subjected to abnormal loads. The analytical procedures incorporated into the computer program described herein take account of the various material and geometric nonlinear effects that become important in the evaluation of structures in a damaged state. In this chapter the main features and capabilities of the nonlinear analysis procedure employed in the present study are presented.

In nonlinear structural analysis, two different types of nonlinearities may be identified (see Reference [15]). The first is material or physical nonlinearity which results from nonlinear constitutive laws. The second is geometric nonlinearity which results from finite changes in geometry. Both material and geometric nonlinearity are accounted for in the current analysis capability. For material nonlinearity, special attention is given to elasto-plastic behavior of frame members, nonlinear moment-rotation characteristics of beam-to-column connections, and shear cracking of infill panels. For the three element types included in the present analysis capability, only the frame member exhibits significant geometric nonlinear behavior. Discussion of the nonlinear material behavior of the various structural elements noted above is deferred until the next chapter.

In the following sections computational procedures to account for nonlinear behavior are discussed. The chapter is divided into essentially two parts. The first part (Sections 3.1-3.4) deals with the formulation and solution of material and geometric nonlinear problems. The direct stiffness method of analysis is discussed first since it forms the basis for the nonlinear solution technique employed in the current study. Next, the incremental stiffness procedure, which has been adopted for this study, is outlined. The nonlinear incremental stiffness matrix for the beam-column element is then developed using a formulation based on a moving, or updated, coordinate system. Finally, two solution procedures which have been implemented are explained. They are the simple-step procedure and the predictor-corrector procedure. The second part of the chapter (Sections 3.5-3.7) is devoted to a discussion of several features included in the analysis program for the implementation of the nonlinear solution techniques. These features include the step termination criteria, the load-step tolerance, and post-collapse behavior.

3.1 Direct Stiffness Method

In matrix methods of structural analysis (see, for example, References [15-17]), a structure is idealized as an assemblage of deformable elements or members. These elements are connected at nodes or joints. The exact or approximate deformation and force states within a structure subjected to a system of forces applied at the nodes may be completely defined by a set of displacement parameters associated with each node. In the stiffness method, these displacement parameters are the primary unknowns or degrees of freedom of the system. For the current case of a planar frame, three degrees of freedom are considered

at each node; two translational displacements and one rotational displacement.

Before considering the displacement degrees of freedom, the distinction between global and local coordinate axes must first be made. The global axes are those established for the complete structure. A set of orthogonal axes designated by X and Y is used in the present study. The local (or element) axes are fixed to the respective elements and are designated by x and y. The global coordinate axes and the local coordinate axes for a line element are shown in Figure 3.1.

The displacement components required for the definition of the behavior of a structure may be written in terms of either the local or global coordinate directions. For the global axes, these displacement components for the i-th node are given by *

$$\{r_i\}^T = \lfloor U_i \; V_i \; \theta_i \rfloor \tag{3.1}$$

in which U_i is the translation in the global X-coordinate direction, V_i is the translation in the global Y-coordinate direction, and θ_i is the rotation about the global Z-coordinate direction (orthogonal to X and Y). For the local coordinate axes, the displacement components for the j-th node of an element are given by

$$\{q_j\}^T = \lfloor u_j \; v_j \; \theta_j \rfloor \tag{3.2}$$

in which u_j is the translation in the local x-coordinate direction,

---

*$\lfloor \; \rfloor$ indicates a row vector, $\{ \; \}$ a column vector, and the superscript T denotes the matrix transpose.

v_j is the translation in the local y-coordinate direction, and θ_j is the rotation about the local z-coordinate direction. The positive sense of the global displacement components and the local displacement components for a representative element coordinate system is shown in Figure 3.1.

The element stiffness relates the force and deformation characteristics of an element to the local displacement degrees of freedom associated with the element nodes. The matrix expression for the element equilibrium equation is

$$[k]\{q\} = \{Q\} \tag{3.3}$$

in which $[k]$ is the element stiffness matrix, $\{q\}$ is a vector of element displacements, and $\{Q\}$ is a vector of element forces. Note that these quantities are written with respect to the local element coordinate system. Once the element stiffness matrix has been formulated in local coordinates, it may be transformed to the global coordinate directions by the following transformation.

$$[k]_{global} = [\Gamma]^T[k][\Gamma] \tag{3.4}$$

in which $[k]_{global}$ is the element stiffness matrix referenced to the global axes, $[k]$ is the element stiffness matrix referenced to the local axes, and $[\Gamma]$ is the transformation matrix which consists of direction cosines relating the local and global coordinate directions.

Based on compatibility of displacements at the nodes and equilibrium of the nodal forces, the equations representing the behavior of the complete structure may be formed from the individual element stiffness relations and load vectors. In the direct stiffness method, the total

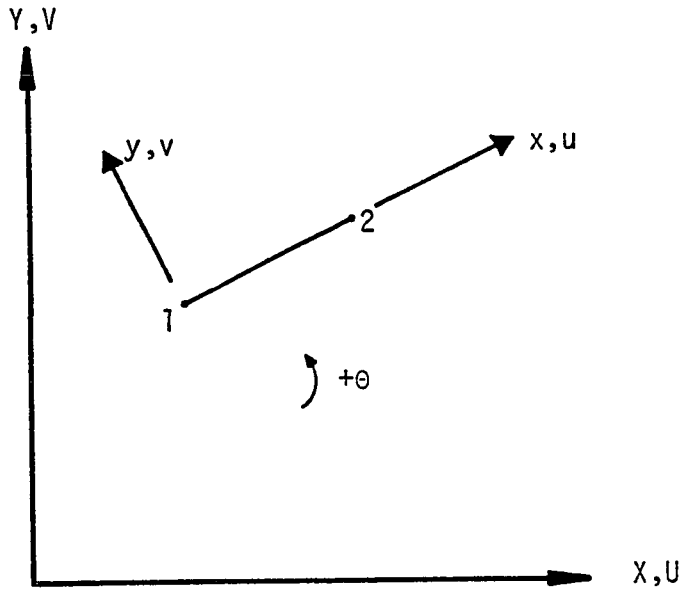

Figure 3.1 Coordinate System and Displacement Degrees of Freedom

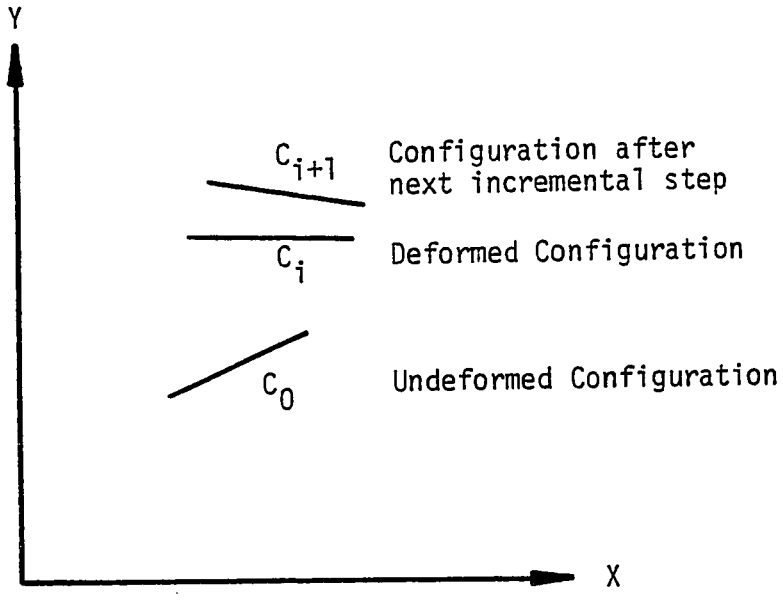

Figure 3.2 Deformation Path of Element

structure stiffness is formed by simply adding the stiffness coefficients associated with each active degree of freedom. Similarly, the total structure load vector is assembled by adding the element nodal forces associated with each active degree of freedom. The equilibrium relation for the complete structure is written in matrix form as

$$[K]\{r\} = \{R\} \tag{3.5}$$

in which $[K]$ is the stiffness matrix for the complete structure, $\{r\}$ is the vector of global displacements, and $\{R\}$ is the vector of global node forces. Equation 3.5 represents a set of simultaneous linear algebraic equations which may be solved by any of several well known techniques. In the next section it will be shown how the direct stiffness formulation is extended to the analysis of nonlinear structural behavior.

3.2 Incremental Nonlinear Analysis

The direct stiffness method was first extended to the analysis of geometric nonlinear structures by Turner, Dill, Martin, and Melosh [18]. Early studies such as this, and works by Martin [19], Argyris [20], and Felippa [21] used an incremental approach whereby the nonlinear problem was analyzed as a sequence of linear problems. Since these pioneering studies a considerable amount of attention has been directed toward the formulation and solution of nonlinear structural problems. The reader is directed to several survey papers [22-27] for a comprehensive assessment of the solution of nonlinear structural problems.

Solution procedures for nonlinear structural analysis may be divided into essentially three classifications; incremental procedures, iterative procedures, and step-iterative or mixed procedures. Incremental

procedures approximate the nonlinear problem as a sequence of linear problems. That is, the load is applied as a sequence of sufficiently small increments so that the structure can be assumed to behave linearly during each increment. The nonlinear load-deflection path is therefore only approximated and equilibrium is not satisfied. Iterative procedures seek to satisfy the nonlinear relations at a specific load level by applying successive linear corrections to an initial linear solution until equilibrium is satisfied to some predefined degree of accuracy. Mixed procedures, as the name implies, are combinations of incremental and iterative techniques. They attempt to combine the most attractive features of each method. For example, the true load-deflection curve may be traced by applying an iterative technique for several increments of applied load.

Iterative procedures, such as Newton-Raphson and successive approximations, are the most widely accepted methods for problems involving geometric nonlinearity alone. The Newton-Raphson method, in particular, is very efficient. Tillerson, Stricklin, and Haisler [28] indicate, however, that it is the iterative nature of these formulations which generally precludes their use in material nonlinear, path dependent applications. The Newton-Raphson procedure, for example, fails to converge when elastic unloading occurs [25]. Since the response of building structures subjected to extreme loads is path-dependent, iterative solution procedures are considered to be unnecessarily restrictive for this class of problems.

Incremental procedures, on the other hand, are particularly attractive since they permit the combined effects of material and geometric nonlinearity to be incorporated in a straightforward manner [29]. Also, the entire load history may be traced using an incremental approach.

This is not necessarily the case with iterative procedures unless the load is applied in increments and equilibrium is achieved by iteration at each step (mixed procedure). In addition, the post-collapse behavior (unstable region) may be traced with relative ease using the incremental procedure. This topic is covered in more detail in Section 3.7. The nonlinear analysis program described herein employs an incremental procedure.

One of the major drawbacks of the simple incremental procedure, as compared with various iterative procedures, is that equilibrium is, in general, not satisfied. That is, the solution tends to "drift" from the true load-deflection relation. The results can be improved by reducing the load increment which, of course, tends to increase the solution time. A "mid-point" or "predictor-corrector" scheme, as described by Felippa [21], may be employed to improve the solution accuracy. This method is used in the present study and is described in Section 3.4.2.

The nonlinear load-deflection characteristics of a structure may be closely approximated by employing the incremental method of solution. With this technique the load is applied as a sequence of sufficiently small increments so that the structure can be assumed to respond linearly within each increment. The solution is thereby reduced to a series of linear steps in which the structure stiffness is recomputed at each load increment. The updated stiffness is a function of both the deformed geometry and state of stress at the start of an increment and is commonly referred to as the "tangent stiffness." Displacement increments are computed for each step and are accumulated to give the total displacement. The corresponding increments of stress are computed from the displacement

increments and are accumulated to give the total stress at any stage of loading. This incremental process is repeated until the desired load level is reached. In this manner the entire load history may be traced.

3.3 Formulation of Beam-Column Stiffness

Large displacement stiffness equations may be developed in an incremental form by direct application of energy principles of structural mechanics. Such equations will accurately predict nonlinear structural behavior for small increments of load starting from a known equilibrium position. This section deals with the formulation of the incremental element stiffness matrix for the beam-column element which accounts for the geometric nonlinear behavior resulting from an axial force acting on the member.

There are essentially two different approaches to incremental nonlinear finite element analysis [27]; the large-displacement stiffness equations may be referenced to either a stationary or a moving coordinate system. Consider an element in its path of deformation as shown in Figure 3.2. C_0 represents the undeformed state, C_i is the current deformed configuration, and C_{i+1} is the deformed state for the next incremental step. In the first approach the incremental stiffness relations are written in terms of the undisplaced coordinates of the structure (C_0). The second approach is based on an updated coordinate system which describes the structure in some known, displaced equilibrium configuration (C_i). The nomenclature presented by Bathe, Ramm, and Wilson [27] is adopted here in which the first approach, based on the initial, undisplaced configuration is termed the Total Lagrangian

formulation while the second approach, based on an updated configuration, is termed the Updated Lagrangian formulation. Bathe and Bolourchi [30] have shown that, for a three-dimensional beam element, the two formulations yield identical element stiffness matrices and nodal point force vectors. In addition, they conclude that the Updated Lagrangian formulation is computationally more efficient.

The principle of minimum potential energy provides a variational basis for the direct formulation of element stiffness equations (see Reference [16]). The potential energy (Π) of an element is given by the strain energy of deformation plus the potential of the applied loads. The principle states that of all admissible displacements, those that satisfy the equilibrium conditions make the potential energy assume a stationary value, or $\delta\Pi(\{q\}) = 0$. That is, the first variation of Π with respect to the displacements is equal to zero.

To evaluate the total potential energy of an element, an expression for the element strain must be obtained. Consider a linear element in which the local x-axis coincides with the centroidal axis of the member and the local y-axis is normal to the x-axis. For the planar frame beam element, the x-component of direct strain may be expressed as [31]

$$\varepsilon_1 = \frac{\partial u}{\partial x} + \frac{1}{2}\left(\frac{\partial u}{\partial x}\right)^2 + \frac{1}{2}\left(\frac{\partial v}{\partial x}\right)^2 \tag{3.6}$$

in which u and v are the local x- and y-components of displacement respectively. The in-plane bending strain, or curvature, for a slender member, is given by [32]

$$\varepsilon_2 = \frac{\frac{\partial^2 v}{\partial x^2}}{\left[1 + \left(\frac{\partial v}{\partial x}\right)^2\right]^{3/2}} \tag{3.7}$$

If it is assumed that rotations are small, the quantity $(\partial v/\partial x)^2$ becomes very small in comparison with unity and Equation 3.7 may be approximated by

$$\varepsilon_2 \simeq \frac{\partial^2 v}{\partial x^2} \tag{3.8}$$

Shear strain is also neglected in the present study since, for slender elements, shear distortions are considerably smaller than bending distortions. The linear beam curvature expressed by Equation 3.8 produces a component of direct strain in the x-direction which is linearly proportional to the distance from the centroidal axis. The axial strain for the beam element may, therefore, be written as

$$\varepsilon_x = \varepsilon_1 - y\varepsilon_2 \tag{3.9}$$

in which y is measured normal to the centroidal axis of the beam and d is the death of the beam. The sign convention used in Equation 3.9 is consistent with the definition of positive bending shown in Figure 3.3. Upon substitution of the expressions for ε_1 and ε_2 into the above equation and the rearrangement of terms, the following equation is obtained for the x-component of strain:

$$\varepsilon_x = \frac{\partial u}{\partial x} - y\frac{\partial^2 v}{\partial x^2} + \frac{1}{2}\left(\frac{\partial u}{\partial x}\right)^2 + \frac{1}{2}\left(\frac{\partial v}{\partial x}\right)^2 \tag{3.10}$$

The first two terms in the above expression are linear in the displacement derivatives while the last two terms are nonlinear.

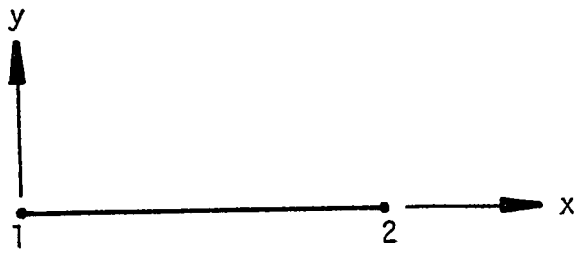

Figure 3.3 Member Force Components

The element strains may be expressed as the sum of the linear and nonlinear components. Thus, the element strains may be written in vector form as

$$\{\varepsilon\} = \{\varepsilon^L\} + \{\varepsilon^N\} \tag{3.11a}$$

in which, for the current case,

$$\{\varepsilon^L\} = \{\frac{\partial u}{\partial x} - y \frac{\partial^2 v}{\partial x^2}\} \tag{3.11b}$$

and

$$\{\varepsilon^N\} = \{\frac{1}{2}\left(\frac{\partial u}{\partial x}\right)^2 + \frac{1}{2}\left(\frac{\partial v}{\partial x}\right)^2\} \tag{3.11c}$$

The superscripts L and N refer to linear and nonlinear terms respectively. Note that, for the present case, the vector $\{\varepsilon\}$ contains only ε_x. The formulation presented herein uses the nonlinear strain expression given by Equation 3.11a as a basis for the formulation of the element stiffness equations.

Consider again a body in its path of deformation (Figure 3.2). The body is initially in an undisplaced ($\{q_0\} = \{0\}$) configuration represented by C_0. After application of the i-th increment of load, the body is in the known equilibrium state, C_i. A solution for the next increment, C_{i+1}, is sought.

In the Updated Lagrangian formulation all quantities are referred to the displaced equilibrium configuration, C_i. This state is, therefore, the reference state for this formulation. In this reference state the body is subjected to a known set of nodal loads, $\{Q_i\}$. Similarly, all displacements $\{q_i\}$ and stresses $\{\sigma_i\}$ are known with respect to the reference state. It is desired to obtain a solution for the next

increment. At the end of this increment the vector of applied nodal loads is given by

$$\{Q_{i+1}\} = \{Q_i\} + \{\Delta Q\} \tag{3.12}$$

in which $\{\Delta Q\}$ is a finite increment of load. Similarly, the displacements and stresses at the end of the next increment may be written as

$$\{q_{i+1}\} = \{q_i\} + \{\Delta q\} \tag{3.13}$$

and

$$\{\sigma_{i+1}\} = \{\sigma_i\} + \{\Delta \sigma\} \tag{3.14}$$

in which $\{\Delta q\}$ is the vector of incremental nodal displacements and $\{\Delta \sigma\}$ is the vector of incremental element stresses. For the present case the vector $\{\sigma\}$ contains only the axial stress, σ_x. Again it is emphasized that all quantities in the above equations are expressed in terms of the reference state.

The incremental strains measured with respect to the reference state are $\{\Delta \varepsilon\}$. The total potential energy of an element may be written with respect to the reference state in terms of the incremental strains and incremental displacements. If it is assumed that the loads are applied only at the element nodes, the following expression for the element total potential energy is obtained:

$$\Pi = \frac{1}{2}\int_V \lfloor \Delta\varepsilon \rfloor [E] \{\Delta\varepsilon\} dV + \int_V \lfloor \sigma_i \rfloor \{\Delta\varepsilon\} dV - \lfloor \Delta q \rfloor \{Q_{i+1}\} \tag{3.15}$$

in which $\{\Delta \varepsilon\}$ is a vector of incremental strain components, $[E]$ is a matrix of material constitutive relations, $\{\sigma_i\}$ is a vector of initial stresses, $\{\Delta q\}$ is a vector of generalized incremental nodal displacements,

$\{Q_{i+1}\}$ is the vector of applied nodal loads, and V refers to integration over the volume of the element. The first term in the above expression represents the strain energy of the element as it undergoes deformation. The second term accounts for initial element stress in the reference state. And the third term is the potential of the applied element nodal loads. Note that the general matrix notation for the element stresses and strains is maintained.

The incremental strain may also be represented by the sum of linear and nonlinear components as in Equation 3.11a giving

$$\{\Delta\varepsilon\} = \{\Delta\varepsilon^L\} + \{\Delta\varepsilon^N\} \tag{3.16}$$

in which $\{\Delta\varepsilon^L\}$ is the vector of linear strain increments and $\{\Delta\varepsilon^N\}$ is the vector of nonlinear strain increments. Now, upon substitution of the expression for the strain increments given by Equation 3.16 into the equation for the potential energy in Equation 3.15, the following relation is obtained:

$$\begin{aligned}\Pi = \frac{1}{2}\int_V \lfloor\Delta\varepsilon^L + \Delta\varepsilon^N\rfloor[E]\{\Delta\varepsilon^L + \Delta\varepsilon^N\}dV \\ + \int_V \lfloor\sigma_i\rfloor\{\Delta\varepsilon^L + \Delta\varepsilon^N\}dV - \lfloor\Delta q\rfloor\{Q_{i+1}\}\end{aligned} \tag{3.17}$$

In accordance with the principle of minimum potential energy, the first variation of the above expression is taken with respect to the incremental displacements and the result is set equal to zero. The first term in the above expression is found, upon taking the variation, to be nonlinear in the displacements. To obtain a linear set of stiffness equations, the nonlinear component of the incremental strain is neglected

in the first integral. For small changes in geometry and, therefore, small incremental strains, this linearization is justified. The nonlinear strain term is retained in the second integral since no linearization is required. The incremental potential energy is thus approximated as

$$\Pi = \frac{1}{2}\int_V \lfloor \Delta\varepsilon^L \rfloor [E] \{\Delta\varepsilon^L\} dV + \int_V \lfloor \sigma_i \rfloor \{\Delta\varepsilon^L\} dV + \int_V \lfloor \sigma_i \rfloor \{\Delta\varepsilon^N\} dV - \lfloor \Delta q \rfloor \{Q_{i+1}\} \tag{3.18}$$

In the stiffness approach to finite element analysis the potential energy expression is discretized through the introduction of displacement fields expressed in terms of generalized node displacements (see Reference [16]). For the beam element considered here, a linear displacement field is assumed for the u-displacement component and a cubic displacement field is assumed for the v-displacement component. The displacements at any point in the element are written in terms of the generalized node displacements as

$$u = \lfloor N_x \rfloor \{q\} \tag{3.19a}$$

$$v = \lfloor N_y \rfloor \{q\} \tag{3.19b}$$

in which $\lfloor N_x \rfloor$ and $\lfloor N_y \rfloor$ are the displacement interpolation functions and are given by

$$\lfloor N_x \rfloor = \left\lfloor \left(1 - \frac{x}{L}\right) \quad 0 \quad 0 \quad \left(\frac{x}{L}\right) \quad 0 \quad 0 \right\rfloor \tag{3.20a}$$

$$\lfloor N_y \rfloor = \left\lfloor 0 \quad 1 - \frac{3x^2}{L^2} + \frac{2x^2}{L^3} \quad x - \frac{2x^2}{L} + \frac{x^3}{L^2} \right.$$

$$0 \quad \frac{3x^2}{L^2} - \frac{2x^2}{L^3} \quad - \frac{x^2}{L} + \frac{x^3}{L^2} \Big] \tag{3.20b}$$

and $\{q\}$ is the vector of element node displacements

$$\{q\}^T = \lfloor u_1 \; v_1 \; \theta_i \; u_2 \; v_2 \; \theta_2 \rfloor \tag{3.20c}$$

in which the subscripts 1 and 2 refer to ends 1 and 2 of the beam element, respectively. The incremental displacements may also be written in terms of the element incremental node displacements using the displacement interpolation functions given above. Thus

$$\Delta u = \lfloor N_x \rfloor \{\Delta q\} \tag{3.21a}$$

$$\Delta v = \lfloor N_y \rfloor \{\Delta q\} \tag{3.21b}$$

in which $\{\Delta q\}$ is the vector of element incremental node displacements

$$\{\Delta q\}^T = \lfloor \Delta u_1 \; \Delta v_1 \; \Delta\theta_1 \; \Delta u_2 \; \Delta v_2 \; \Delta\theta_2 \rfloor \tag{3.21c}$$

and the subscripts again refer to ends 1 and 2 of the element. The partial derivatives of the incremental x- and y-displacement components are, then

$$\frac{\partial \Delta u}{\partial x} = \frac{\partial}{\partial x} \lfloor N_x \rfloor \{\Delta q\} = \lfloor N_x' \rfloor \{\Delta q\} \tag{3.22a}$$

$$\frac{\partial \Delta v}{\partial x} = \frac{\partial}{\partial x} \lfloor N_y \rfloor \{\Delta q\} = \lfloor N_y' \rfloor \{\Delta q\} \tag{3.22b}$$

in which the prime (') indicates differentiation with respect to the variable x. Similarly, the second partial derivative of the incremental y-displacement component is

$$\frac{\partial^2 \Delta v}{\partial x^2} = \frac{\partial^2}{\partial x^2} [N_y]\{\Delta q\} = [N_y'']\{\Delta q\} \tag{3.23}$$

The axial strain, expressed in terms of the first and second derivatives of the displacements, may now be expressed in terms of the interpolation functions. The linear and nonlinear incremental strain terms are written in matrix form as

$$\{\Delta \varepsilon^L\} = [B^L]\{\Delta q\} \tag{3.24a}$$

$$\{\Delta \varepsilon^N\} = \frac{1}{2}[\Delta q][B^N]^T[B^N]\{\Delta q\} \tag{3.24b}$$

in which

$$[B^L] = [LN_x'] - y[N_y'']] \tag{3.24c}$$

and

$$[B^N] = \begin{bmatrix} [N_x'] \\ [N_y'] \end{bmatrix} \tag{3.24d}$$

Upon substitution of the matrix expressions for the linear and nonlinear strain terms given by Equations 3.24a and 3.24b into the total potential energy expression, the following equation is obtained:

$$\begin{aligned} \Pi = \frac{1}{2}\int_V [\Delta q][B^L]^T[E][B^L]\{\Delta q\}dV + \int_V [\Delta q][B^L]^T\{\sigma_i\}dV \\ + \frac{1}{2}\int_V [\Delta q][B^N]^T[\sigma_i][B^N]\{\Delta q\}dV - [\Delta q]\{Q_{i+1}\} \end{aligned} \tag{3.25}$$

in which $[\sigma_i]$ is a matrix containing initial stress components and for the present case is simply $\sigma_x[I]_{2\times 2}$. Finally, the first variation of the above expression is taken with respect to $\{\Delta q\}$ and the result is

set equal to zero producing the following incremental element equilibrium equation in matrix form:

$$\delta\Pi(\{\Delta q\}) = 0 = \int_V [B^L]^T[E][B^L]dV\{\Delta q\} + \int_V [B^L]^T\{\sigma_i\}dV + \int_V [B^N]^T[\sigma_i][B^N]dV\{\Delta q\} - \{Q_{i+1}\} \tag{3.26}$$

or, upon the rearrangement of terms,

$$\left[\int_V [B^L]^T[E][B^L]dV + \int_V [B^N]^T[\sigma_i][B^N]dV\right]\{\Delta q\} = \{Q_{i+1}\} - \int_V [B^L]^T\{\sigma_i\}dV \tag{3.27}$$

The axial stress in the reference state may be written in terms of the element axial force and bending moment. The positive sense of these generalized force components is shown in Figure 3.3. The element stress in the reference state may be written as

$$\sigma_{xi} = \frac{P_i}{A} + \frac{M_i y}{I} \tag{3.28a}$$

in which

$$M_i = M_{1i}(1 - \frac{x}{L}) + M_{2i}(\frac{x}{L}) \tag{3.28b}$$

and P is the axial force in the element, A is the cross sectional area, M_{1i} and M_{2i} are the bending moments at ends 1 and 2 respectively, I is the moment of inertia of the beam section, and L is the member length. Upon evaluation of the integrals in Equation 3.27, the following incremental equilibrium expression is obtained:

$$\left[[k] + [k_g]\right]\{\Delta q\} = \{Q_{i+1}\} - \{F_i\} \tag{3.29a}$$

in which

$$[k] = \int_V [B^L]^T [E][B^L] dV \tag{3.29b}$$

$$[k_g] = \int_V [B^N]^T [\sigma_i][B^N] dV \tag{3.29c}$$

$$\{F_i\} = \int_V [B^L]^T \{\sigma_i\} dV \tag{3.29d}$$

The matrix $[k]$ is the linear elastic stiffness matrix and, as can be seen from Equation 3.29b, contains terms representing the linear portion of the strain energy expression. $[k_g]$ is termed the "initial stress" matrix. This matrix results from the energy contribution of the initial stresses and nonlinear incremental strains. $\{F_i\}$ is a vector of nodal point forces equivalent in an energy sense to the element stresses at the beginning of the increment. If the element is in equilibrium at the start of the increment, $\{F_i\} = \{Q_i\}$ and since $\{Q_{i+1}\} - \{Q_i\} = \{\Delta Q\}$, the incremental stiffness relation may be written as

$$\left[[k] + [k_g]\right]\{\Delta q\} = \{\Delta Q\} \tag{3.30a}$$

or

$$[k_t]\{\Delta q\} = \{\Delta Q\} \tag{3.30b}$$

in which $[k_t] = \left[[k] + [k_g]\right]$ is the tangent stiffness for the increment. The explicit form of both $[k]$ and $[k_g]$ is given in Appendix A for the beam-column element.

For the Updated Lagrangian formulation, the transformation from local to global coordinates is based on the displaced configuration. The matrix

used to effect this transformation is, therefore, a function of the displaced geometry. This relation may be expressed as

$$[\Gamma_i] = [\Gamma(\{q_i\})] \tag{3.31}$$

in which $\{q_i\}$ is the displacement vector in configuration C_i. The transformation matrix, $[\Gamma_i]$, is written as

$$[\Gamma_i] = \begin{bmatrix} \lambda_{x'} & \mu_{x'} & 0 & 0 & 0 & 0 \\ \lambda_{y'} & \mu_{y'} & 0 & 0 & 0 & 0 \\ 0 & 0 & 1 & 0 & 0 & 0 \\ 0 & 0 & 0 & \lambda_{x'} & \mu_{x'} & 0 \\ 0 & 0 & 0 & \lambda_{y'} & \mu_{y'} & 0 \\ 0 & 0 & 0 & 0 & 0 & 1 \end{bmatrix} \tag{3.32a}$$

in which λ and μ are the cosines of the angle between the locas axes and the global X- and Y-axes, respectively. The direction cosines are computed as follows:

$$\lambda_{x'} = \frac{X_{2i} - X_{1i}}{L_i} \qquad \mu_{x'} = \frac{Y_{2i} - Y_{1i}}{L_i} \tag{3.32b,c}$$

and

$$\lambda_{y'} = \frac{Y_{1i} - Y_{2i}}{L_i} \qquad \mu_{y'} = \frac{X_{2i} - X_{1i}}{L_i} \tag{3.32d,e}$$

and X and Y are the spatial coordinates of the member ends of the reference state C_i, and L is the deformed member length. The transformation to global stiffness is again expressed as

$$[k_t]_{global} = [\Gamma_i]^T[k_t][\Gamma_i] \tag{3.33}$$

in which $[k_t]_{global}$ is the tangent stiffness in global coordinates, $[k_t]$ is the tangent stiffness in local coordinates, and $[\Gamma_i]$ is the transformation matrix based on the geometry of the structure at the start of the i-th step.

3.4 Incremental Solution Techniques

In the above discussion the incremental step procedure was briefly described. Here, this method of solution is formalized and the required equations for the application of the procedure are provided. Two methods are presented; the simple-step procedure and the predictor-corrector procedure. The following development is based on equilibrium equations written for the entire structure and expressed in global coordinates (see Equation 3.5).

3.4.1 Simple-Step Procedure

The equations representing the simple-step approach are given here. The development follows closely that presented by Desai and Abel [15]. Let the initial loads and displacements be given by $\{R_o\}$ and $\{r_o\}$, respectively, in which the subscript o represents the initial or reference state. After application of the i-th increment, the load is given by

$$\{R_i\} = \{R_o\} + \sum_{j=1}^{i} \{\Delta R_j\} \tag{3.34}$$

in which the Δ notation indicates a finite increment. Similarly, the displacements after the i-th step are

$$\{r_i\} = \{r_o\} + \sum_{j=1}^{i} \{\Delta r_j\} \tag{3.35}$$

The stiffness for the i-th increment is based on the results of the previous step. The set of simultaneous linear equations which must be solved for each incremental step is written as

$$[K_{i-1}]\{\Delta r_i\} = \{\Delta R_i\} \tag{3.36a}$$

in which

$$[K_{i-1}] = [K(\{r_{i-1}\}, \{R_{i-1}\})] \tag{3.36b}$$

and $[K_{i-1}]$ is the value of the stiffness at the beginning of the increment. Equations (3.34-3.36) provide the necessary relations for application of the simple-step procedure. A one-degree-of-freedom schematic representation of this procedure is shown in Figure 3.4.

The accuracy of this method is dependent on the step size. The smaller the incremental step the more accurately the nonlinear load-deflection curve is traced. Since a new incremental stiffness must be formed for each step, this improved accuracy results in additional computational effort. A two-step or predictor-corrector method may be employed to improve the solution accuracy.

3.4.2 Predictor-Corrector Procedure

The predictor-corrector method involves a two-step process. In the first step (predictor) the load increment is applied and the displacement increments are computed as above. The stiffness equation is

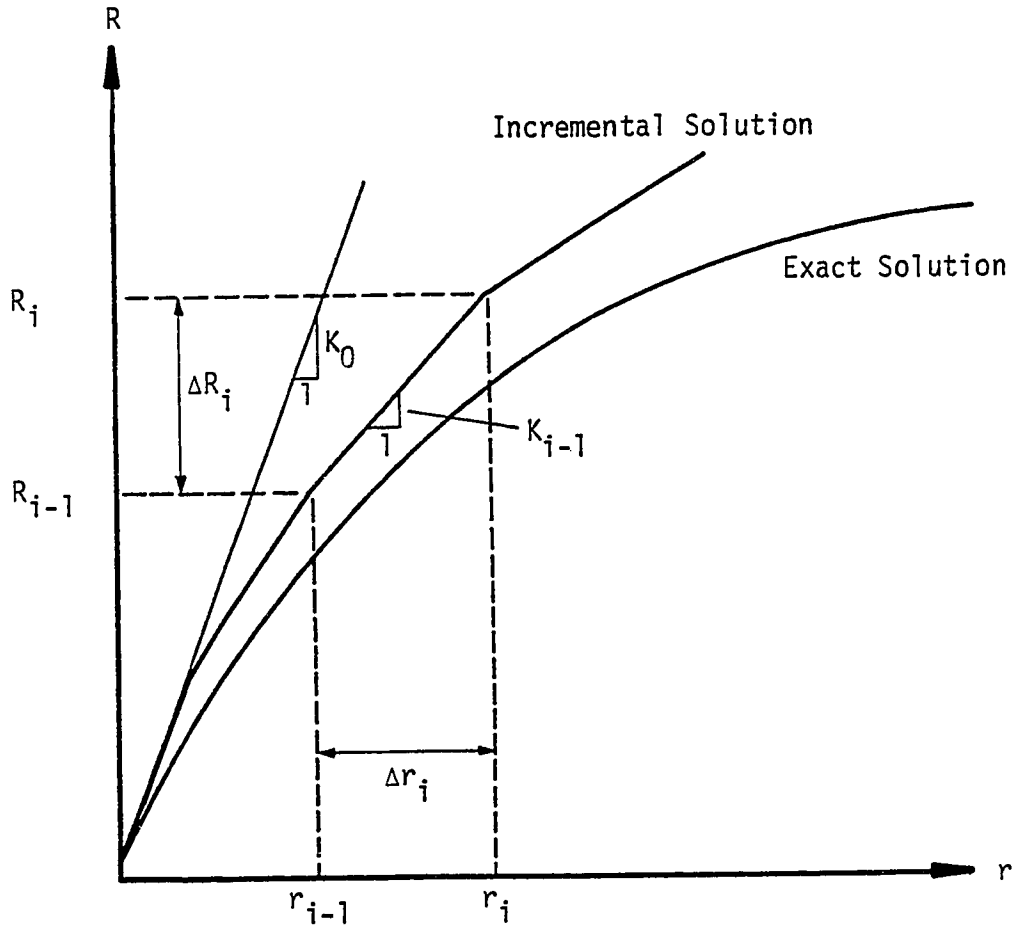

Figure 3.4 Schematic of Simple-Step Procedure

$$[K_{i-1}]\{\Delta r_i^*\} = \{\Delta R_i\} \tag{3.37}$$

which is the same as Equation 3.33a except that the superscript * indicates temporary values. Since each step is linear, the displacements at half the load increment are computed by

$$\{r_{i-\frac{1}{2}}\} = \{r_{i-1}\} + \{\frac{\Delta r_i^*}{2}\} \tag{3.38}$$

Similarly, the load at the midpoint of the increment is

$$\{R_{i-\frac{1}{2}}\} = \{R_{i-1}\} + \{\frac{\Delta R_i}{2}\} \tag{3.39}$$

A new stiffness is computed on the basis of the displacement and forces at the midpoint of the increment:

$$[K_{i-\frac{1}{2}}] = [K(\{r_{i-\frac{1}{2}}\}, \{R_{i-\frac{1}{2}}\})] \tag{3.40}$$

A second step (corrector) is taken using this updated stiffness

$$[K_{i-\frac{1}{2}}]\{\Delta r_i\} = \{\Delta R_i\} \tag{3.41}$$

In effect, $[K_{i-\frac{1}{2}}]$ is an approximation of the stiffness at the midpoint of the i-th increment. Therefore, it is an improvement over the stiffness computed at the beginning of the increment using Equation 3.36b.

The predictor-corrector procedure is shown schematically in Figure 3.5 for a one-degree-of-freedom system. This method provides a better approximation to the true curve than simply halving the load increment and applying the simple-step procedure. This procedure has been used by Felippa [21] and by Porter and Powell [33] for elastic-plastic large displacement analyses. Either of these two methods, the simple-step or

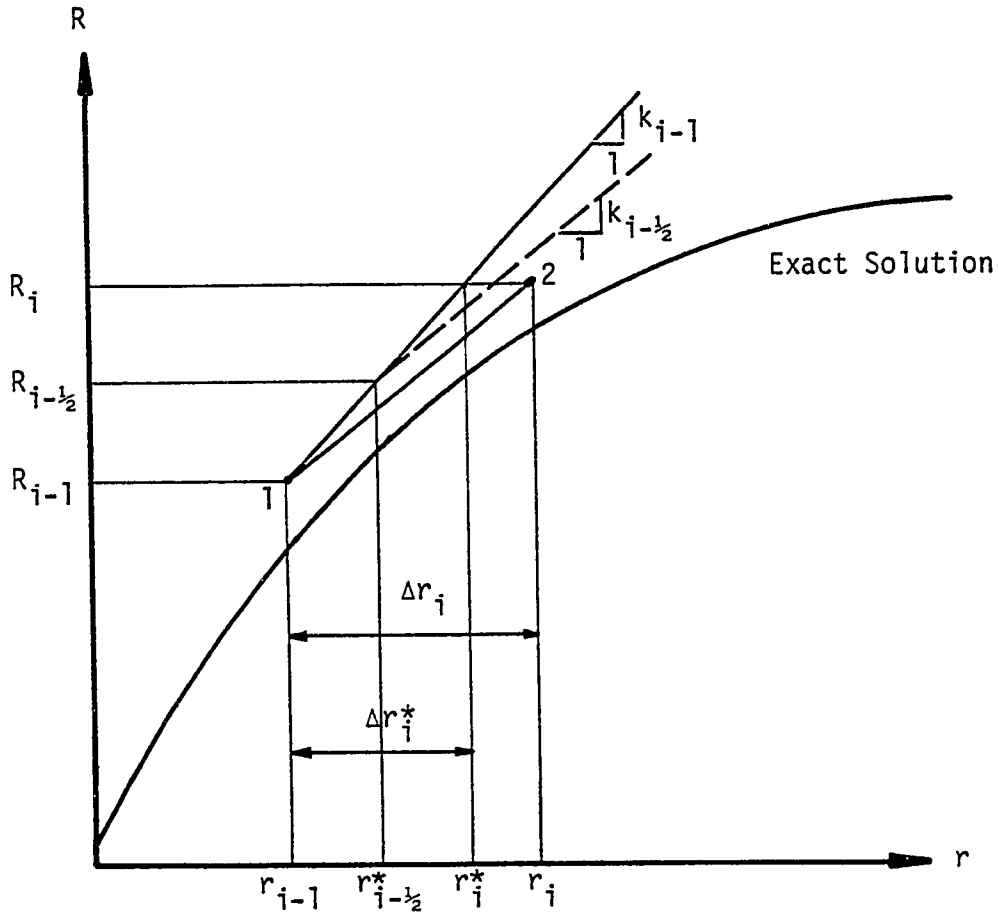

Figure 3.5 Schematic of Predictor-Corrector Procedure

predictor-corrector, may be selected in the analysis program described herein. For problems in which the geometric effects are assumed to be negligible, the simple step procedure will give acceptable results. In general, the predictor-corrector method should be used for problems which exhibit moderate to significant geometric nonlinearities.

3.5 Step-Termination Criteria

In the foregoing discussion it was assumed that the incremental step size was specified and that the entire step could always be applied. For the current analysis procedure, this is not always the case. Any of several conditions may arise during the incremental step which preclude the entire load increment from being applied. For example, a step is terminated when a plastic hinge forms in a beam-column member or when a shear panel reaches its cracking stress. These conditions are distinguished by an abrupt change in stiffness which is accounted for in the next incremental step. In this section the various criteria which determine the actual size of the incremental step which may be applied are discussed.

3.5.1 Change of Member Stiffness

It is assumed in the current analysis that all members yield or crack suddenly instead of gradually. For each of the elements included in the analysis program, a yield or failure criterion is defined such that the element exhibits an abrupt change in stiffness when this criterion is satisfied. The load-deflection curve for such behavior exhibits marked slope discontinuities as a result of this sudden change

of stiffness. A representative load-deflection curve depicting abrupt changes in slope is shown in Figure 3.6. To follow the load-deflection behavior accurately, the stiffness of the structure must reflect such changes as result from yielding or cracking. Therefore, if the failure criterion for any member is reached during a load step, only that portion of the load to just cause the member to yield or crack is applied. Thus, a load increment may be terminated as a result of a change of member stiffness.

For each of the elements described in Chapter 4, the yield criteria are represented by linear functions of the member forces or stresses. At the end of each increment, all members are checked to determine if any have yielded or cracked. If so, the step size to just cause yielding or cracking is computed. This load step size determines the largest load increment that can be applied without changing the yield or cracking configuration. A method for preventing excessively small load increments is given in Section 3.6.

3.5.2 Load Increment Constraint

If a structure exhibits significant nonlinear geometric behavior, it may be necessary to restrict the increment of load applied during each step to trace accurately the nonlinear load-deflection characteristics. The load step size may be specified for each incremental step. The step size must, of course, be greater than zero.

A maximum load factor may also be specified. This maximum is expressed as a fraction of the defined load. It may be greater than 1.0 but must not be less than zero. A step is terminated when this

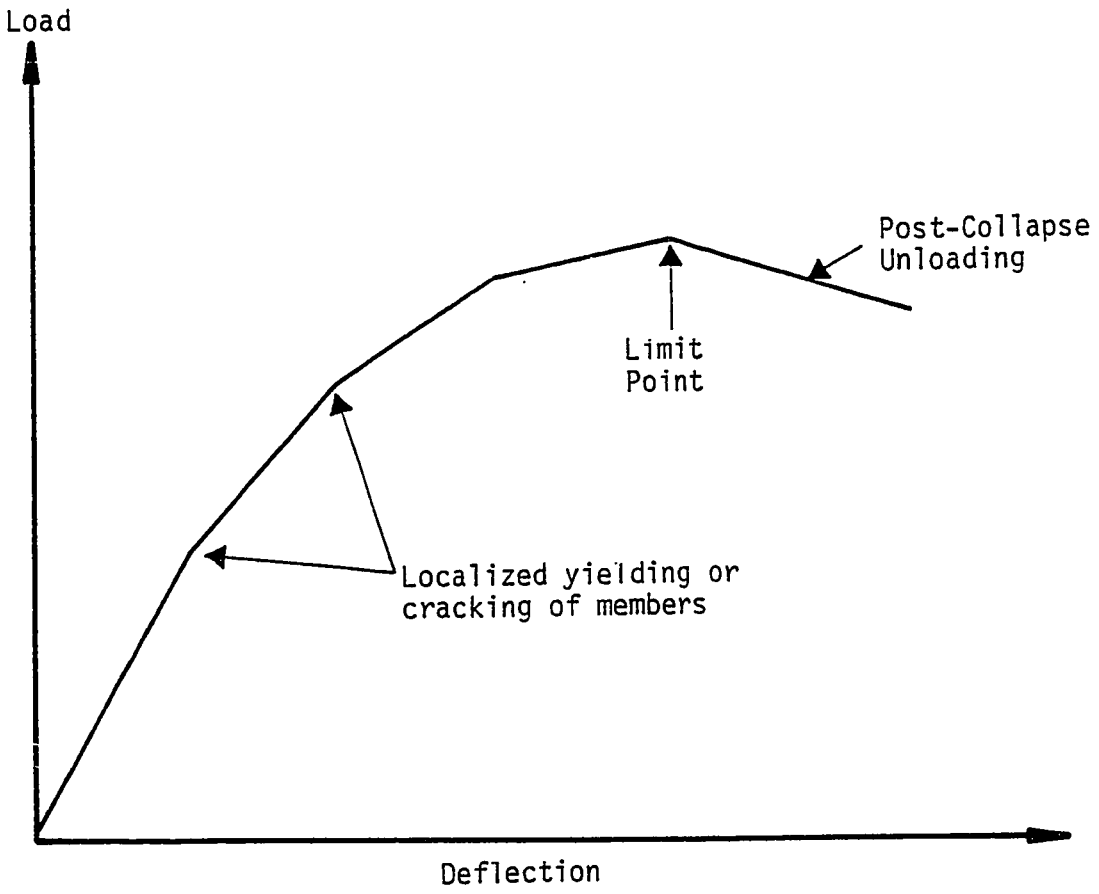

Figure 3.6 Load-Deflection Curve Exhibiting Abrupt Changes in Stiffness

maximum load factor is reached. For example, if results are desired at 50% of the applied load, the maximum load factor would be set to 0.5. Alternatively, a maximum load factor of 2.0 would permit the structure under analysis to be loaded with two times the defined load. The maximum load factor may be changed between load steps thus enabling considerable control over the incremental step process.

When a structure reaches collapse, the loads are removed in the same incremental fashion as they were applied (see Section 3.6). The program will terminate when all of the applied load has been removed. If more than one load case has been applied, each will be removed in turn.

3.5.3 Maximum Displacement Constraint

Two displacement constraints may be specified: a limit on the maximum displacement permitted during a load step, and a limit on the maximum total displacement permitted. A step will be terminated when either of these limits is reached. Limits may be specified for each of the three displacement components individually. For those constraints which are not specified, no checks are performed. This feature is useful in those situations where a small increment of load causes a large corresponding increment of displacement.

3.6 Load-Step Tolerance

The program terminates a load step when any element reaches a change of stiffness as described in Section 3.5.1. To prevent an excessive number of small load steps a load step tolerance feature is

provided. The load step tolerance is defined as a fraction of the total load. This feature insures that all changes of stiffness which would ordinarily occur within this tolerance, occur at the end of the current step. Suppose, for example, that a load step tolerance of 0.02 is specified. Upon termination of a step, all elements are checked to determine those which would meet a change of state constraint within an additional 2% of the defined load. These elements are then assumed to have met the change of state criteria during the current step. This guarantees that no step smaller than 0.02 will result. Typically a much smaller value is used for the load step tolerance. Porter and Powell [33] report that a value of 10^{-5} works well and this is used as a default value in the current program. The load step tolerance may be redefined at any step of the analysis.

3.7 Post-Collapse Behavior

Figure 3.6 shows a characteristic load-deflection curve for a structure loaded to collapse (limit point) and into the post-collapse or unstable region. The incremental procedure described above is applicable up to the limit point. Numerical difficulties arise, however, beyond this point. The descending branch of the load-deflection curve is characterized by a negative-definite stiffness matrix [34]. Therefore, the structure can only withstand a decreasing load. A procedure which accounts for this situation is necessary if the entire load history, through collapse, is to be traced.

Several procedures to follow the post-collapse behavior have been reported. Wright and Gaylord [35] have developed a scheme for

multistory frames with sidesway whereby fictitious springs are added to assure that the stiffness matrix remains positive-definite. A similar procedure is used by Sharifi and Popov [34] for the buckling analysis of sandwich arches. Argyris [20] suggests incrementing the displacements instead of the loads to insure a unique solution in the post-collapse region. A third approach is that used by Porter and Powell [33] in which the sign of the load increment is simply reversed after the collapse load has been reached. It is this procedure which has been adopted in the present study.

To apply this method the point at which the stiffness matrix becomes negative-definite must be determined. This is done by detecting the presence of a negative term on the diagonal of the reduced stiffness matrix. For subsequent incremental steps the negative of the displacement and load increments is used. The post-collapse unloading behavior can therefore be followed. This procedure has been successfully applied to building frame structures as will be shown in Chapter 6.

4. DESCRIPTION OF ELEMENTS

In the direct stiffness method of analysis described in Chapter 3 a structure is idealized as an assemblage of deformable elements. The purpose of this section is to describe the theoretical development of the various elements included in the progressive collapse analysis computer program. Since the intent of the program is to analyze structures at or near collapse, the elements presented here must be capable of representing accurately the behavior of the various structural components as damage is incurred. Considerable attention is devoted to the inelastic and nonlinear behavior of these elements. The elements are all compatible with the direct stiffness formulation and incremental solution procedure presented in Chapter 3. In addition, the detection of local yield or failure (change of stiffness) is consistent among the elements so they may be used in combination. Additional elements may, of course, be added to the current capability as required. Several examples demonstrating the use of the elements for a variety of problems are presented in Chapter 6.

4.1. Beam-column

By far the most common structural elements in building construction are frame members. For steel structures, these members are generally wide flange sections, or members built up from flat plates. This type of member is usually connected at its ends by either bolted or welded connections. An element used to model connection behavior is given in Section 4.3. Frame structures can usually be expected to behave

in a linear elastic fashion throughout the working load range. However, damage to a portion of the structure may cause severe loading in the frame members. If the moment capacity of a cross section is exceeded, local yielding will occur. This may significantly affect the subsequent behavior of the member and should be accounted for in the analysis. Although the behavior of frame members is often governed by bending, the effects of axial load in column members is also significant. A compressive axial load in a member reduces its bending stiffness; this is the so-called "second order" or "geometric" effect. In addition, the moment capacity of a cross section is reduced in the presence of axial force. This section describes an element which models beam-column members for analysis.

Considerable theoretical work has been conducted on the effects of the two sources of nonlinear structural frame behavior, namely material and geometric nonlinearity. These effects are treated separately by most researchers. Under certain simplifying assumptions, however, they can be combined in a consistent manner to model realistically the behavior of nonlinear, inelastic frames.

4.1.1. Background

Many investigations have been conducted on the elastic, nonlinear behavior of beam-column members. Several alternative formulations have been reported for taking large deflections and the effects of axial force into account [36-40]. Approximate solution techniques have been developed to account for the elasto-plastic behavior of frame structures assuming the yielding of a cross section to be a function of

bending moment alone [41-46]. That is, the influence of axial force on the moment capacity of a cross section and the inelastic interaction between the axial force and bending moment are neglected. Generally, such investigations have assumed elastic-perfectly plastic behavior and, therefore, have ignored strain hardening and the spread of plasticity. Clough, Benuska, and Wilson [43] account for strain hardening in an approximate way using a dual component, parallel member model.

In general, the yield condition of a member cross section is not a function of bending moment alone but is influenced by several stress resultants, such as axial force and bending moment. Also, the inelastic response of a member cross section is a function of the interaction of these stress resultants used to define the yield criteria (see Hodge [47]). Morris and Fenves [48] have developed a general procedure for the analysis of inelastic frames which accounts for cross sections deforming plastically under combined flexural and torsional moments and axial force. The members are assumed to be elastic-plastic and yielding occurs at generalized hinges. Each member cross section is assumed to have a shape factor of 1.0, thus, the transition from elastic to plastic behavior is immediate. A similar procedure was adopted by Nigam [49] for the analysis of inelastic frames under dynamic loads. Here the members are assumed to yield at generalized hinges governed by two-dimensional smooth yield surfaces. For each load increment the member end forces at each hinge are constrained to move tangent to the yield surface. Again, no strain hardening is taken into account. In both of these studies the effects of geometric nonlinearities are not included.

A general method for modifying the member stiffness matrix to account for the formation of generalized hinges is given by Porter and

Powell [33]. The procedure is essentially the same as that of Nigam but is presented in concise matrix form. Two-dimensional yield surfaces are used whereby each surface is represented by a series of linear segments. Thus, a yield surface of almost any shape or complexity may be specified. The procedure is also able to handle the behavior at yield surface discontinuities. Effects of geometric nonlinearity are also included. The procedure presented by Porter and Powell is believed to be more direct than those previously cited and is adopted in the present study.

Wen and Farhoomand [50] have extended the above approach by considering the finite length of yielded regions. In addition, a continuous yield surface is used and an iterative procedure is employed to insure that the force point remains on the yield surface at all times. Works by Gupta and Hollmeier [51] and Gupta [52] use the yielding approach presented by Hodge and by Morris and Fenves. Strain hardening is included in both of these works and the length of yielded region is considered in Reference [52]. Neither of these methods which consider the spread of plasticity takes geometric nonlinear effects into account. When the material is assumed to behave in an elastic-perfectly plastic manner and hinges form at discrete points with no spread of plastification, geometric and material nonlinearities may be combined in a straightforward manner.

4.1.2. Assumptions and Limitations

Formulation of the beam-column element is based on the following assumptions and limitations:

(1) The members are assumed to be straight and prismatic.

(2) Loads may be applied only at the joints.

(3) Transverse shear deformations are ignored.

(4) The material is assumed to be linearly elastic-perfectly plastic and the stress-strain characteristics are assumed to be independent of time.

(5) The member cross sections are assumed to have a shape factor of 1.0.

(6) Plastic deformations are restricted to concentrated points at the member ends.

(7) The member yield criterion is defined by a two-dimensional yield surface depending only on bending moment and axial force. The yield surface consists of straight line segments; it is convex and encloses the origin.

(8) Plastic flow of the material is governed by the normality criterion.

(9) Both elastic and plastic deformations are assumed to be small for each incremental step.

(10) Local failure by web or flange buckling or brittle fracture is ignored.

4.1.3. Yield Surface Representation

In the analysis of frame structures it is convenient to express the yield condition as an equation which defines the combination of force components necessary to initiate inelastic deformation at a member cross section. If the shape factor is assumed to be equal to

1.0 and the material is assumed to be elastic-perfectly plastic, the yield condition represents the relationship among the force components at the onset of unrestricted plastic flow at that cross section. The yield condition is often described by the function ϕ as

$$\phi = \phi(\{S\}) = 1.0 \tag{4.1}$$

in which $\{S\}$ represents the vector of force components. The yield condition for a planar frame member is often described by an interaction between the member axial force, P, and bending moment, M; the shear force is neglected. A two-dimensional yield surface for a representative wide flange section bent about its strong axis is shown in Figure 4.1. The yield surface is generally continuous except where it intersects the positive and negative P axis [53], and it is always convex [54].

The derivation of yield surface equations for a cross section subjected to a combination of several force components is generally quite difficult. Morris and Fenves [53] describe a procedure for deriving approximate lower bound yield surface equations using a method suggested by Hodge [47]. For the current analysis, a linearized approximation to the yield surface is used. The member yield criterion is described by a two dimensional surface representing the interaction between the member axial force and bending moment. Figure 4.2 shows a two dimensional yield surface which is approximated by a series of straight line segments. Each segment is defined by the linear yield condition ϕ_i in which i refers to the particular segment. The yield surface may represent either a "best fit" or lower bound approximation. To describe the yield surface the analyst must specify the coordinates

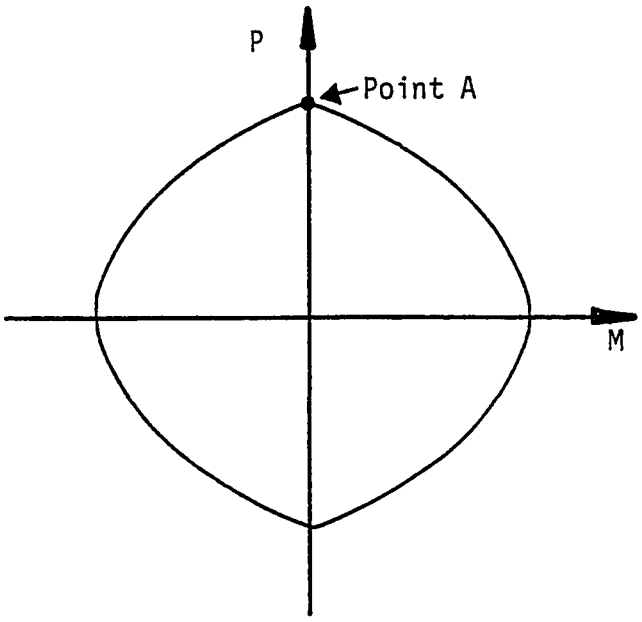

Figure 4.1 Interaction Curve for Wide Flange Section

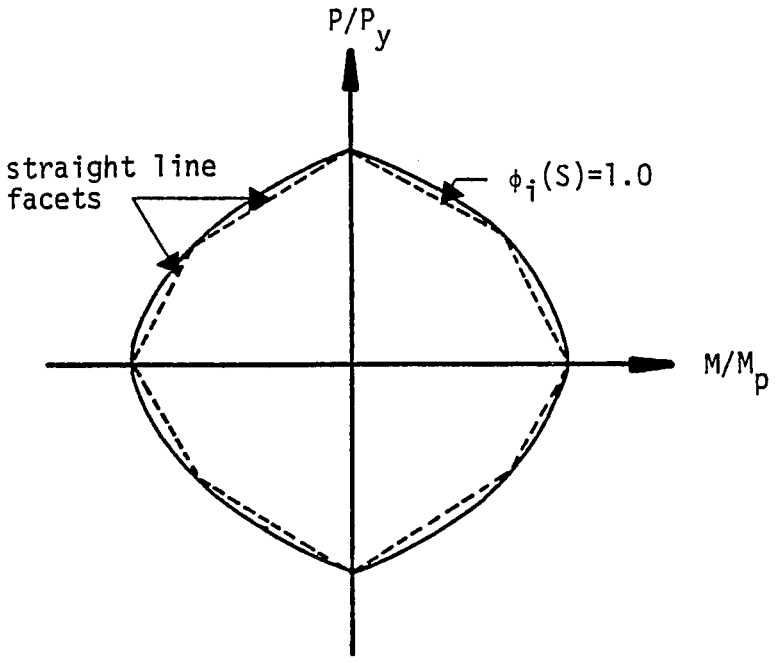

Figure 4.2 Straight Line Approximation to Yield Surface

of the vertices of the linear approximation.

As an example, the AISC interaction formulae for members subject to combined axial load and bending moment may be used to construct an approximate yield surface. Equation 2.4-3 of the AISC Code [55] states

$$\frac{P}{P_y} + \frac{M}{1.18M_p} \leq 1.0 \tag{4.2a}$$

$$M \leq M_p \tag{4.2b}$$

in which P represents the member axial force (compression), M the applied moment, and P_y and M_p are the axial yield load and plastic moment capacity, respectively. Figure 4.3 shows one quadrant of the interaction diagram resulting from the AISC formulae. The dashed line is representative of an actual interaction relation for a wide flange section bent about its strong axis while the solid line corresponds to the approximate AISC formulae. The six-faceted member yield surface which is constructed for a symmetrical section is shown in Figure 4.4. The linear functions ϕ_i, $(i = 1,2,\ldots,6)$ are formed from Equations 4.2a and 4.2b. The axial force for end 1 of the member is F_{x1} (compression is positive) and the bending moment is M_{z1}. The first two constraints are, then

$$\phi_1 = \left(\frac{1.0}{M_p}\right) M_{z1} = 1.0 \tag{4.3a}$$

$$\phi_2 = \left(\frac{-1.0}{P_y}\right) F_{x1} + \left(\frac{-0.85}{M_p}\right) M_{z1} = 1.0 \tag{4.3b}$$

For a symmetrical section, the remaining four constraints are constructed in an analogous manner.

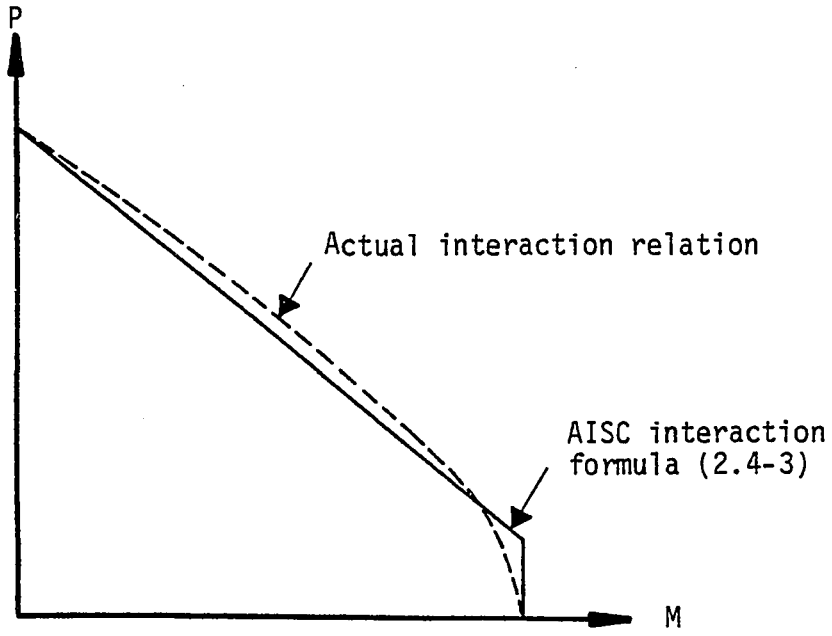

Figure 4.3 AISC Interaction Curve

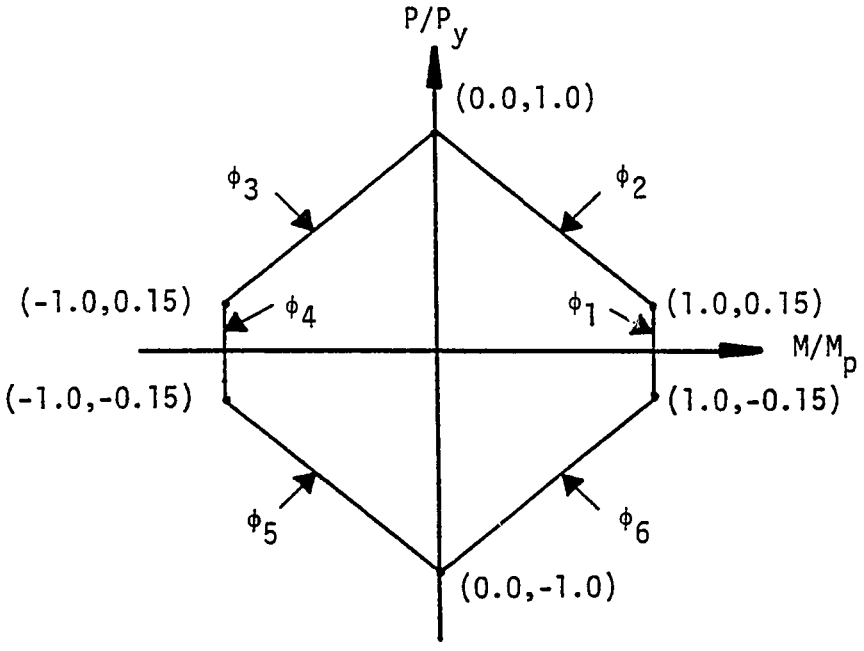

Figure 4.4 Six-Faceted Yield Surface

Porter and Powell [33] have proposed another method for computing the yield surface for wide flange sections. The cross section and recommended yield surface are shown in Figure 4.5. The coordinates of the vertices of the faceted surface are given by the following formulae:

$$F_1 = \sigma_y A \tag{4.4a}$$

$$M_1 = \sigma_y Z_x \tag{4.4b}$$

$$F_2 = \frac{.75(1-2t_f/h)C}{1+(1-2t_f/h)C} \times F_1 \tag{4.4c}$$

$$M_2 = 1 - \frac{.563(1-2t_f/h)^2 C}{2(1-t_w/b)(1-t_f/h)C} \times M_1 \tag{4.4d}$$

in which b, h, t_f, and t_w are as shown in Figure 4.5, $C = ht_w/2bt_f$, σ_y is the yield stress, A is the cross sectional area, and Z_x is the plastic section modulus. The surfaces resulting from these equations are reported to be satisfactory approximations to the true yield surfaces.

4.1.4. Element Stiffness Formulation

In this section the elasto-plastic stiffness matrix which represents the tangent stiffness of a yielding member is presented. The element was formulated by Porter and Powell [33] and the reader is referred to their work for a complete derivation. The effects of geometric nonlinearities are temporarily ignored and will be considered subsequently. The stiffness matrix is formed in local (deformed) coordinates. It is later transformed to the global coordinate system (refer to Section 3.3). A beam element in local coordinates is shown in Figure 4.6. The six degrees of freedom for the member are

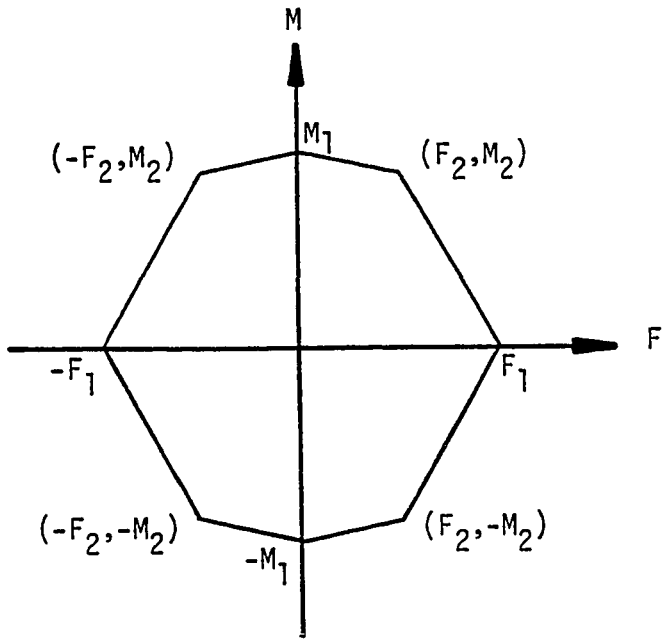

$$C = \frac{h\ t_w}{2bt_f}$$

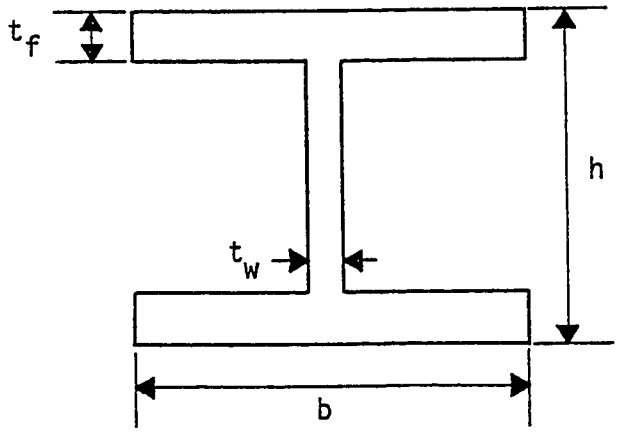

Figure 4.5 Recommended Yield Surface for Wide Flange Sections

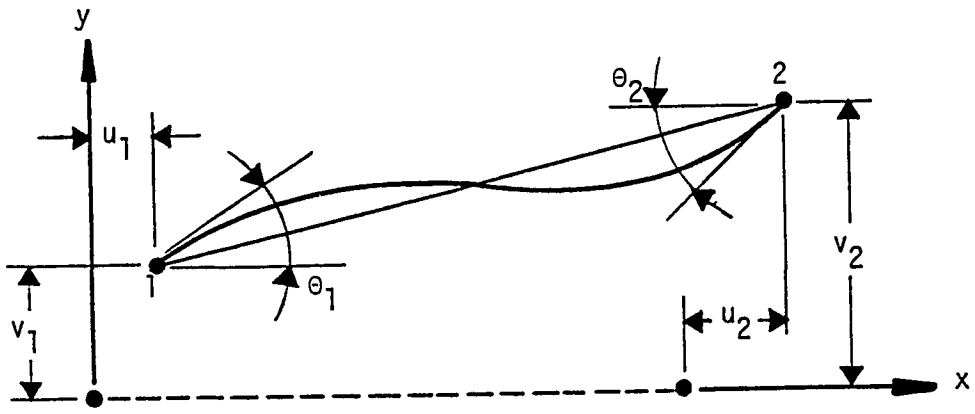

Figure 4.6 Beam-Column Element Degrees of Freedom

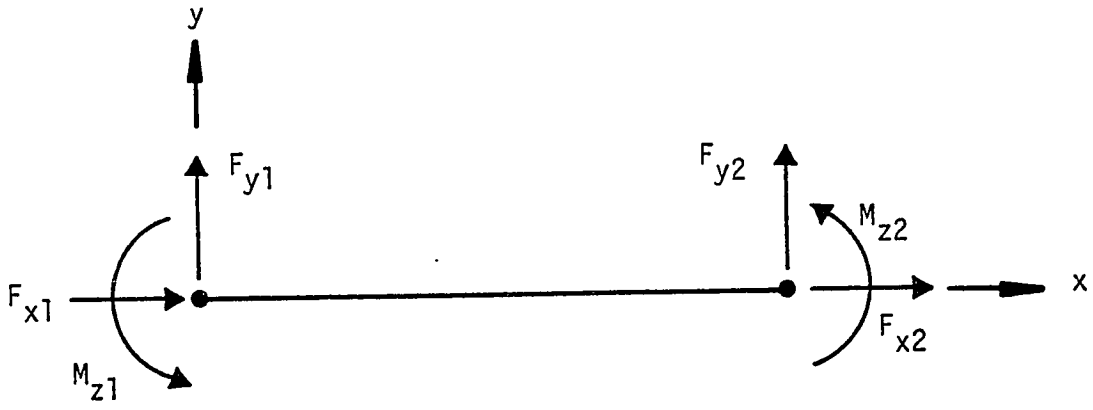

Figure 4.7 Beam-Column Element Force Components

$$\{u\}^T = \lfloor u_1 \; v_1 \; \theta_1 \; u_2 \; v_2 \; \theta_2 \rfloor \tag{4.5}$$

and are shown in Figure 4.6 for a deflected member. The corresponding force components are shown in Figure 4.7 and are

$$\{S\}^T = \lfloor F_{x1} \; F_{y1} \; M_{z1} \; F_{x2} \; F_{y2} \; M_{z2} \rfloor \tag{4.6}$$

Increments of displacement and force are $\{\Delta u\}$ and $\{\Delta S\}$, respectively. The joint displacements are composed of elastic and plastic components. That is,

$$\{u\} = \{u_e\} + \{u_p\} \tag{4.7}$$

in which $\{u_e\}$ is the vector of elastic displacement components and $\{u_p\}$ is the vector of plastic displacement components. The plastic deformations are computed in a straightforward manner as will be described later. Plastic hinges are located only at the member ends and all plastic deformations are concentrated at these hinges. The portion of the member between the hinges remains elastic.

For the current development, the plastic flow rule follows that defined by Drucker's normality criterion [54] and, as such, the plastic deformation increments are assumed to be normal to the yield surface. The outwardly directed normal to facet i of the yield surface is computed by taking the partial derivative of ϕ_i with respect to each of the member end forces, or

$$\{\phi_{i,S}\} = \left\{\frac{\partial \phi_i}{\partial S}\right\} \tag{4.8}$$

in which ϕ_i is the linear expression for facet i, and $,S$ represents differentiaion with respect to S. For example, the vectors

defined by Equation 4.8 for the AISC interaction relation are computed from Equations 4.3a and 4.3b which yield

$$\{\phi_{1,S}\} = \begin{Bmatrix} 0 \\ 0 \\ \frac{1}{M_p} \\ 0 \\ 0 \\ 0 \end{Bmatrix}, \qquad \{\phi_{2,S}\} = \begin{Bmatrix} \frac{-1}{P_y} \\ 0 \\ \frac{-.85}{M_p} \\ 0 \\ 0 \\ 0 \end{Bmatrix} \tag{4.9a,b}$$

The vector $\{\phi_{i,S}\}$, which represents the components of the outward normal, is used in constructing the stiffness of a yielding member.

The tangent stiffness matrix developed by Porter and Powell for an elasto-plastic member excluding geometric nonlinear effects is given by

$$[\hat{k}_t] = [k_e] - [k_e][\phi_{,S}] \left[[\phi_{,S}]^T[k_e][\phi_{,S}]\right]^{-1} [\phi_{,s}]^T[k_e] \tag{4.10}$$

in which $[\hat{k}_t]$ is the tangent stiffness of the elasto-plastic but geometrically linear member, $[k_e]$ is the linear elastic stiffness matrix for a planar frame member, and $[\phi_{,S}]$ is a matrix having a column for each of the segments on which a force point lies, where each column is $\{\phi_{,S}\}$ given by Equation 4.8. Note that the order in which the columns in matrix $[\phi_{,S}]$ are arranged makes no difference. The second term on the right hand side of Equation 4.10 may be interpreted as the required correction to the elastic stiffness which constrains the force increments to be tangent to the yield surface. When this stiffness is used, force points which lie on the yield surface are

automatically constrained to remain on the yield surface. If there is no yielding, the matrix $[\phi_{,S}]$ has zero columns, and $[\hat{k}_t]$ is simply $[k_e]$.

As noted earlier, the plastic deformation components may be computed at each incremental step. The increments of plastic deformation are

$$\{\Delta u_p\} = [\phi_{,S}]\{\hat{\lambda}\} \tag{4.11}$$

The vector $\{\hat{\lambda}\}$, which contains the plastic deformation magnitudes for all member ends whose force points lie on the yield surface, is computed as follows:

$$\{\hat{\lambda}\} = \left[[\phi_{,S}][k_e][\phi_{,S}]\right]^{-1}[\phi_{,S}]^T[k_e]\{\Delta u\} \tag{4.12}$$

The matrix which multiplies the incremental displacement vector in the above expression is the plastic deformation transformation matrix. This matrix is formed at the same time that the element stiffness matrix is formed.

Geometric nonlinear effects are accounted for by adding the initial stress matrix to the elastic stiffness matrix as described in Chapter 3. The resulting tangent stiffness matrix is

$$[k_t] = [k_e] + [k_g] \tag{4.13}$$

in which $[k_e]$ is the elastic stiffness matrix based on the member geometry at the beginning of the load step and $[k_g]$ is the geometric stiffness which depends on both the member axial load and the geometry at the start of the incremental step. The explicit form of both

$[k_e]$ and $[k_g]$ is given in Appendix A. When geometric nonlinearities are included in the analysis, the elastic stiffness matrix in Equations 4.10 and 4.12 is replaced by the tangent stiffness matrix $[k_t]$ from Equation 4.13. Thus, in the case of combined geometric and material nonlinearity, the tangent stiffness matrix for an elasto-plastic member and the plastic deformation vector are, respectively

$$[\bar{k}_t] = [k_t] - [k_t][\phi_{,S}]\left[[\phi_{,S}]^T[k_t][\phi_{,S}]\right]^{-1}[\phi_{,s}]^T[k_t] \tag{4.14}$$

and

$$\{\bar{\lambda}\} = \left[[\phi_{,S}]^T[k_t][\phi_{,S}]\right]^{-1}[\phi_{,S}][k_t]\{\Delta u\} \tag{4.15}$$

4.1.5. Loading Between Member Ends

For the element described here, no consideration has been given to loading between nodal points. In general, a beam element is subjected to both concentrated and distributed loads. The formulation presented herein can be extended to include intermediate loads by dividing the beam into a series of segments. The distributed load is then replaced by equivalent concentrated loads applied to the intermediate nodes. This procedure is used in several of the examples given in Chapter 6.

4.1.6. Strain Hardening

The effects of strain hardening may be accounted for in an approximate way by assuming a dual component, parallel element model (Figure 4.8). One component behaves elasto-plastically while the other remains elastic. This technique was introduced by Clough, Benuska,

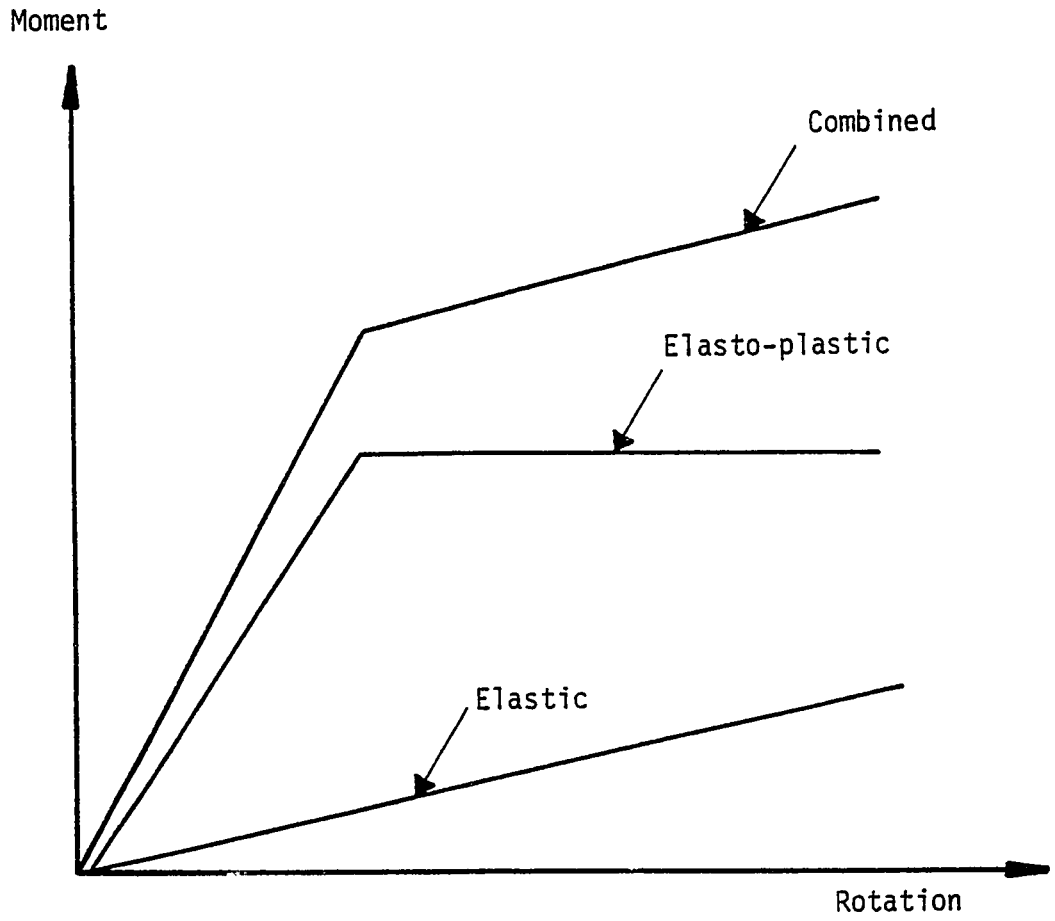

Figure 4.8 Dual Component Model for Strain-Hardening

and Wilson [43] and has been used successfully by Anderson abd Bertero [56], Porter and Powell [33], and El-Hafez and Powell [57]. Mahin and Bertero [58] note that, for the cases studied, analytical results are similar for dual component models and for single component models with bilinear moment-rotation relations, even though the models are not theoretically equivalent unless the rate of strain hardening is zero.

In the current analysis the value of the strain hardening modulus, E_{sh}, as well as the elastic modulus, E, must be specified. The yield criteria are scaled by the ratio of $(E-E_{sh})/E$. If a value of zero is specified for the strain hardening modulus the default value of $1 \times 10^{-8} E$ is used in the program. A non-zero strain hardening stiffness prevents the possibility of a joint instability. Such a condition would ordinarily arise when all members framing into a joint form plastic hinges at that joint.

4.1.7. Axial Plastic Load Limit

Under extreme loads resulting from partial collapse, frame elements may reach their full axial plastic load as described by point A in Figure 4.1. Since the same yield criterion is used for both ends of an element in the current analysis program, two generalized hinges will form. Unlike the case where the moment is non-zero, the case of yielding under pure axial load presents a computation difficulty. Consider a member which is part of a larger structure and which has just reached its tensile yield load (see Figure 4.9). If the load is monotonically increased, plastic deformations will occur during the next load increment. These plastic deformations may occur at either

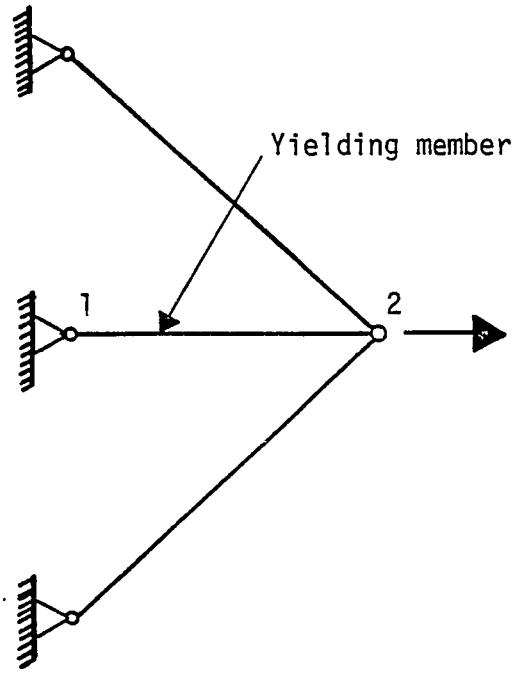

Figure 4.9 Member at Axial Plastic Load Limit

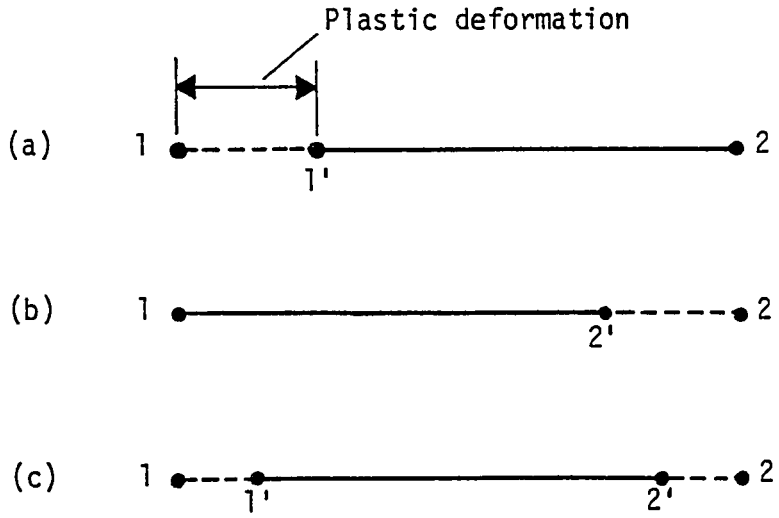

Figure 4.10 Alternative Plastic Deformation States

end of the member while the portion between the yielding sections remains elastic. Three alternatives are shown in Figure 4.10; (a) all plastic deformations occur at end 1, (b) all plastic deformations occur at end 2, and (c) some plastic deformations occur at each end with the total deformation being equal to that in cases (a) and (b). Thus, an indeterminate condition exists since there is an infinite number of plastic deformation states which will satisfy the nodal displacements. With the exception of Harung and Millar [59], previous researchers have failed to account for this particular condition. In Harung and Millar's analysis an element which has reached its axial yield load is removed from the structure. However, no mention is made of the possibility of unloading and the resulting return to elastic behavior.

To accommodate this axial yield condition, a modification in the procedure presented by Porter and Powell is required. When a member has reached its axial plastic load limit, two generalized hinges form and the matrix

$$[\phi k \phi] = [\phi_{,S}]^T [k_t][\phi_{,S}] \tag{4.16}$$

becomes singular. When this singularity is detected in the current program, one of the hinges is eliminated. All plastic deformations are thus forced to occur at one end of the yielding member. This feature is illustrated in the overloaded beam problem presented in Chapter 6.

4.1.8. Stability of Beam-Columns

The development presented above permits plastification only at the ends of the beam-column element. For certain structures where inelastic

stability is important, the formation of plastic hinges at any point along a beam-column must be considered. It is necessary, in this case, to divide these members into a series of smaller segments as was done for the case of intermediate loads. An example using this procedure for the analysis of a member subjected to cyclic axial loading is given in Reference [60].

4.2 Shear Infill Panel

The effect of shear infill panels on the lateral stiffness of frame building structures has long been recognized. For normal working loads the infill panels are typically under very low stress. In the event of abnormal loading and subsequent localized failure, however, the infill panels may significantly affect the response of the building and may, in fact, contribute substantial strength. For this reason it is very important that they be considered in analysis for damage and collapse.

4.2.1. Background

Infills are often of concrete or masonry construction. It is assumed here that masonry may be described using the same physical model as that used for plain concrete. The analytical procedures which attempt to determine the stress and deformation states in such members are, indeed, very complex. Several factors which contribute to the complexity are: (1) the nonlinear load-deformation response, (2) the effect of progressive cracking of concrete, (3) the difficulty in formulating failure criteria for the various stress states, and (4)

the effect of reinforcement. The element considered here and implemented in the analysis program is limited to the case of unreinforced concrete.

Recently, a considerable amount of research has been conducted in the application of the finite element method to the study of plain and reinforced concrete structures (see References [61-71]). Great advances have been made and, while no single approach has obtained universal approval, very promising results have been obtained by a number of researchers. The following sections are devoted to a discussion of several aspects of the analysis of shear walls by the finite element method and the selection of a scheme for inclusion in the progressive collapse analysis program.

4.2.2. Assumptions and Limitations

Formulation of the shear infill element described here is based on the following assumptions and limitations:

(1) The elements are represented by four noded quadrilaterals.

(2) The elements are planar with only in-plane loads.

(3) Loads may be applied only at the joints.

(4) The material is assumed to have shear stiffness only.

(5) Shear cracking is defined by a one-dimensional failure criterion represented by the shear cracking stress.

(6) Post-cracking shear stiffness may be specified.

(7) The shear stress is computed at the element centroid.

(8) Geometric nonlinear effects are ignored.

4.2.3. Behavior of Concrete

As seen in Figure 4.11 the uniaxial stress-strain relation for concrete is nonlinear. For the purpose of analysis, concrete is often assumed to be elastic-plastic in compression and elastic-brittle in tension. This assumed relationship is also shown in Figure 4.11. In the presence of biaxial stress the behavior of concrete is somewhat more complex. In such a case, it is well known that the effective stiffness of concrete is increased due to the presence of normal compressive stresses. The primary cause of this stiffening effect is the confinement of microcracking. Liu, Nilson, and Slate [82] have proposed a stress-strain relation for the biaxial stress condition which accounts for microcrack confinement as well as the Poisson effect. In addition, they have stated the biaxial relations in the form of matrix constitutive relationships which are well-suited to plane stress finite element analysis.

The failure envelope for plain concrete in a biaxial stress state is shown in Figure 4.12. This curve was proposed by Kupfer, Hilsdorf, and Rusch [73] based on a number of tests. The effect of a normal compressive stress on the ultimate compressive strength of concrete is readily apparent. An increase of twenty to thirty percent of the uniaxial compressive strength may be realized depending on the ratio of principal stresses.

In the current investigation it is assumed that a piecewise linear failure criterion can be used to represent the actual biaxial failure condition adequately. Each segment of the linearized failure envelope is represented by an expression of the form

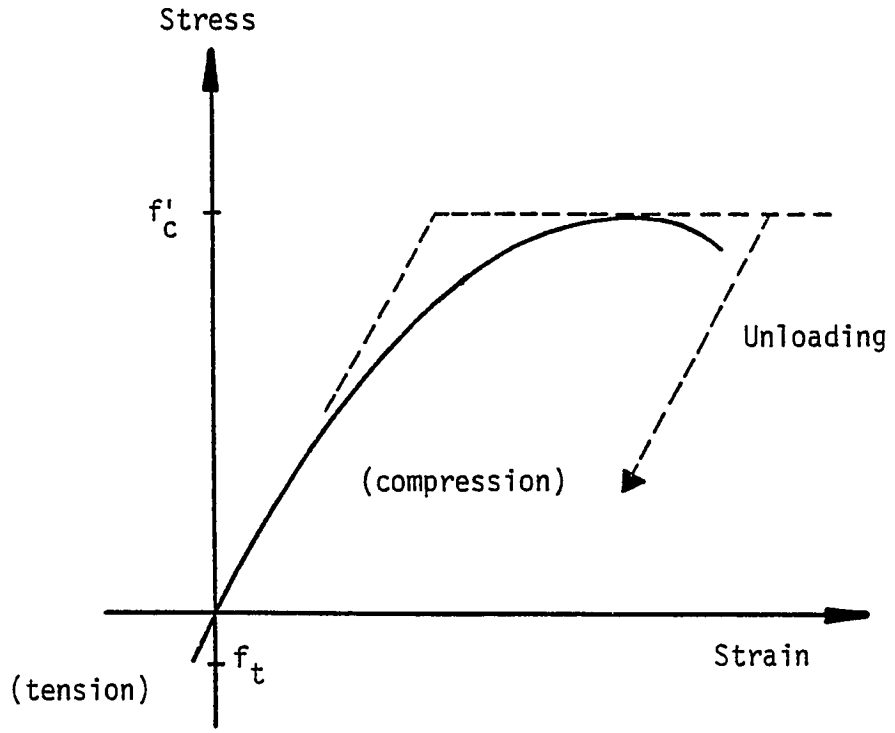

Figure 4.11 Uniaxial Stress-Strain Relation for Concrete

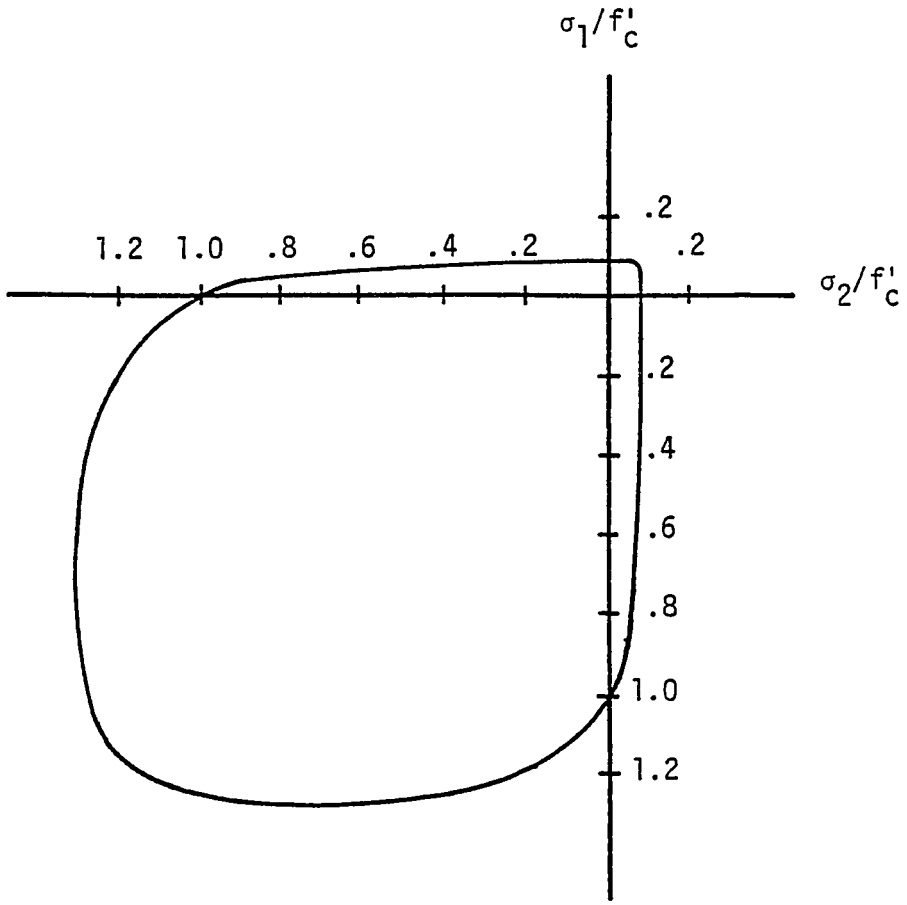

Figure 4.12 Failure Envelope for Plain Concrete in Biaxial Stress State

$$\phi_i = \phi_i(\{\sigma\}) = 1.0 \tag{4.17}$$

in which $\{\sigma\}$ is the vector of principal stresses. The function ϕ_i has a value of 1.0 on the failure surface and is less than 1.0 within it. The failure surface must be convex and enclose the origin.

Based on experimental results, Liu, et al. have proposed the empirical failure envelope for concrete under biaxial compression shown in Figure 4.13. It is often assumed that in biaxial tension the failure criterion is a constant equal to the uniaxial concrete tensile strength. In the tension-compression zone the straight line shown in Figure 4.13 is consistent with test results. A biaxial failure criterion such as this is readily accommodated by the analysis method used in this study.

The nonlinear response of concrete is caused by two major effects, cracking of the concrete in tension and yielding in compression. In the following sections only these two effects are considered. Several other nonlinear effects are assumed to be of lesser importance and are not included. Among these are various time-dependent effects such as creep, temperature, and shrinkage.

Two basic schemes have been reported in the literature for representing the cracking behavior of concrete. Ngo and Scordelis [68] used an approach whereby cracking is accounted for by the separation of nodes. This same procedure was also employed by Nilson [69] in a paper which extended the work by Ngo and Scordelis. This procedure has two major drawbacks. First, as cracking progresses the topology of the problem is continually being altered, thus making an automated

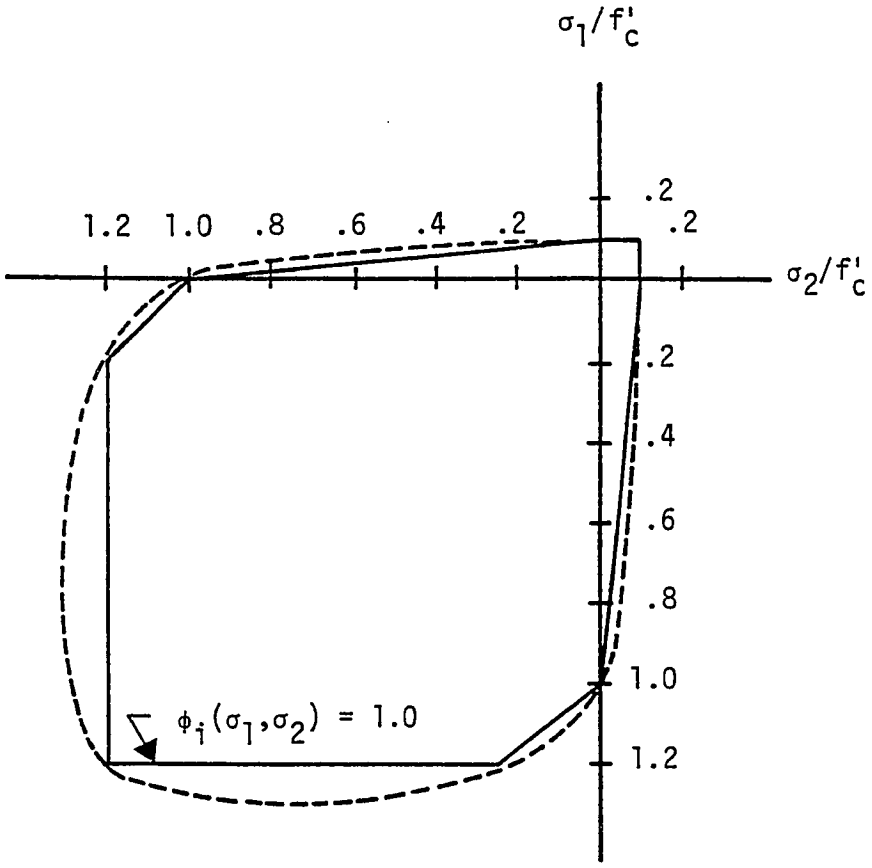

Figure 4.13 Idealized Failure Envelope for Plain Concrete

approach difficult. Second, the crack pattern is prejudiced in that cracks may form only along element boundaries. This second problem may be alleviated when the general pattern of cracking is known beforehand or when a very fine element mesh is used in critical cracking zones. A second approach is that adopted by Franklin [63] and several others whereby the cracking is taken into account by modifying the material constitutive matrix involved in formulating the element stiffness matrix. In this approach the cracking is distributed over an entire element or, if a numerical integration approach is used in the element formulation, over a portion of the element. While both procedures appear to produce satisfactory results, the distributed cracking method is computationally more attractive. This procedure is used in the current investigation and is explained in more detail below.

Concrete is assumed to yield in biaxial compression consistent with the failure criteria defined above. When yielding does occur, the concrete is assumed to behave in a purely plastic fashion. Krishnamoorthy and Panneerselvam [65] note that the assumption of unconstrained plastic flow is reasonable for the analysis of reinforced concrete framed structures since the nonlinear effects due to the cracking of concrete and yielding of the reinforcing steel dominate the behavior.

4.2.4. Material Constitutive Relations

The behavior of concrete may be characterized by three different modes; elastic, cracked, or plastic. In an incremental solution procedure the material stiffness matrix reflects the current element

behavior and, in a sense, represents the secant modulus for the incremental step. The material constitutive relations are described below for elastic, cracked, and plastic behavior of plain concrete.

Concrete is assumed to behave as an isotropic material prior to cracking or yielding. The material constitutive relationships take the form (see Reference [16])

$$[E] = \frac{E_c}{1-\nu^2} \begin{bmatrix} 1 & \nu & 0 \\ \nu & 1 & 0 \\ 0 & 0 & \frac{1-\nu}{2} \end{bmatrix} \tag{4.18}$$

in which E_c is the modulus of elasticity of the concrete and ν is Poisson's ratio. For the isotropic case the shear modulus, G, may be written in terms of the elastic modulus of the concrete $G = E_c/2(1+\nu)$ as above.

When one of the principal stresses becomes equal to the tensile strength of the concrete, cracking will occur in a direction normal to the direction of maximum tensile stress. An element with a crack oriented at an angle of α measured from the x-direction is shown in Figure 4.14. It is assumed that no stress can be carried in a direction normal to the crack. Thus, a state of orthotropy exists where the stiffness in the direction normal to the crack is zero. For a local axis shown in Figure 4.14, the values of E_1 and ν_1 in the general orthotropic constitutive relationship are set to zero.

For this case of extreme anisotropy, the value of the shear modulus is difficult to evaluate. Franklin [63] approached this problem by computing an expression for the shearing modulus in the cracked element

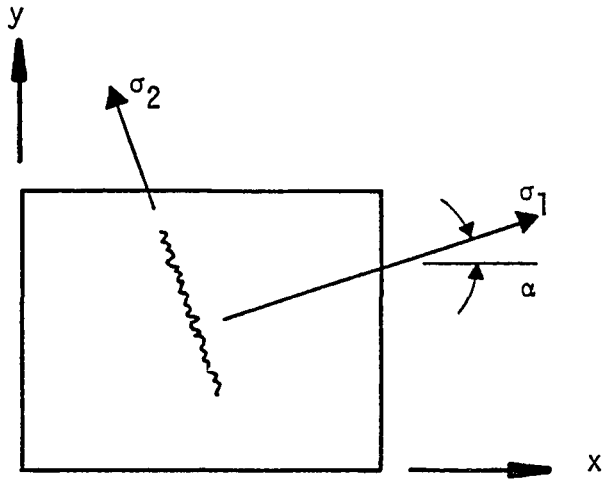

Figure 4.14 Element with Tensile Cracking in One Direction

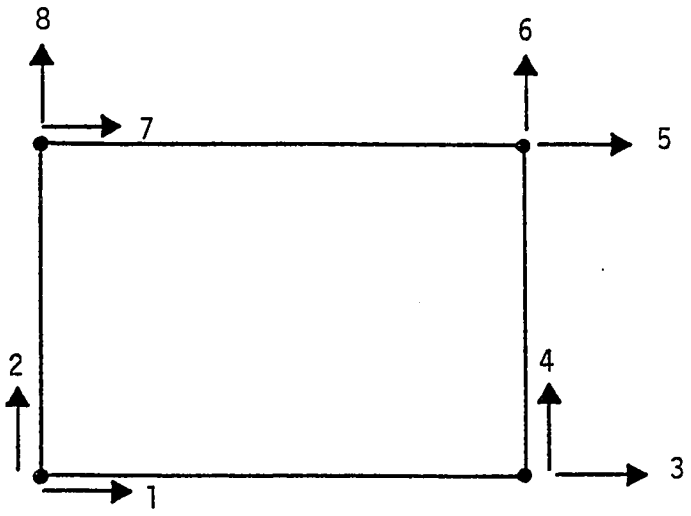

Figure 4.15 Shear Infill Element Description

for an apparent state of isotropy obtained by a local axis rotation through 45°. He thus obtained

$$G = \frac{E_1(1-\nu_2) + E_2(1-\nu_1)}{4(1-\nu_1\nu_2)} \tag{4.19}$$

which reduces to the usual expression for the isotropic shear modulus when E_1 is equal to E_2 and ν_1 is equal to ν_2. For cracking in one direction E_1 and ν_1 are taken to be zero and an estimate for the cracked element shear modulus is given by

$$G_{cr} = \frac{E_c}{4} \tag{4.20}$$

For a value of $\nu = 0.20$ the cracked shear modulus may be expressed in terms of the isotropic shear modulus as

$$G_{cr} = 0.60\,G \tag{4.21}$$

While tests show that this value is fairly accurate, its derivation neglects several contributions to the shear stiffness of a cracked element such as aggregate interlock. Thus it appears advantageous to use the more general expression

$$G_{cr} = \beta G \tag{4.22}$$

in which β is the shear transfer factor and G is the isotropic shear modulus. Suidan and Schnobrich [71] note that the retention of some shear stiffness is necessary but that results are not particularly sensitive to the proportion, β. In their analysis, Suidan and Schnobrich use a value of $\beta = 0.5$.

The general constitutive relationship for an element which has cracked due to an excessive tensile stress in the principal stress direction 1 is

$$[E'_{cr}] = \begin{bmatrix} 0 & 0 & 0 \\ 0 & \frac{E_c}{1-\nu^2} & 0 \\ 0 & 0 & \beta G \end{bmatrix} \tag{4.23}$$

in which the prime (') denotes reference to the principal stress coordinate axes. If both principal stresses exceed the tensile strength the concrete will crack in both principal stress directions. The matrix $[E'_{cr}]$ is then

$$[E'_{cr}] = \begin{bmatrix} 0 & 0 & 0 \\ 0 & 0 & 0 \\ 0 & 0 & \beta G \end{bmatrix} . \tag{4.24}$$

As noted earlier, the concrete in biaxial compression is assumed to behave in an elastic-perfectly plastic fashion. The constitutive matrix which governs the material behavior on the yield surface is the elasto-plastic matrix $[E_{ep}]$. For a piecewise linear representation of the failure envelope as shown in Figure 4.13, the expression for segment i is given by Equation 4.17. Alternatively, this expression can be written in matrix form as

$$\phi_i = [\phi_{i,\sigma}]\{\sigma\} = 1.0 \tag{4.25}$$

in which $,\sigma$ denotes differentiation with respect to each of the principal stresses. Let $[\phi_{,\sigma}]$ be a matrix having a column for each of the linear segments comprising the failure envelope on which a stress point lies; that is, each column is $\{\phi_{i,\sigma}\}$. Then the elasto-plastic material constitutive matrix may be written as follows:

$$[E_{ep}] = [E] - [E][\phi_{,\sigma}]\left[[\phi_{,\sigma}]^T[E][\phi_{,\sigma}]\right]^{-1}[\phi_{,\sigma}]^T[E] \qquad (4.26)$$

in which $[E]$ is the isotropic material stiffness matrix. The development of Equation 4.26 is given in Appendix B.

As was noted earlier, geometric nonlinear effects are neglected for the shear infill panel. This assumption is justified since, in general, deformations of an infilled frame are small.

4.2.5. Element Stiffness Formulation

Finite elements with a variety of assumed displacement functions may be found in the literature for the two dimensional plane stress problem. Several of the elements applied to the analysis of plain or reinforced concrete structures are noted here. A triangular element using a linear displacement representation (CST) was used by both Cervenka [62] and Moss [67]. Kanaan and Powell [64] used an isoparametric four node quadrilateral (Q4) for a shear infill panel. A quadrilateral plane stress element constructed from two linear strain triangles was used by Franklin [63]. In this case a linear displacement variation was imposed on the element sides and the internal degree of freedom was eliminated by static condensation. McLeod [66] has proposed a rectangular element with rotational degrees of freedom at the

four corner nodes for shear wall analysis. The purpose of such an element is to assure compatibility of the plane stress elements with line elements in bending. An incompatible linear strain quadrilateral was reported by Krishnamoorthy and Panneerselvam [65] for problems involving significant bending. The isoparametric four node quadrilateral element has been selected for the current investigation. The element has eight displacement degrees of freedom as shown in Figure 4.15. The development of such an element using a bilinear displacement representation is detailed in Reference [16].

For the current study, a simplified version of the bilinear isoparametric quadrilateral element is used. This version has resistance to shear only. That is, only the shear modulus term in the material constitutive matrix (Equation 4.18) is nonzero. Because the element is in a state of pure shear the principal stress components are always equal in magnitude and opposite in sign. Therefore, failure in all cases is by tension cracking in the tension-compression region of the failure envelope (see Figure 4.16). The shear modulus prior to cracking is given by G and after cracking by βG. Instead of defining a failure envelope, however, only the value of the shear stress at which cracking occurs need be specified. As a reasonable approximation, the uniaxial tensile strength of concrete may be used.

The element stiffness matrix is formed using the following relation:

$$[K] = \int_V [D]^T[E][D]dV \tag{4.27}$$

in which $[K]$ is the global element stiffness matrix, $[D]$ is the strain-displacement matrix, $[E]$ is the material constitutive matrix,

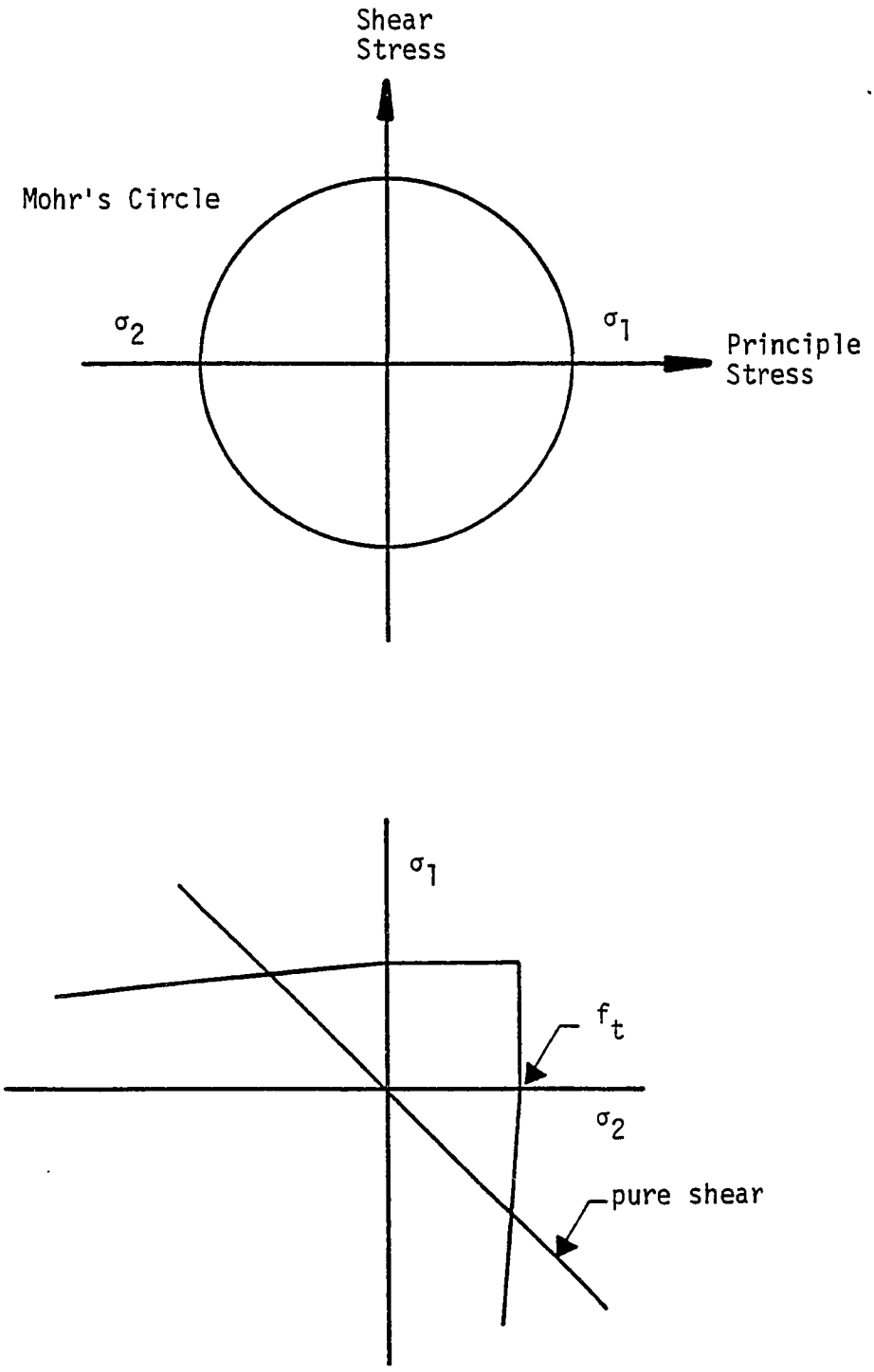

Figure 4.16 Shear Failure in Tension-Compression Region

and V refers to integration over the volume of the element. A detailed discussion of the form of the strain-displacement matrix in isoparametric form is given in Reference [16]. For the present case the material constitutive matrix is simply equal to G or βG depending on whether the element is uncracked or cracked. The integration in Equation 4.27 is performed numerically using a two-by-two Gaussian scheme (see Reference [15]). The strain-displacement matrix is evaluated at the element centroid. It should be noted that for the isoparametric formulation the stiffness matrix is obtained with respect to the global coordinate system.

4.3. Semi-Rigid Connection

When modeling frame structures, it is usually assumed that connections are either perfectly rigid or perfectly pinned. Such is not the case in real building frames. A connection designed for rigid behavior will have some flexibility; similarly, a pinned or simple connection will have a degree of rigidity. The semi-rigid connection element provides a means to represent more accurately the physical behavior of beam-to-column connections encountered in frame construction.

4.3.1. Background

Under extreme loads frame connections tend to behave in a nonlinear and inelastic fashion. Figure 4.17 shows a representative nonlinear moment-rotation relation for a typical frame connection. Since a connection may yield at a load substantially below the limit of adjacent members, the full capacity of the frame members may not

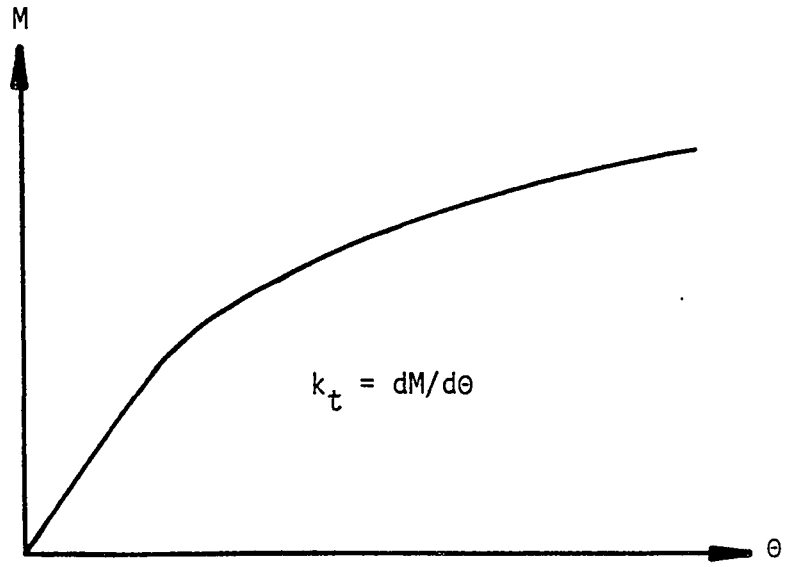

Figure 4.17 Nonlinear Moment-Rotation Relation for Typical Frame Connection

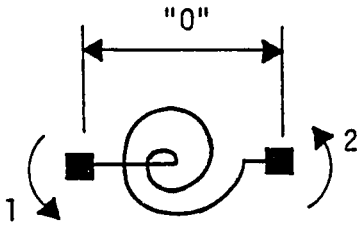

Figure 4.18 Semi-Rigid Connection Element Description

be realized. In general, nonlinear and inelastic behavior of frame connections greatly affects the overall behavior of a structure. It is important that this type of behavior be modeled accurately when evaluating a framed building for its resistance to progressive collapse.

The behavior of most connections in the nonlinear range is complex. Reference [74] contains a detailed discussion of steel frame connection behavior. A representative moment-rotation curve for a particular connection is usually obtained by experimental tests. Popov and Pinkney [75] have conducted tests of numerous connection specimens and have concluded that the Ramberg-Osgood relation (see Reference [76]) provides a satisfactory mathematical model of the moment-rotation curve for the case of monotonic loading. Krishnamurthy and Panneerselvam [77] have developed finite element models for determining the moment-rotation characteristics of bolted steel connections. These moment-rotation relations for a connection are incorporated into the matrix stiffness method of analysis. Several researchers [33, 64, 78] have employed this discrete element approach in the analysis of structures including the effects of semi-rigid connections. A thorough discussion of nonlinear, inelastic building frame connections can be found in Reference [60].

4.3.2. Assumptions and Limitations

Formulation of the semi-rigid connection element is based on the following assumptions and limitations:

(1) The element is defined by two rotational degrees of freedom and has zero length.

(2) Only in-plane loads are permitted.

(3) The moment-rotation relation is assumed to be given by either a linear segmented representation or the Ramberg-Osgood relation.

(4) Elastic unloading is permitted.

(5) Geometric nonlinear effects are ignored.

4.3.3. Element Stiffness Formulation

The semi-rigid connection element was developed and implemented in the current analysis program by Mutryn [60]. The connection element has two rotational degrees of freedom which allow for a relative rotation between connected members. The element has zero length and the translational degrees of freedom at the connection nodes are coupled. Figure 4.18 shows the semi-rigid element and its associated displacement degrees of freedom. Two analytical models are available to represent the moment-rotation characteristics of a connection; a piecewise linear representation and the Ramberg-Osgood relation. They will be discussed in the following two sections.

The stiffness matrix for a connection model is derived as follows. The relative rotation between the connection nodes is related to the rotational degrees of freedom by

$$d\Theta_{rel} = \lfloor 1 \; -1 \rfloor \begin{Bmatrix} d\Theta_1 \\ d\Theta_2 \end{Bmatrix} \tag{4.28}$$

in which $d\Theta_{rel}$ is the increment of relative rotation, and $d\Theta_1$ and $d\Theta_2$ are the increments of rotational displacement at nodes 1 and 2,

respectively. The tangent stiffness, k_t, is the slope of the moment-rotation curve for the connection and is written as

$$k_t = \frac{dM}{d\Theta} \tag{4.29}$$

in which dM is the increment in moment and $d\Theta$ is the increment in relative rotation. The moment at each node of the connection element is equal but opposite in sign. Equations 4.28 and 4.29 are combined to write the element stiffness relation as follows:

$$\begin{Bmatrix} dM_1 \\ dM_2 \end{Bmatrix} = k_t \begin{bmatrix} 1 & -1 \\ -1 & 1 \end{bmatrix} \begin{Bmatrix} d\Theta_1 \\ d\Theta_2 \end{Bmatrix} \tag{4.30}$$

and the global stiffness matrix for the connection element is, simply,

$$[K_t] = k_t \begin{bmatrix} 1 & -1 \\ -1 & 1 \end{bmatrix} \tag{4.31}$$

The determination of the rotational stiffness coefficient, k_t, for both the linear segmented model and Ramberg-Osgood model, is discussed next.

4.3.4. Linear Segmented Representation

The continuous moment-rotation relation can be approximated by a series of straight line segments. In such a representation, the tangent stiffness changes at discrete points. Figure 4.19 shows a typical multi-segmented approximation to a continuous moment-rotation relation. This type of representation fits well into the analysis procedure previously described since the mechanism exists for detecting stiffness changes and modifying the load increment accordingly.

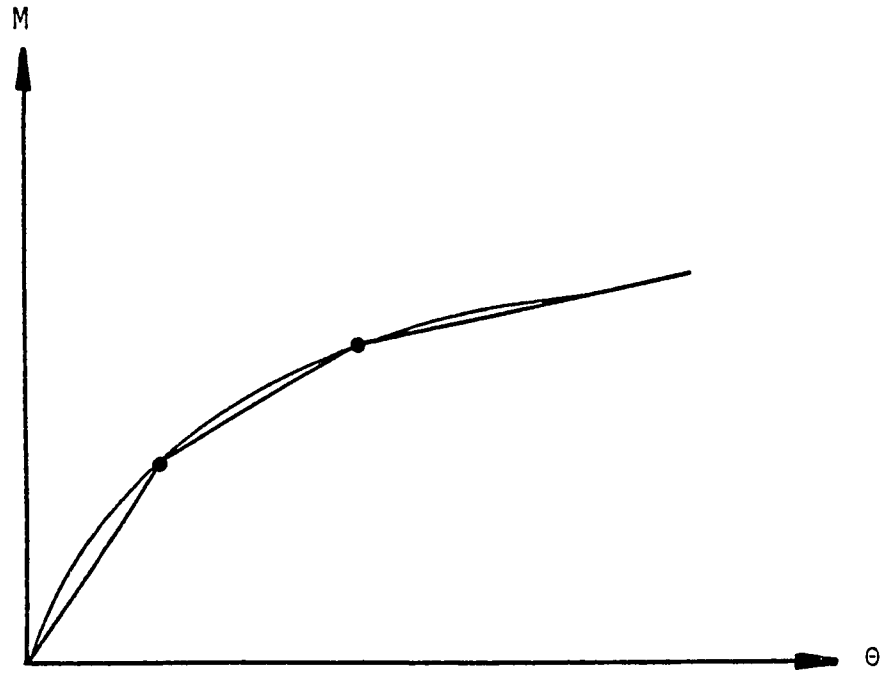

Figure 4.19 Linear Segmented Representation of Moment-Rotation Curve

The three segment model shown in Figure 4.20 is used here to illustrate the response of this representation. Sequential yielding is defined by the intersection of the current loading path and the next parallel dashed line as shown in the figure. Elastic unloading occurs along the path defined by the initial stiffness, In this way the Baushinger effect is accounted for.

A linear elastic connection or elastic rotational spring can be modeled with this procedure by defining a single segment moment-rotation relation. Elastic-perfectly plastic behavior can be represented with a bilinear model where the second segment has a stiffness of zero. Similarly, a perfect hinge can be described by specifying a value of zero for the initial stiffness. In this way a pin-ended beam or column may be modeled.

4.3.5. Ramberg-Osgood Representation

A continuous moment-rotation curve can be described by the Ramberg-Osgood relation [76]. This function is generally written in the following form:

$$\frac{\Theta}{\Theta_y} = \frac{M}{M_y} + k\left(\frac{M}{M_y}\right)^r \qquad (4.32)$$

in which Θ is the rotation, M is the moment, Θ_y and M_y are the yield values of rotation and moment respectively, and k and r are constants. Figure 4.21 shows a typical curve defined by Equation 4.32. A procedure for determining the values of r and k for a given moment-rotation curve is outlined in Reference [76]. Based on an analysis of test results, Popov and Pinkney [75] suggest values of

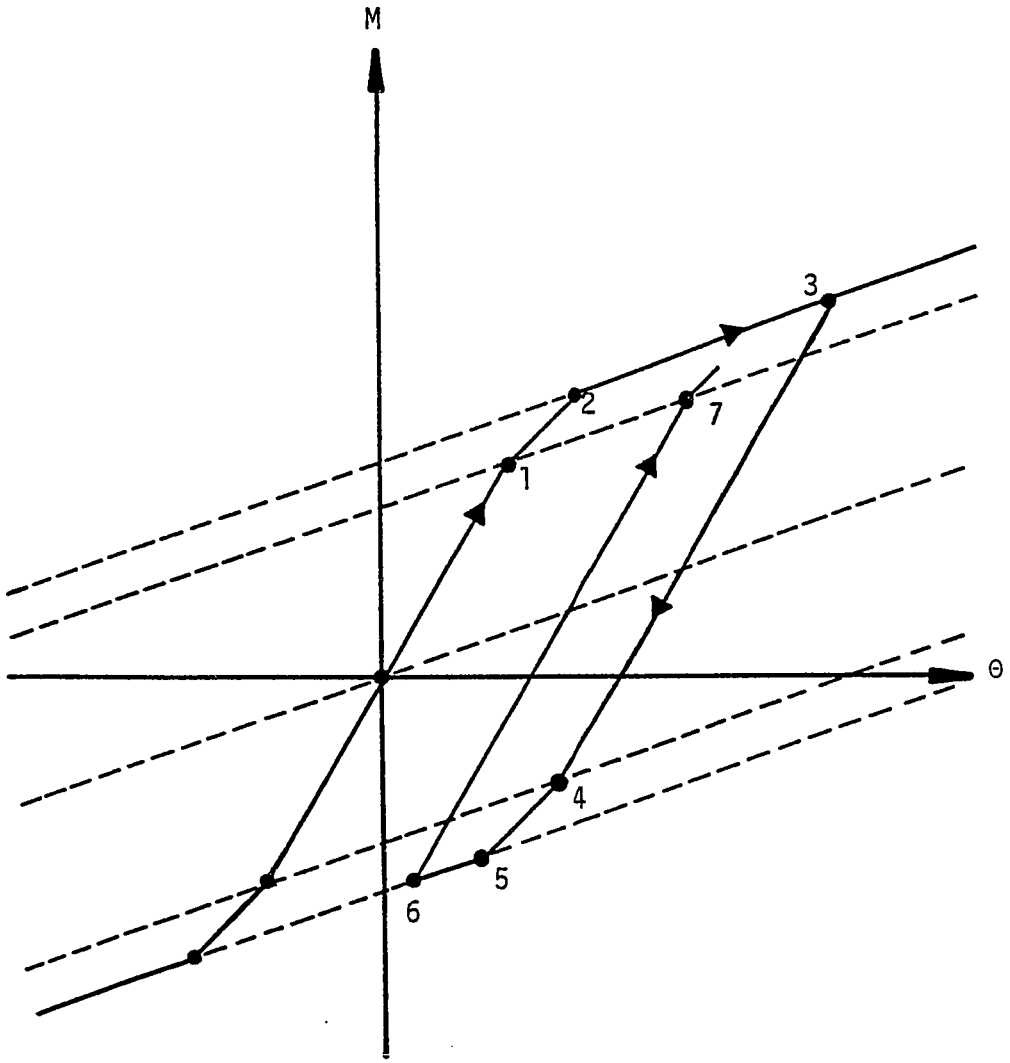

Figure 4.20 Three Segment Moment-Rotation Curve with Bounding Lines

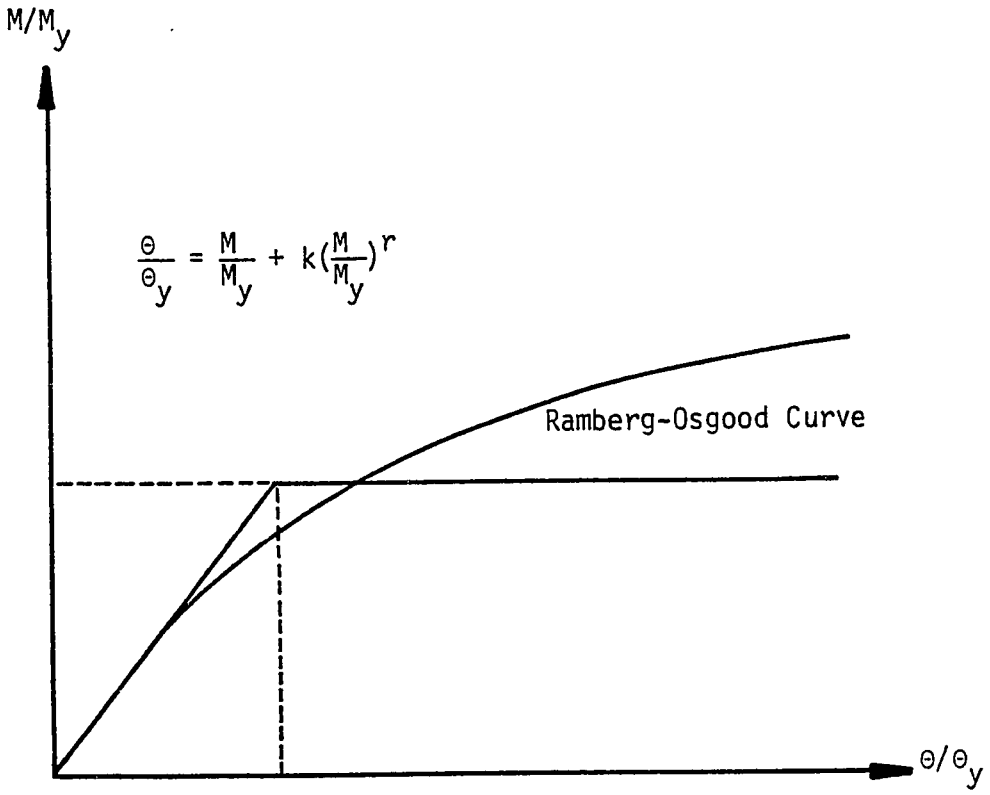

Figure 4.21 Typical Ramberg-Osgood Curve

$k = 0.5$ and $r = 8$ for connections free of slip. To accommodate negative moment and rotation, Equation 4.32 may be written in the following form:

$$\frac{\Theta}{\Theta_y} = \frac{M}{M_y}\left(1 + k\left|\frac{M}{M_y}\right|^{r-1}\right) \tag{4.33}$$

Equation 4.33 may be generalized to account for unloading by the following expression:

$$\frac{\Theta-\Theta_i}{2\Theta_y} = \frac{M-M_i}{2M_y}\left(1 + k\left|\frac{M-M_i}{M_y}\right|^{r-1}\right) \tag{4.34}$$

in which Θ_i and M_i define the point at which the direction of the load was last reversed. Figure 4.22 shows the Ramberg-Osgood curve for loading and unloading as expressed by Equations 4.33 and 4.34.

Since there is no distinct change in stiffness with the Ramberg-Osgood model, the incremental analysis is performed by limiting the allowable load step. For a given relative rotation, the corresponding value of moment is determined from either Equation 4.33 or 4.34 by an iterative process. Once the moment is known, a value of the tangent stiffness may be obtained for the loading curve by differentiating Equation 4.33 with respect to M giving

$$k_t = \frac{M_y}{\Theta_y\left(1 + kr\left|\frac{M}{M_y}\right|^{r-1}\right)} \tag{4.35}$$

A similar expression for k_t is obtained for the unloading curve by differentiating Equation 4.34

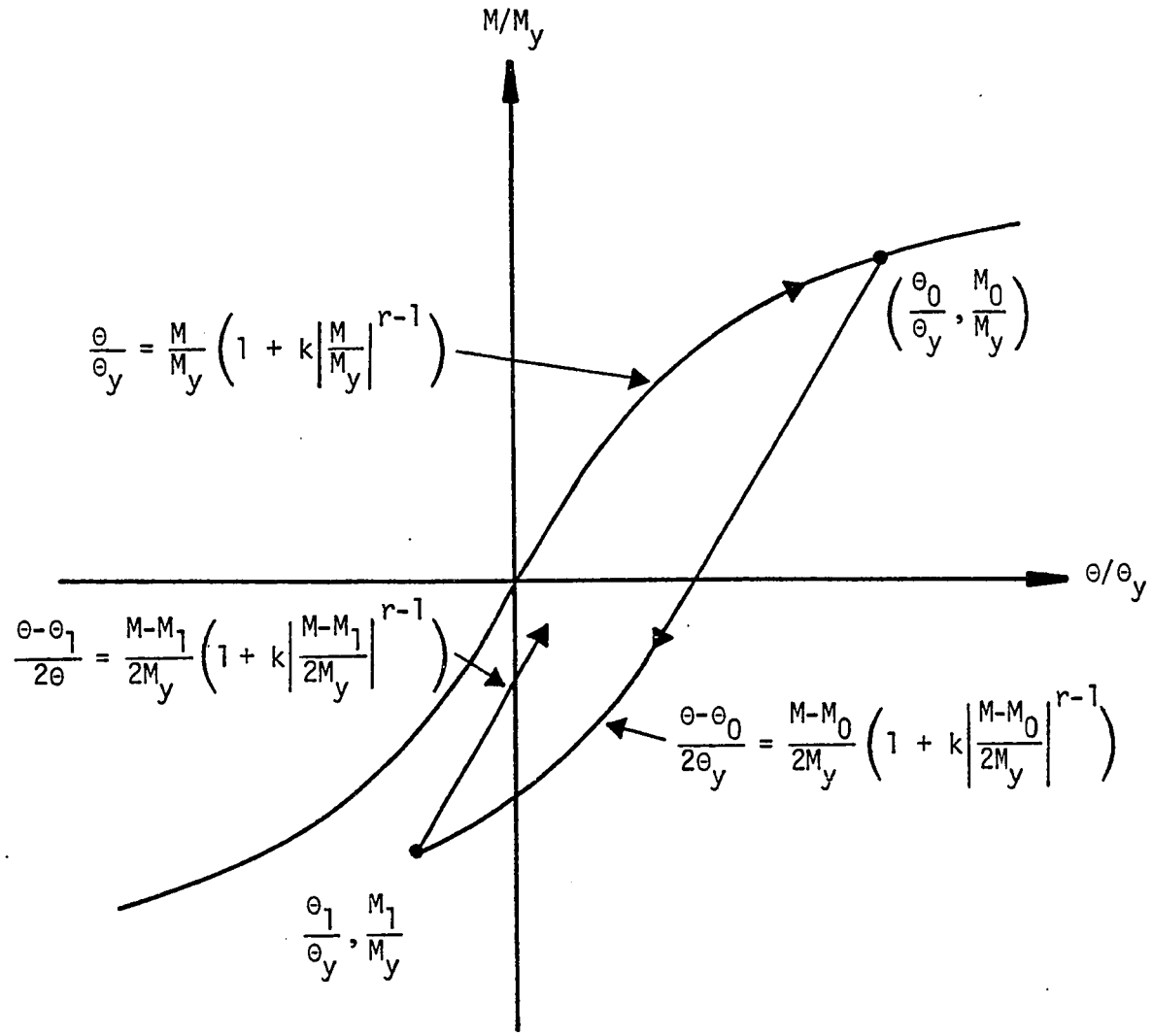

Figure 4.22 Ramberg-Osgood Curve for Loading and Unloading

$$k_t = \frac{M_y}{\theta_y\left(1 + k_r\left|\frac{M-M_i}{2M_y}\right|^{r-1}\right)} \tag{4.36}$$

For the predictor-corrector method, Mutryn averages the values of the tangent stiffness obtained at the beginning and end of a step. This procedure is computationally efficient and has been found to give good results.

5. PROGRESSIVE COLLAPSE ANALYSIS SYSTEM

The computer system described in this chapter is specifically designed for the analysis of building structures subjected to abnormal loads. It can be employed in any of several ways to implement the various progressive collapse design strategies described in Chapter 2. The distinguishing feature of the present capability is that it permits selective removal of one or more load carrying members during the course of analysis. This feature is discussed in Section 5.2.3.

A progressive collapse analysis may be conducted in accordance with the following procedure. First, the structure is subjected to the loads which may reasonably be expected to occur during normal service; for example, the full dead load of the structure plus some fraction of the live load and wind load (see Section 2.5). Typically, small deflections result and, for a properly designed building, the member forces and stresses can be expected to be well below their specified limits. Next, based on the location and magnitude of a postulated abnormal load, one or more structural members are removed. The reverse of the forces acting on the damaged members prior to removal, or "reverse forces," are then applied to the remaining structure. If the structure is able to withstand the application of these forces, it can be concluded that it has the capacity to redistribute the loads previously carried by the removed members. In this case the structure does not collapse. If, on the other hand, the remaining structure is not able to carry the reverse forces, collapse is indicated. In either case, the extent of further damage to the structure may be assessed from the analysis results.

Considerable time and effort is spent in generating the data for nonlinear analysis and in obtaining and interpreting results. Gallagher [79] notes that estimates of current costs of input/output data preparation range from 60 to 85% of the total analysis cost. The use of interactive computer graphics significantly alleviates the problems associated with input data generation and output result interpretation. Although typically viewed as separate from analysis, computer graphics can have a direct role in engineering research [80]. The progressive collapse analysis system described herein makes extensive use of the latest graphic display devices and interactive techniques. The ability to interact with the computer provides the user with the means to define a structure quickly, perform an analysis, modify the structure for member removal, and display the analysis results. The ease and speed with which this process can be performed makes such a system particularly attractive for the evaluation of alternative member removal schemes.

The system just described can, of course, be applied to ordinary nonlinear analysis and design problems (see, for example, References [81 and 82]). The speed with which design changes can be implemented and subsequent analyses performed makes such a system extremely valuable as a design tool. In addition, the ability to review rapidly the results of an analysis using interactive computer graphics provides a ready means for the analyst to assess the response of any complex structure.

The intent of this chapter is to describe the computer programs developed for the interactive analysis of building structures for progressive collapse. A definition of interactive computer graphics, as it relates to the immediate problem of adaptive structural analysis, is

first provided. Next, the independent program modules which constitute the progressive collapse analysis system are briefly described. Photographs of either black and white or color displays are used to illustrate the type of feedback and interaction provided by this system. Finally, the data base and the associated data flow between the independent program modules is described. Several examples which demonstrate the versatility of this system for a variety of problems are given in the next chapter.

5.1. Interactive Computer Graphics

A computer graphics system may be defined as one in which alphanumeric, numerical, and pictorial input, output, and process stages can be displayed on black and white or color graphic devices [83]. Control is exercised by the operator through a keyboard terminal or directly through a device such as a digitizing tablet. Movement of a stylus on this tablet is duplicated by a small cross, or "cursor", displayed on the screen. This provides the capability of identifying a particular area of the screen or feature of the display by simply "pointing" to it. Through the manual operation of the digitizing tablet, figures may be drawn, commands issued, and the flow of a program controlled. A detailed description of the Cornell computer graphics facility is given in Reference [84].

There are two major distinguishing features of an interactive graphics process. First, the response to the user is immediate; that is, any change in the display, such as the deletion of a member, is realized immediately. Second, the means of communication is graphical in the

sense that the user initiates actions by indicating a portion of the graphic display rather than by employing digital means such as keyed-in numbers or commands. These two features allow the analyst to exercise intimate control over the computer processes and graphical displays.

5.2 System Description

The system described in this chapter is a collection of program modules designed to facilitate the analysis of building structures to determine their resistance to progressive collapse. The analysis process may be divided into four functional areas: problem description, analysis control, member removal, and result interpretation. Each of these four functional areas is discussed in the following sections. Extensive use of interactive computer graphics is made in all phases of the analysis process.

The independent modules making up the progressive collapse analysis system are linked through an executive program. The "menu" which displays the available program options is shown in Figure 5.1. Here control over the analysis process is exercised by simply pointing to the next operation to be performed. For example, the program for defining a new structure may be initiated by pointing to the appropriate option. When the input data has been completely specified, control is returned to the executive program and the executive menu is again displayed. In this way the analyst may control the execution sequence of the programs which comprise the system.

Data is transferred between the various independent program modules by means of disk files. The input data generation program, for example,

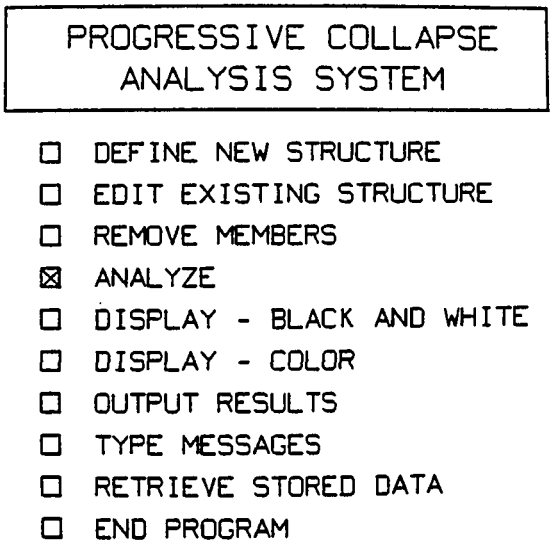

Figure 5.1 Executive Control Menu Display

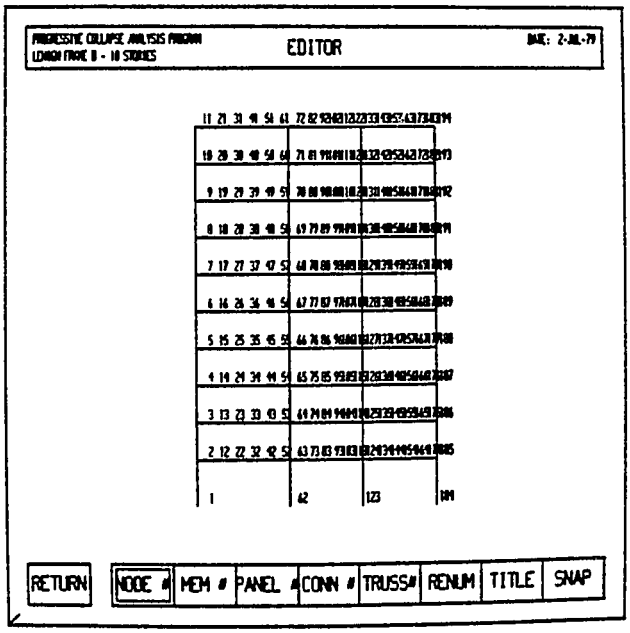

Figure 5.2 Structure Definition Editor

creates several files which contain all necessary data for a complete nonlinear analysis. The analysis program then reads these files and creates, in turn, several files containing the analysis results. Since all relevant data is written to file at each stage, the sequence may be interrupted at any time and restarted later. A more complete description of the data base organization is presented in Section 5.3.

5.2.1 Problem Definition

The preprocessing program is a rather conventional one which allows for both the definition and modification of the structure's geometry and attributes. Topologies can be generated by defining either a nodal grid or a member grid. Individual nodes can be defined by specifying their coordinates. Members can be added or deleted and material properties can be defined.

Additional capabilities allow for input of the different element types: beam-column, semi-rigid connection, and shear infill panel. Once an element type is specified, the user need only point to the nodes defining the location of the element. The element is then added to the description of the structure. Figure 5.2 shows a structure in the process of being described. In this figure the beam and column members are shown and the nodal numbering system generated by the program is displayed.

Element properties are also input using the graphics devices. If material nonlinearities are considered, element behavior beyond the elastic range must be defined. When this behavior is input, the program graphically displays the relevant information, whether it be a member

yield surface or a characteristic force-displacement diagram. The display of the beam-column element property editor is shown in Figure 5.3. Element properties, including the coordinates of the vertices of the yield surface are entered using the display keyboard. The yield surface is displayed thus providing the analyst with visual feedback on the correctness of the data entered. Figure 5.4 shows the property editor page for the semi-rigid connection. In this example the Ramberg-Osgood representation is specified and the curve corresponding to the parameters entered is displayed. The element properties are assigned by simply pointing to the appropriate members.

Nodal fixity is specified by selecting an active fixity type from a list of possible fixity conditions and assigning it to the appropriate nodes. The input/editing capabilities also allow for the specification of either independent load cases or cyclic loads. A cyclic load description can be modified interactively to accommodate any desired loading.

5.2.2 Analysis Control

The interactive analysis capabilities give the analyst intermediate control over the incremental solution procedure. At the end of each load step, a synopsis of the analysis results, including the amount of load applied and any detected change in member behavior, is reported. The analyst is able to use this information, together with more detailed analysis results available from the interactive post-processing programs, to assess the condition of the structure. Based on this updated information regarding the structure response, the user may choose to alter one or more of the analysis parameters.

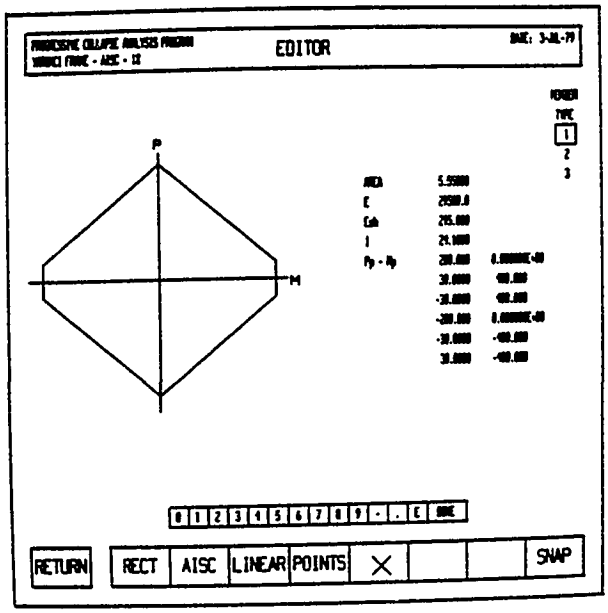

Figure 5.3 Beam-Column Element Property Editor

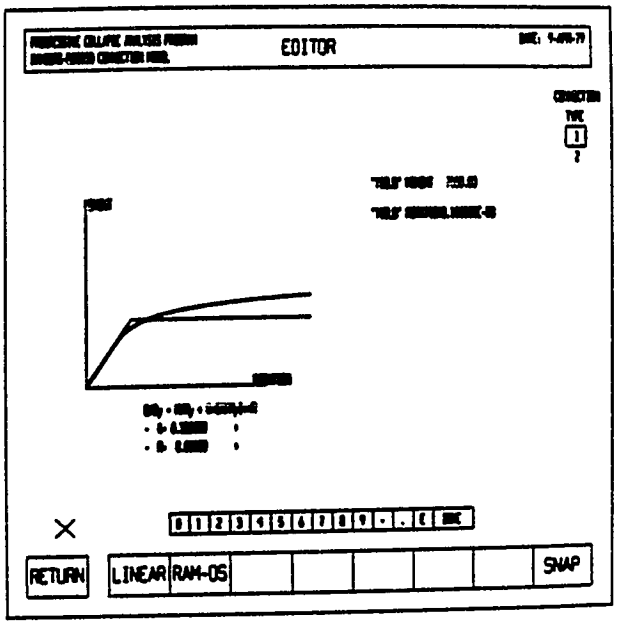

Figure 5.4 Semi-Rigid Connection Element Property Editor

The parameters which are under user control at any stage of the incremental analysis procedure are displayed on the menu shown in Figure 5.5. Values are specified by the analyst using the display keyboard shown at the bottom of the screen. Only those parameters which are to be changed must be entered. For example, the analyst may wish to alter the step size, the displacement constraints, or the load step tolerance. Large displacement effects and material nonlinearity may be included by specifying the appropriate value for the solution parameter. Or, another load case may be applied without having fully applied the current load case. This capability has been used in conjunction with displacement constraints to reproduce test data for structures subjected to cyclic loads in strain-controlled experiments.

5.2.3 Member Removal

The member removal capabilities provide a means for investigating the susceptibility of structures to a progressive collapse type of failure. After the structure has been analyzed for imposed loads, for example, dead load and a portion of the service live load, the user may selectively remove one or more members from the structure to simulate the loss, through accident, of the load carrying capacity of the member. Removal is accomplished by pointing to the members to be eliminated. Figure 5.6 shows a display of a frame structure with an exterior column removed. The data defining the structure and the nodal force vector are modified to reflect the change.

When an element is deleted from a loaded structure, a reverse force vector $\{T\}$ is added to the nodal force vector to account for

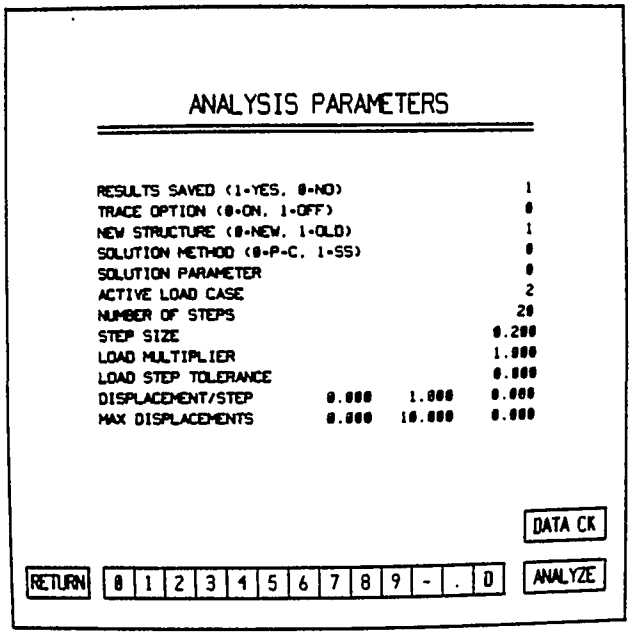

Figure 5.5 Analysis Parameter Menu Display

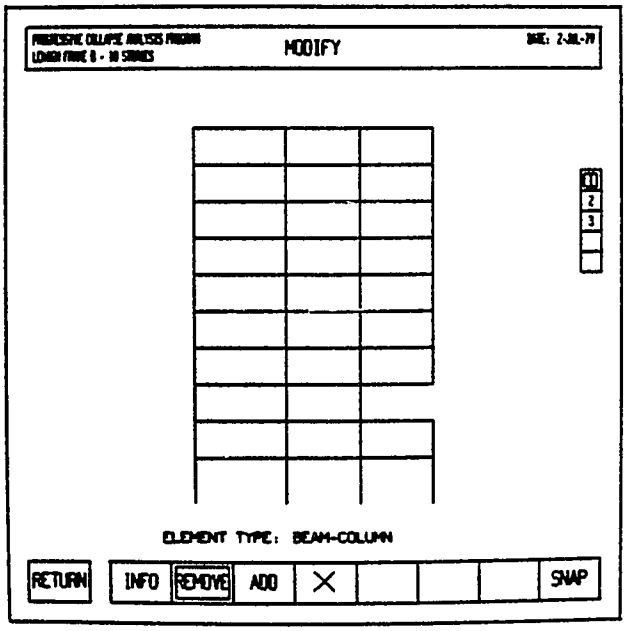

Figure 5.6 Member Removal Display

the resulting lack of equilibrium. This vector is computed as follows. The incremental forces in global coordinates associated with the element to be removed are computed by a transformation of Equation 3.30b, giving

$$\{\Delta S_i\} = -[\Gamma_i]^T\{\Delta Q_i\} = -[\Gamma_i]^T k_t \{\Delta q_i\} \tag{5.1}$$

The total element force vector is obtained by summing the incremental forces for each load step,

$$\{S_i\} = \sum_{j=1}^{i} \{\Delta S_j\} \tag{5.2}$$

These forces are removed with the deleted element by applying a reverse element force vector given by

$$\{T_i\} = -\{S_i\} \tag{5.3}$$

A reverse force vector is added to the global nodal force vector for each element which is removed.

The member removal program performs several important functions. First, since the original structure definition must be preserved, the program sets a flag to instruct the analysis program to disregard the contribution of the damaged members. Second, any node which is left without connecting members is compressed out of the system of equations. This is done by constraining the free node to have zero displacement. Also, if a dependent node is eliminated, the program transfers the dependency to the first active node and makes the necessary changes to the constraint matrix. Finally, the loads originally applied to those portions of the structure which are to be removed are redistributed to

active nodes. The analyst need only indicate which members are to be removed and the program makes the appropriate changes to the structure definition and generates the load vector containing the reverse of the element forces before removal.

5.2.4 Result Interpretation

The postprocessing programs display the response of a structure and its components to the imposed loads. After any incremental step, the analyst may invoke the postprocessing routines to examine quantitative and qualitative responses. The black and white vector scope is used to display the structure deflected shape, the load-deflection curve for any degree of freedom, and the structural response of any element.

A display of a typical deflected structure is shown in Figure 5.7. The beam-column elements are drawn as third-order curves. The displacements may be drawn to an exaggerated scale to make interpretation easier and a "zoom" function is available to enlarge any selected portion of the display. This type of display is particularly effective for determining such things as proper definition of displacement constraints, correct application of loads, and symmetry of behavior.

The load-deflection response is of considerable interest in nonlinear analysis. As the load is increased, any change in stiffness due to nonlinear and inelastic behavior is immediately apparent. A characteristic curve showing horizontal load versus lateral deflection for the simple frame discussed by Horne and Merchant [85] is shown in Figure 5.8. This diagram shows the ability to trace the descending

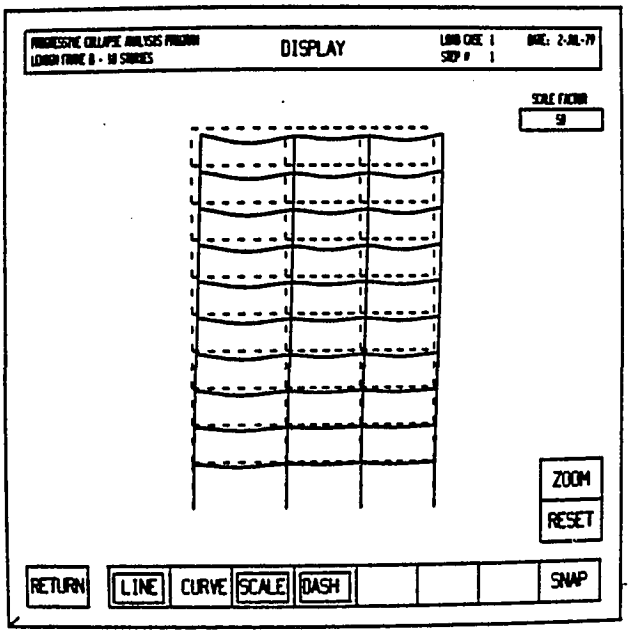

Figure 5.7 Deflected Structure Display

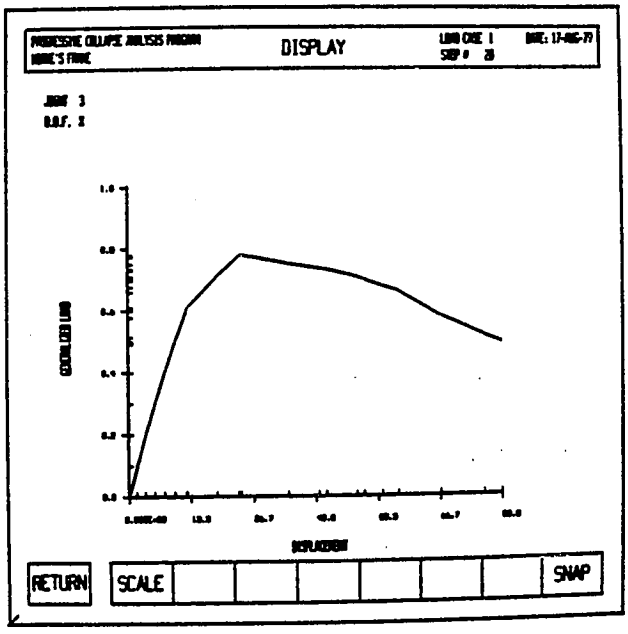

Figure 5.8 Load-Deflection Curve Display for Horne's Frame

branch of the load-deflection curve.

The beam-column element response display depicts the relation of the member end forces to the yield surface. This allows the user to assess the interaction of forces which may lead to plastic hinge formation. Figure 5.9 shows a typical member yield surface and a trace of the bending moment and axial force for a particular cross section as the load is incremented. In this instance the cross section yields and the force point is observed to remain on the yield surface during subsequent load increments. The moment-rotation curve for the connection element graphically depicts the degree of yielding of such an element, and allows the analyst to determine a measure of the energy dissipated during plastic deformation. The response of a connection subjected to several cycles of reversing load is shown in Figure 5.10.

Postprocessing capabilities also include use of a color frame buffer and a color CRT. A structure can be color-coded using, for example, colors corresponding to the proximity of the forces on a beam section to the yield criterion. Plastic hinges at the member ends are drawn as solid dots of a different color. Figure 5.11 shows a structure consisting of beam-column elements displayed in color. A display such as this indicates how close any point in the structure is to its associated failure criteria. It allows the analyst to determine at a glance those portions of the structure which have significant reserve capacity or those areas which have either yielded or are close to yielding. The mechanism causing collapse may also be easily distinguished. This type of display is not intended to replace the actual data available in hard copy or viewed on the vector display;

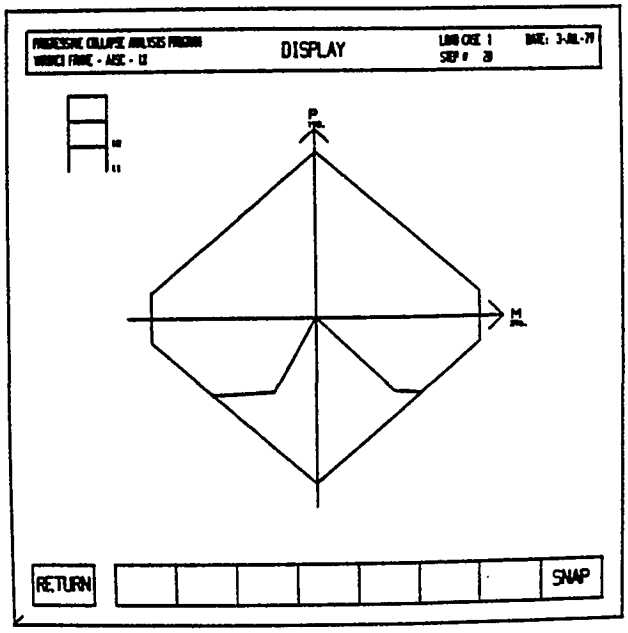

Figure 5.9 Beam-Column Element Response Display

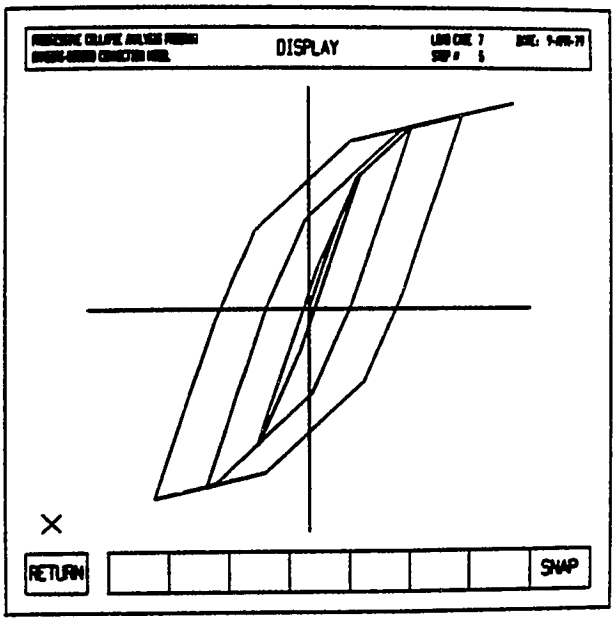

Figure 5.10 Semi-Rigid Connection Element Response Display

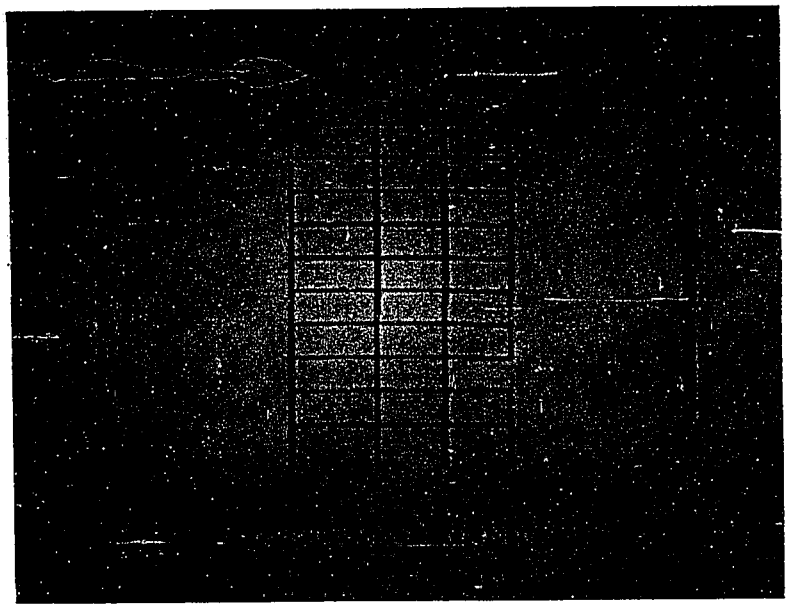

Figure 5.11 Color Display of Beam-Column Frame

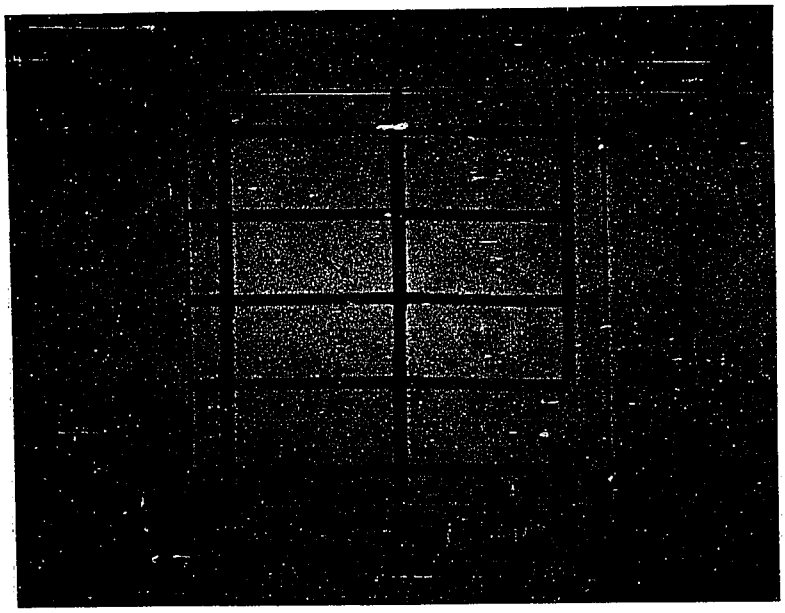

Figure 5.12 Color Display Illustrating "Zoom" Feature

rather it should compliment these other means of reviewing output data and provide the analyst with a general "feel" for the behavior of the structure.

Several features are available to enhance this capability to display element response in color. First, different element types may be displayed in different color ranges to make each element type distinguishable. Eight different ranges consisting of twenty colors each are currently available. A software zoom capability permits the analyst to inspect more closely a particular area of the structure. An example of this is shown in Figure 5.12. A color scale may be drawn adjacent to the structure to permit approximate evaluation of the degree of distress. Another feature permits the analyst to point to a color on the color scale and cause all points on the structure of the same color to be displayed in a blinking mode. Conversely, the analyst may point to any location on the structure and cause the corresponding color on the scale to blink. Figure 5.13 shows an example of this feature in which those portions of the structure within 25% of yielding are blinking (shown as black).

Graphic displays clearly do not always meet the demands of the analyst since quantitative results are often required. An option is available from the executive program to generate a file containing the numerical results in an easily readable form. This file may either be displayed on an alphanumeric terminal, or it may be directed to a line printer to create a permanent record. Selective results may be obtained; that is, either input data or results from any individual or series of incremental steps. For example, after reviewing graphi-

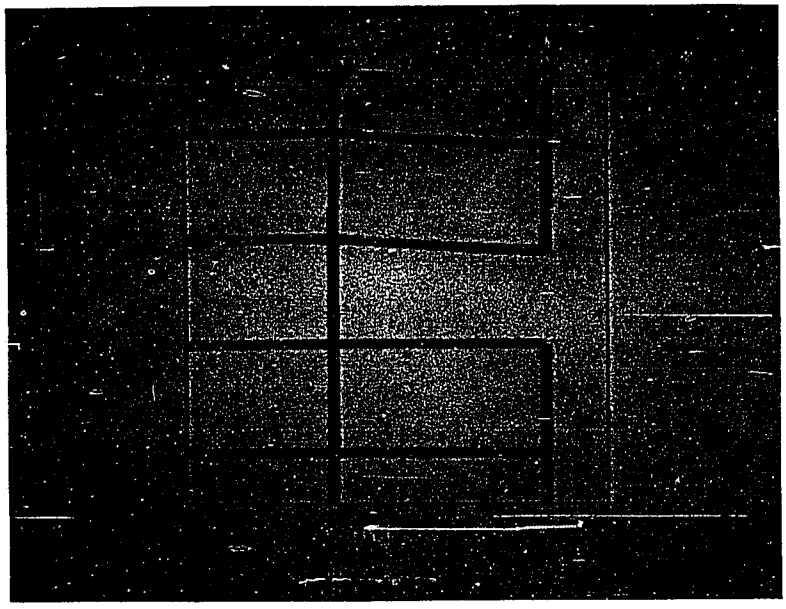

Figure 5.13 Color Display Illustrating "Blinking" Feature

cally the results of several steps of a complex analysis, the analyst may elect to keep a record of only the input data and the last analysis step. Thus, an output report may be generated which consists of only that information which is absolutely necessary.

5.3 Program File Structure and Data Flow

The progressive collapse analysis program is composed of independent program modules. As such, data required by more than one program must be transferred between programs by means of disk files. There are four categories of files in this system: data files, temporary or scratch files, save files, and formatted output files. A diagram showing these four file types and their relation to the various programs which constitute the progressive collapse analysis system is shown in Figure 5.14. The purpose of this section is to describe further the program file structure and flow of data between program segments.

Data files contain both the definition of the structure under consideration and the results of the current analysis step. Together these data completely describe the state of the structure at any stage in the analysis. The structure data is generated by the problem definition or input/edit program. These data are read by the analysis program which in turn creates the files containing the results of the current step. The result files as well as the structure definition files are read by the various graphics programs to display the analysis results.

Since the data files are overwritten at each incremental step, the

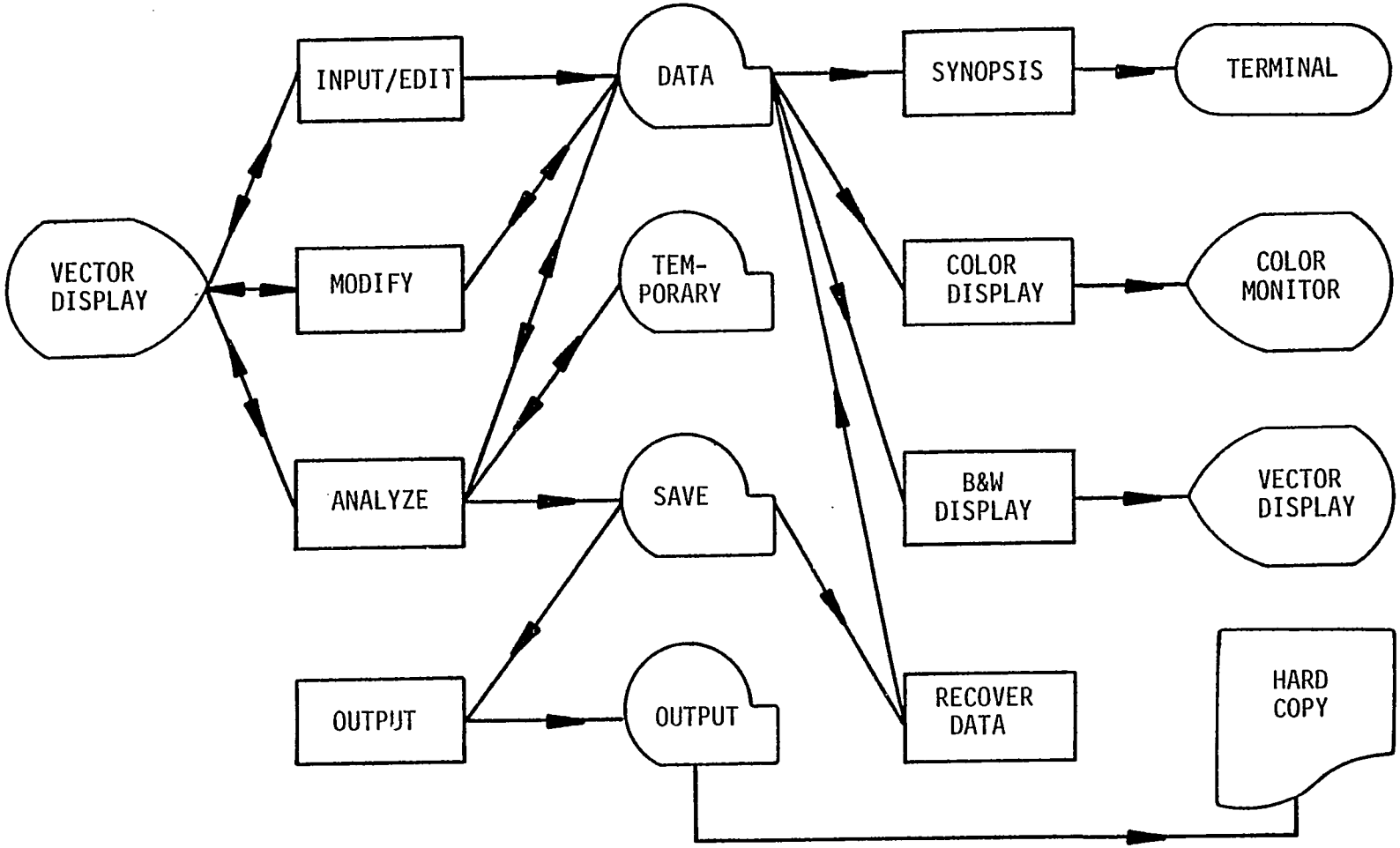

Figure 5.14 Program File Structure and Data Flow

results of previous steps are lost. The option exists to save the results of each incremental step in compressed form; these are the "save" files. The user specifies this option for each analysis step by setting the appropriate flag on the analysis parameter menu shown in Figure 5.5. Data files for any previous step may be recovered from the saved files at any time. The data recovery program is initiated from the executive program (see Figure 5.1).

The save files are also used to generate a formatted output file of the analysis results. This option is again selected from the executive program. The output file may be displayed on the user's terminal or directed to a line printer to produce a hard copy of the analysis results. This sequence is illustrated in Figure 5.14.

This file structure provides the analyst with the ability to compute and store selected analysis results. If desired, the complete analysis history may be stored in compressed form and recovered for display or generation of a final report. A previous load step may be recovered and a different load sequence applied. Alternatively, the analyst may choose to return to a particular stage in the analysis and remove additional members. In this way the user exercises considerable control over the data handling as well as the analysis process.

6. EXAMPLES

In this chapter several examples are presented which illustrate the application of the progressive collapse analysis system. These examples serve several purposes. First is to verify the analysis results by comparison with known solutions. Second is to demonstrate the application of the analysis system to the study of progressive collapse. And third is to illustrate the use of graphic displays to assist in both problem description and interpretation of the analysis results.

The first example compares the results of several analyses with data for a full scale test conducted at Lehigh University. The frame chosen for test was designed to fail in a sway type mode with plastic hinges forming in the columns. Good agreement is found up to and through collapse. The second example demonstrates the ability of the program to analyze large displacement problems. A simple frame toggle is used to illustrate this capability and the results are compared with those of other researchers. Again, good agreement is found and, in fact, the present analysis procedure is found to be more efficient. The next example is that of a small frame which is used to illustrate the behavior of steel frames subjected to abnormal loads and subsequent loss of several members. The effect of removing two different columns is examined and the significant effect of shear infill panels on the collapse resistance is shown. In the fourth example, the capacity of a particular structural element to withstand loads imposed by debris from collapsing floors above is evaluated. A beam section is overloaded to the point where it no longer carries the debris loading by beam action but rather by catenary action. The last example looks at the response of a large

steel building frame to the removal of an exterior column. This example is included to illustrate the ability to analyze large planar frame structures and, more importantly, to illustrate the post-processing capability wherein a vast amount of data can be reviewed rapidly.

6.1 Yarimci Test Frame

A comparison between the results obtained using the analysis program described herein and the experimental results of a full scale test is presented here. Figure 6.1 shows a three story, single bay frame which was tested at Lehigh University by Yarimci [86]. Rolled sections, as indicated in the figure, were used and all connections were fully welded. The loading was non-proportional; the vertical loads were applied first and were maintained constant during the subsequent application of horizontal loads. The axial load versus yield load ratio for lower story columns was 0.445 and the frame was designed to fail in a sway-type mode with plastic hinges forming in the columns.

The structure geometry and member properties were specified using the problem description processor described in the previous chapter. The member properties were taken from test data for the actual rolled selections used in the Lehigh test. These properties are listed in Table 6.1. The loads shown in Figure 6.1 were assigned as two separate load cases with load case 1 consisting of vertical loads and load case 2 consisting of horizontal loads. The analysis included the effects of both geometric and material nonlinearities. Load case 1 was applied in one step since the behavior under gravity loads was assumed to be essentially linear. The horizontal load was then applied incrementally through collapse.

Section	Handbook EI kip-in.^{2} × 10^4	Measured EI kip-in.^{2} × 10^4	Handbook M_p kip-in.	Measured M_p kip-in.
W10 × 25	394	390	1060	1100
M 5 × 18.9	70	73	400	400

Table 6.1 Measured Properties of Beam and Column Sections

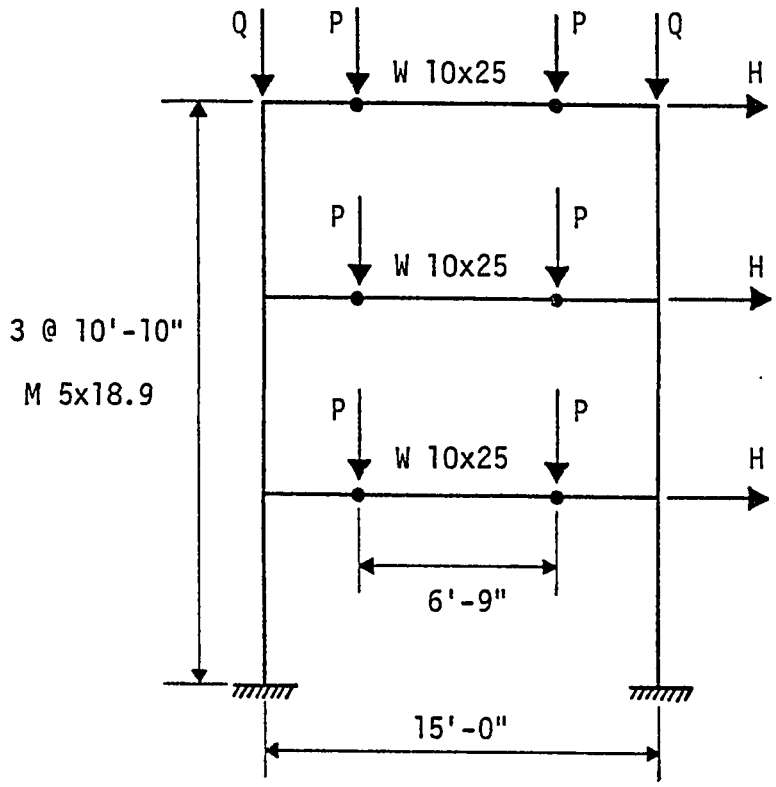

Figure 6.1 Yarimci Test Frame

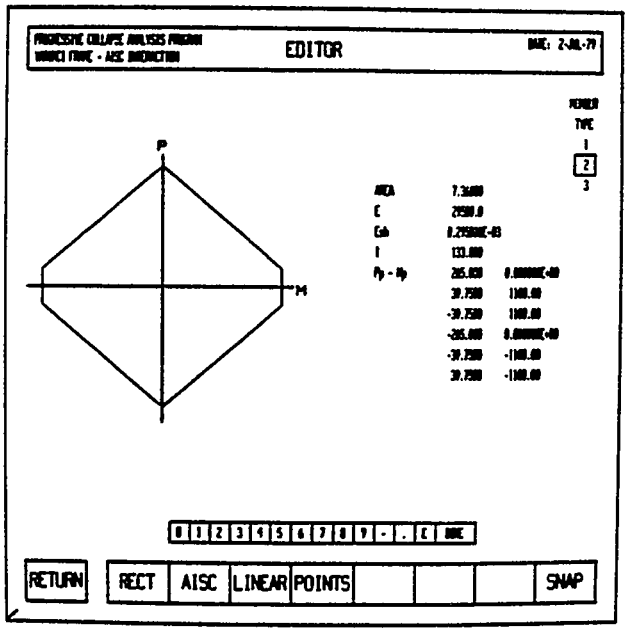

Figure 6.2 AISC Interaction Yield Surface for W 10x25 Section

The load-displacement curve for the sway at the first story is used to compare with the results obtained in the Lehigh test. An analysis was performed using the AISC yield interaction relation. The yield surface for the W 10 × 25 section is shown in Figure 6.2. Figure 6.3 shows a plot of the analysis results along with the test results reported by Yarimci. Excellent agreement is obtained for the collapse load while the lateral displacement at the collapse load is somewhat underestimated. A second analysis was performed including the effects of 1% strain hardening. Results of this analysis are shown in Figure 6.4. As can be seen, the load-deflection curve matches the test results quite closely. Both analyses provide a reasonably accurate account of the behavior of the structure up to and through collapse.

It is possible to neglect the interaction of the axial load and bending moment for the determination of the onset of yield. This is done by simply providing an interaction-free yield surface of rectangular shape. The yield surface for the W 10 × 25 section used in this example is shown in Figure 6.5. A third analysis was performed using interaction-free yield surfaces and no strain hardening. A plot of the lateral deflection of the first story versus the applied lateral load is shown in Figure 6.6. Note that the frame reaches collapse at a load of 2.86 kips which is approximately 77% greater than the collapse load predicted using the AISC interaction relation and no strain hardening. For structures such as this, where the effects of axial loads on the yield criteria are significant, it is essential that the analysis procedure accounts for the interaction of axial load and bending moment.

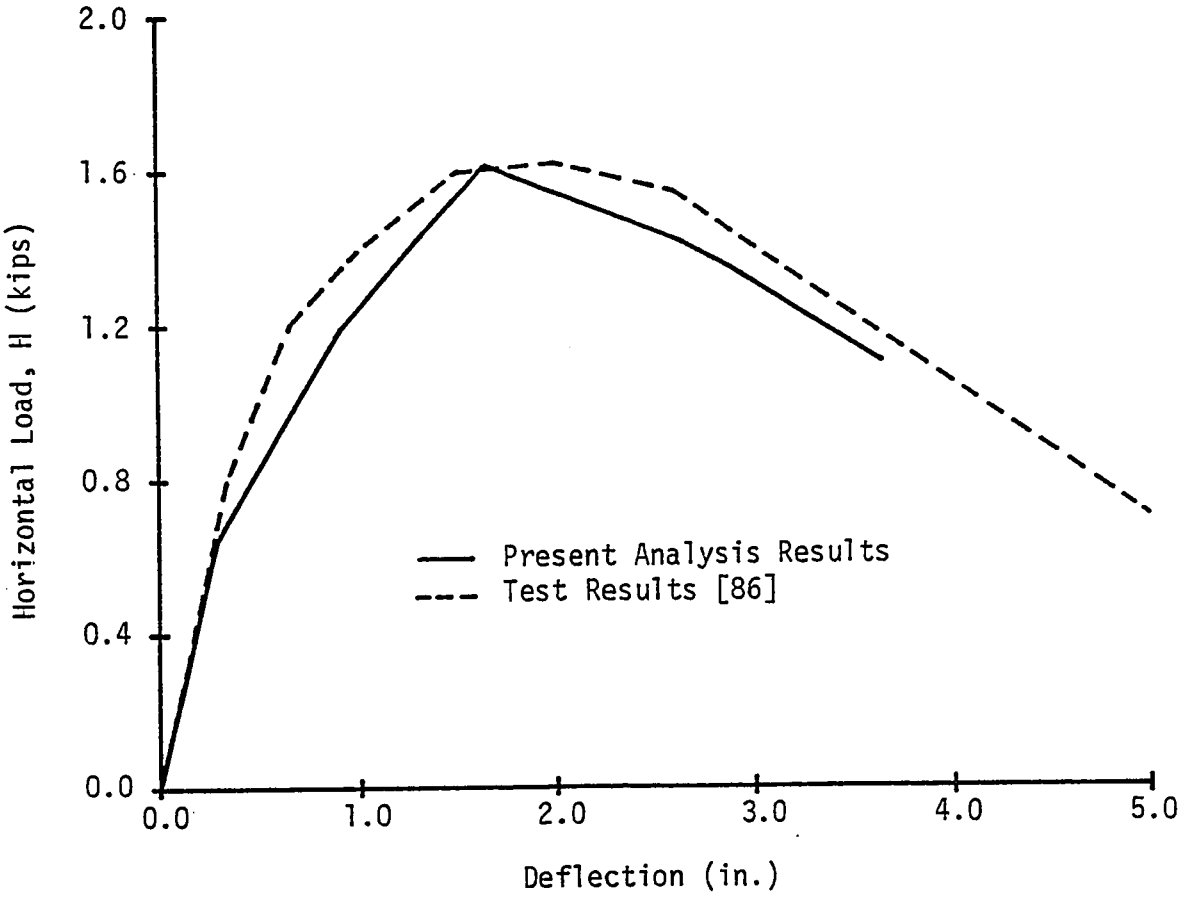

Figure 6.3 Load-Deflection for Sway at First Story - No Strain-Hardening

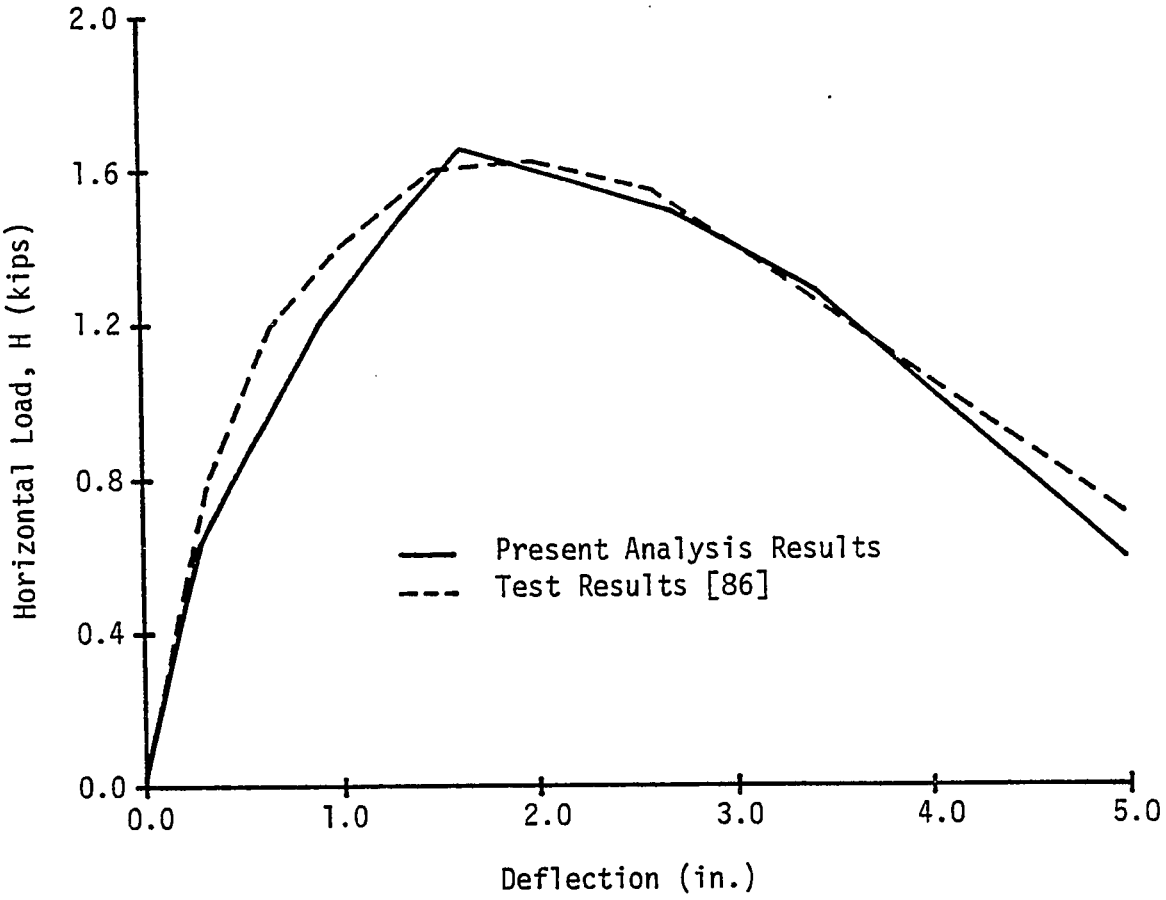

Figure 6.4 Load-Deflection for Sway at First Story - 1% Strain-Hardening

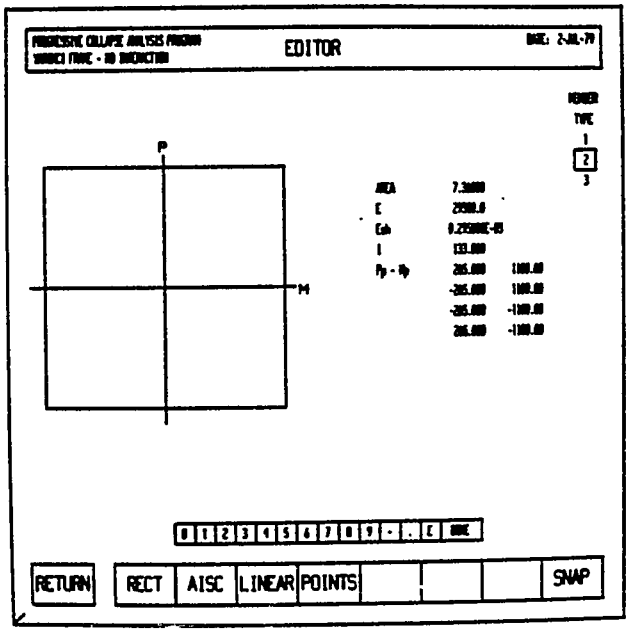

Figure 6.5 Interaction-Free Yield Surface for W 10x25 Section

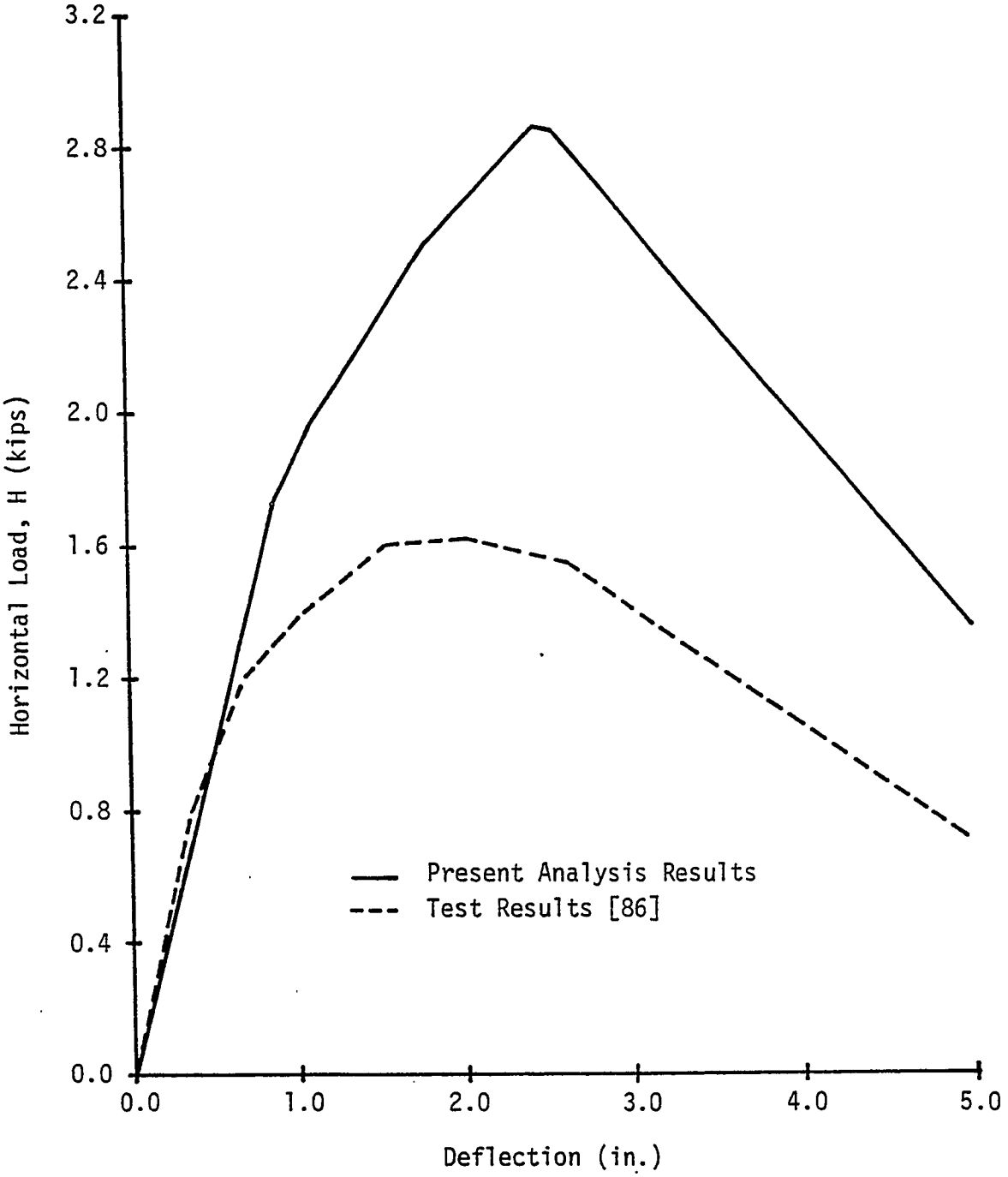

Figure 6.6 Load Deflection for Sway at First Story - No Axial Force-Bending Moment Interaction

6.2 Williams' Toggle

To demonstrate the applicability of the analysis program to problems exhibiting large displacements, the rigid jointed toggle shown in Figure 6.7 was analyzed. This toggle was first studied by Williams [87]. A comparison is made here between the results obtained using the present capability and those obtained by Ebner and Ucciferro [88] using the formulations of Martin [36], Jennings [38], and Powell [89]. The values of $E = 10.278 \times 10$ lb/in, $I = 9.0039 \times 10$ in^4, and $A = 0.1829$ in^2 are those given by Ebner and Ucciferro.

Due to the symmetry, it was only necessary to analyze one half of the structure. Eight elements were used to permit a direct comparison with the incremental solutions presented in Reference [88]. A plot of the centerline deflection versus applied load is shown in Figure 6.8 for both Williams' solution and the solution obtained from the present study. As can be seen, the incremental procedure presented herein gives excellent results.

The results presented by Ebner and Ucciferro for several alternative formulations are given in Table 6.2. The centerline deflection at a load of 80 pounds is used as a basis of comparison. Both load increment and deflection increment solutions are shown. A load increment of one pound was used while the displacement increment was 0.007 inches. The results for the present analysis were obtained using the predictor-corrector procedure and a load increment of four pounds in combination with a displacement constraint of 0.05 inches. This resulted in fifteen steps in which each step required two solutions of the global stiffness equations.

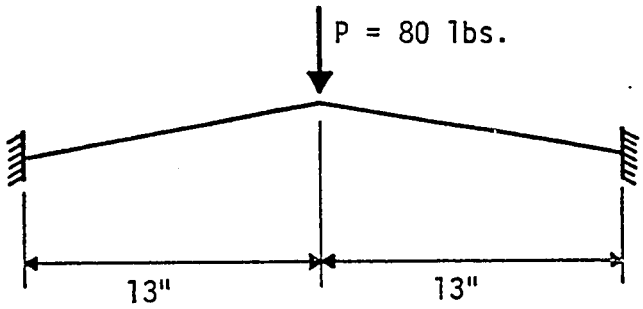

$E = 10.278 \times 10^6$ lb/in^2 $\quad I = 9.0039 \times 10^{-4}$ in^4

$A = 0.1829$ in^2 $\quad$ Rise at centerline = 0.32 in

Figure 6.7 Shallow Toggle with Central Load

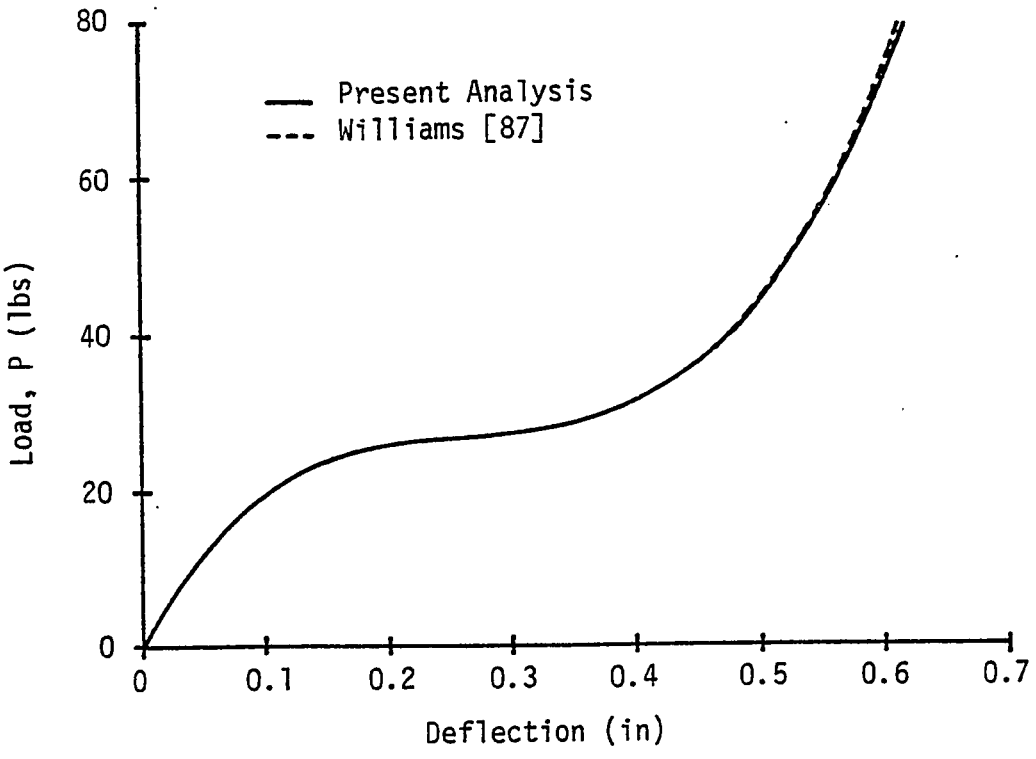

Figure 6.8 Centerline Deflection vs. Applied Load

	Formulation	Centerline deflection (in.)
Williams		0.611
Jennings		0.639
Powell	1 lb load inc.	0.639
Martin		0.640
Martin	0.007 in. displ. inc.	0.621
Jennings		0.616
Present analysis	4 lb. load inc. .05" displ. limit	0.618

Table 6.2 Incremental Solutions for Toggle

It is seen that the results for the present analysis capability are in excellent agreement with the solution given by Williams. The results differ by approximately one percent. The present analysis capability is also seen to give better results than those of the formulations studied by Ebner and Ucciferro. This can be attributed to the use of the predictor-corrector scheme in the present analysis program. It can be concluded that this procedure is quite efficient and should be used in place of the simple-step procedure.

6.3 Four Story, Three Bay Steel Frame

This example is one which demonstrates the capability to remove one or more members in a structure to investigate the ability of the structure to resist a progressive collapse type of failure. The analysis is conducted as follows. First, the structure is subjected to the loads which may reasonably be expected to occur during normal service. The combination of 1.0 Dead load + 0.45 Live load + 0.20 Wind load, as suggested by Leyendecker and Ellingwood [11], is used here. Next, one or more members is removed to simulate the loss, through accident, of load carrying capacity. The reverse of the forces acting on the damaged members prior to removal are then applied to the remaining structure. A determination is made as to whether or not the structure is able to withstand the loss of the selected members. The graphics displays assist greatly in the evaluation of the structure and in the assessment of the severity and extent of damage.

The four story, three bay steel frame shown in Figure 6.9 is used to illustrate this capability. Such a structure represents a typical framing

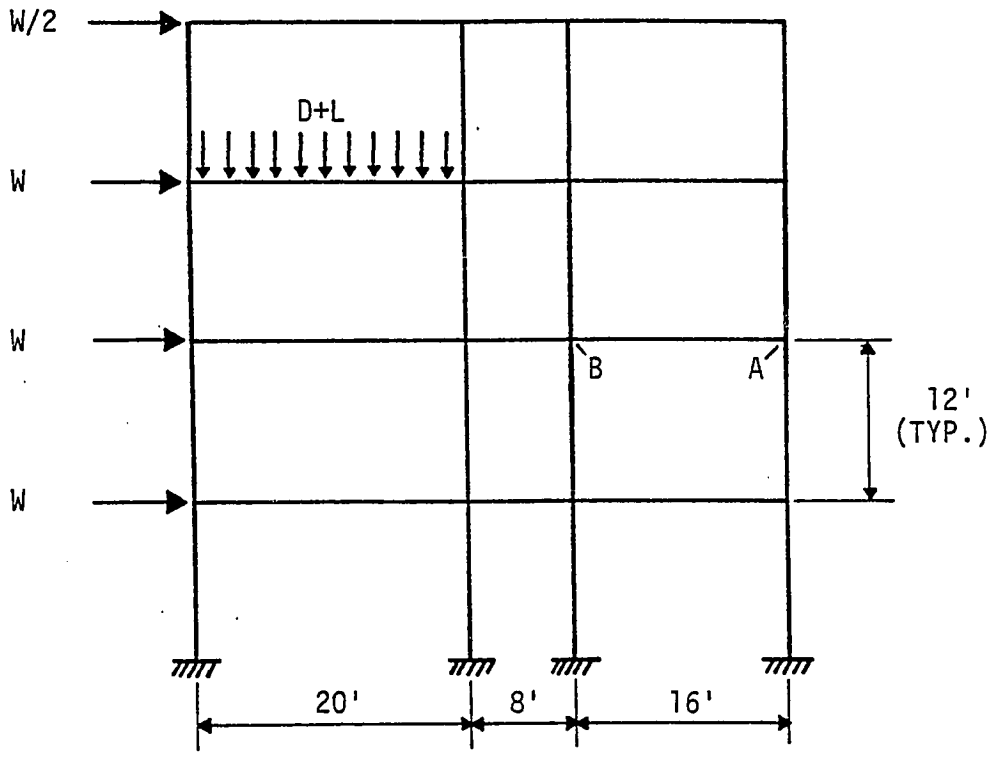

ROOF: D = 60 psf FLOORS: D = 80 psf
L = 30 psf L = 80 psf

WIND: W = 3.84 kips

FRAME SPACING = 16 ft.

Figure 6.9 Four Story, Three Bay Steel Frame

scheme for a low-rise apartment or small office building. The frame is designed in accordance with the AISC Manual of Steel Construction [55]. The loading consists of uniform dead load plus live load on the beam sections and wind load acting on one exterior face of the building. The beams are divided into several segments to approximate the uniformly distributed load using concentrated forces. Similarly, the wind load is applied as concentrated forces acting at the floor elevations. Wide flange sections are used throughout and are shown in Figure 6.10. Several alternative schemes for member removal were investigated.

In the first case, the exterior second story column was removed. It was found that the structure reached collapse at 69% of the applied reverse forces. Thus, for an abnormal load which caused the loss of load carrying capacity of this particular member, the frame was found to collapse. Figure 6.11 shows the deflected shape of the frame at the collapse load. The deflections have been exaggerated for clarity. Significant deflections are obvious in the cantilevered portion of the damaged structure. The load-deflection history for the y-displacement of "point A" is shown in Figure 6.12. A downward deflection of 4.7 inches occurs at the collapse load. Plastic hinging has occurred in several members at this load and a mechanism has formed. A color display of the structure at the collapse load is shown in Figure 6.13. The plastic hinges are indicated by blue dots. A display such as this provides the analyst with a clear picture of the structure behavior and facilitates assessment of the damage.

A second case assumed the removal of an interior column at the second story level. It was found here that the reverse forces were

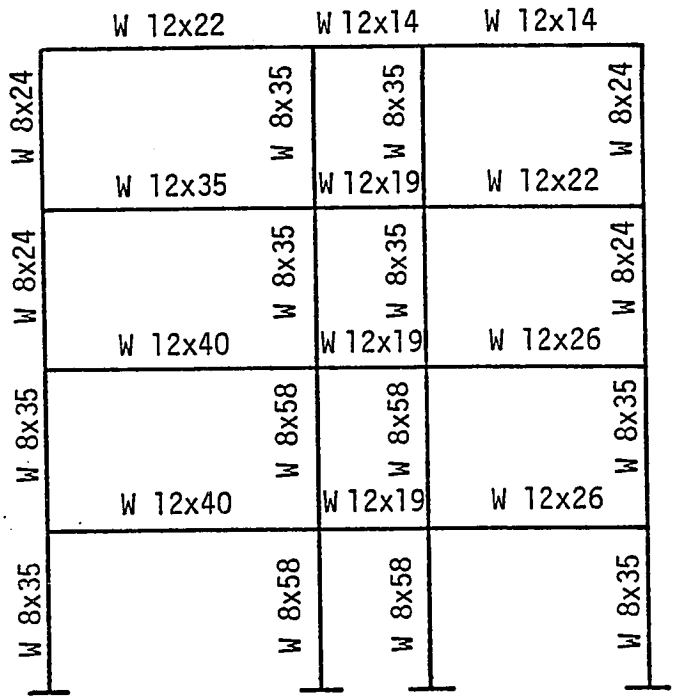

Figure 6.10 Beam and Column Sections for Four Story, Three Bay Steel Frame

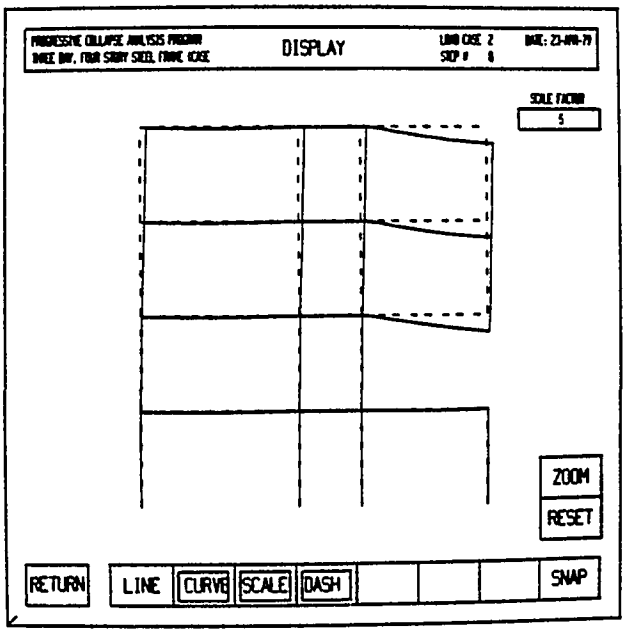

Figure 6.11 Deflected Structure at Collapse Load (case 1)

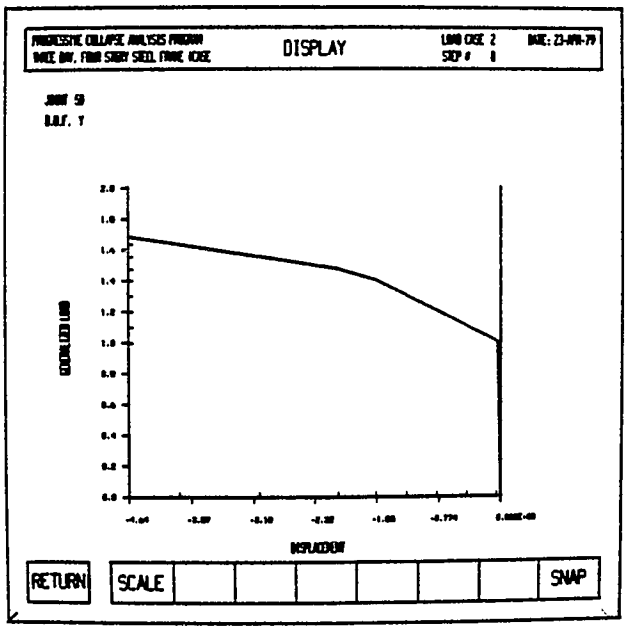

Figure 6.12 Load-Deflection for Point A (case 1)

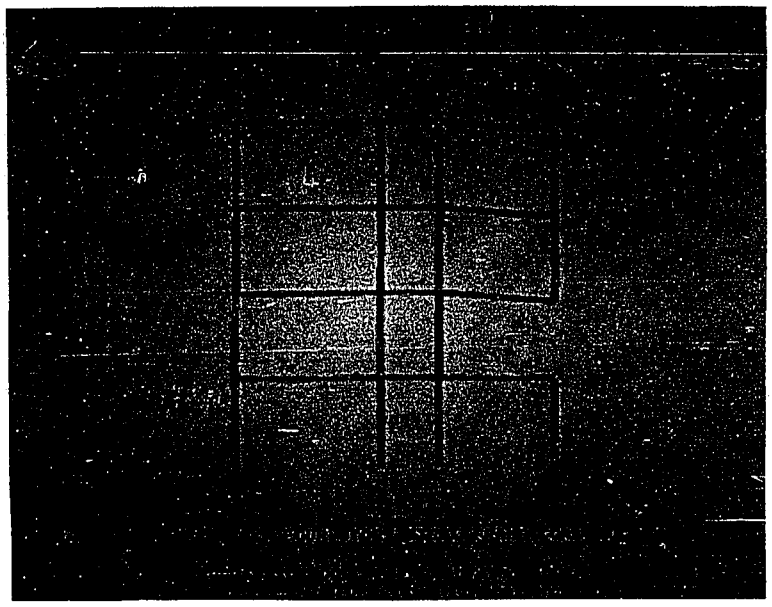

Figure 6.13 Structure Response at Collapse Load (case 1)

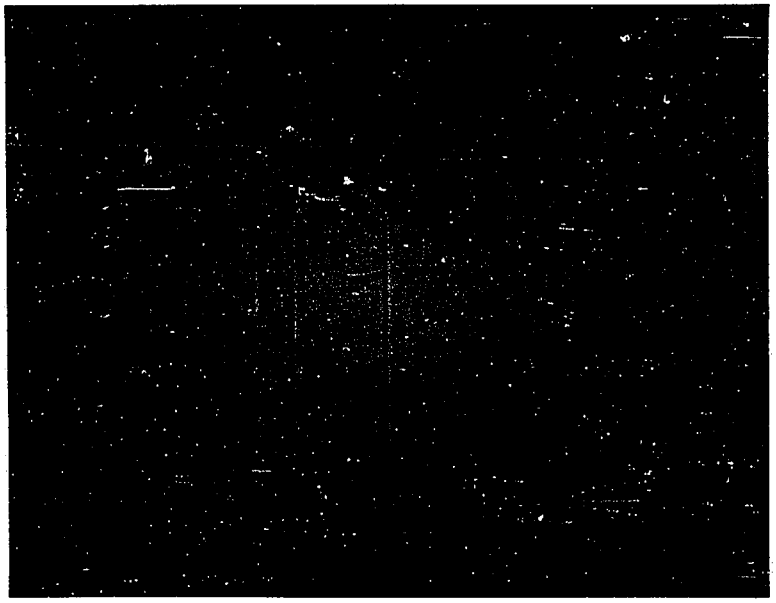

Figure 6.14 Structure Response at Service Load (case 2)

accommodated and the structure, therefore, did not collapse. Damage, in the form of plastic hinging, occurred at several locations in the structure. Figure 6.14 illustrates the ability to enlarge a portion of the color display to facilitate evaluation of the damage. The maximum displacement occurred at "point B" and was equal to 0.8 inches vertically downward. Levels of damage, as determined by this analysis, are within reason and safe evacuation of the building could be accomplished.

In the third case, the effect of shear walls on the behavior of the frame subjected to the removal of an exterior column was investigated. Shear infill panels were added to the exterior spans (the interior span was assumed to be a corridor). The exterior column at the second story and the shear wall in that bay were removed (see Figure 6.15), and twelve analysis steps were performed. The walls were found to provide considerable strength, and, in fact, permitted the service load combination to be carried with only minimal damage to the structure. Cracking was found in the shear wall directly above the removed panel. This is evidenced from the color display shown in Figure 6.16 where the limit is defined as the initiation of first cracking. No plastic hinges were found to occur in the beam sections. Again, damage was limited to the immediate area around the location of the abnormal load event and the structure remained essentially intact. A deflected shape display is shown in Figure 6.17. Note that only beam-column elements are shown in this figure. The deformations are scaled as before but are seen to be considerably smaller than in the previous cases.

In this example it was found that the building collapsed if an exterior column was lost through an abnormal load event. If, on the

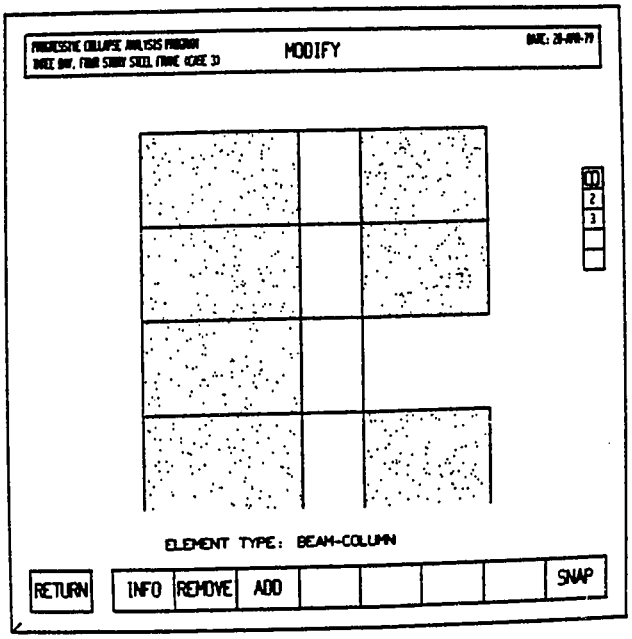

Figure 6.15 Column and Shear Wall Removed (case 3)

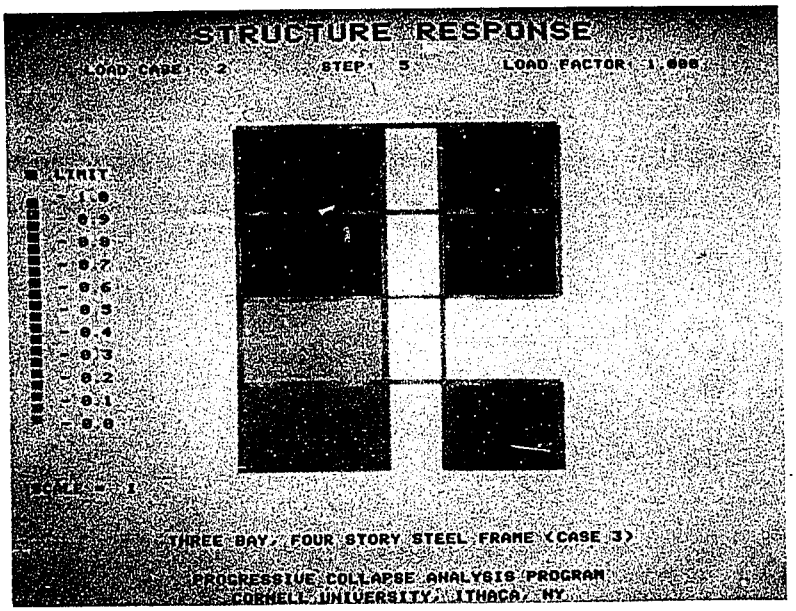

Figure 6.16 Structure Response at Service Load (case 3)

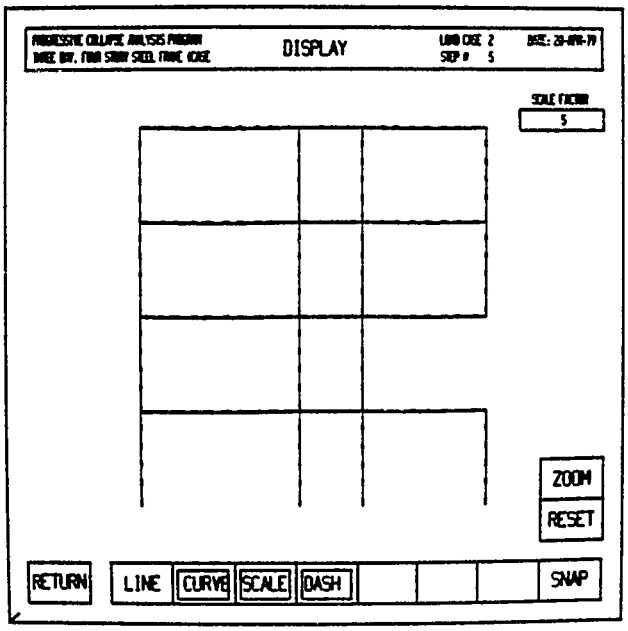

Figure 6.17 Deflected Structure at Service Load (case 3)

other hand, an interior column was removed, the building did not collapse. Thus, the analysis has indicated which members, if lost through accidental loading, would cause the building to collapse. Based on this information, either of two alternative design strategies could be implemented. First, those members which, when removed, initiated collapse could be designed to resist the abnormal load. This is an example of the specific local resistance method discussed in Chapter 2. Alternatively, progressive collapse could be prevented by strengthening the structure so as to provide an alternate path of load resistance. This, of course, is the alternate load path method also discussed in Chapter 2. The progressive collapse analysis program is seen to be applicable to the implementation of both of these design strategies.

A second point should be made regarding the results of this example. It was found that including the shear-infill panels greatly strengthened the frame; the loss of an exterior column as well as one panel did not lead to collapse. While not often considered in design, infill panels are seen to have a significant influence on the stiffness and strength of a frame structure. For an accurate evaluation of the collapse resistance of a frame building, such contributions should not be overlooked.

This example also serves to illustrate the ability to evaluate alternative member removal schemes easily and quickly using interactive computer graphics. Both the black and white and color displays provide the analyst with the information needed to assess the damage caused by the loss of load carrying capacity of one or more members. The speed with which a structure can be modfied to account for the loss of members

as well as the speed with which the results can be evaluated, make computer graphics particularly attractive in progressive collapse analysis.

6.4 Overloaded Beam

When collapse of a portion of a building occurs, the falling debris imposes severe loads on the remaining floors. It is essential to determine whether such an overload can be carried without causing further collapse. In addition, important data regarding required strength, continuity and ductility should be obtained. In this example the case of falling debris imposing an overload condition on a beam section is investigated.

This particular example involves the study of a beam which has a span of 20 feet and which is rigidly supported at its ends. The beam is a W18×35 wide flange with section properties obtained from the AISC Manual of Steel Construction [55]. Due to the symmetry of the support conditions and assumed loading, only one half of the beam was modeled. For purposes of analysis the beam was divided into nine segments as shown in Figure 6.18. Small segments were located at the support and center of the span to permit the spread of plasticity. Solutions were obtained for 0%, 2%, and 5% strain-hardening, expressed as a percentage of the elastic modulus.

In addition to the design dead plus live load which was assumed to be uniformly distributed, the beam was subjected to debris loads with the distribution shown in Figure 6.19. The loading is seen to be symmetrical about the beam centerline. The values of the debris load shown

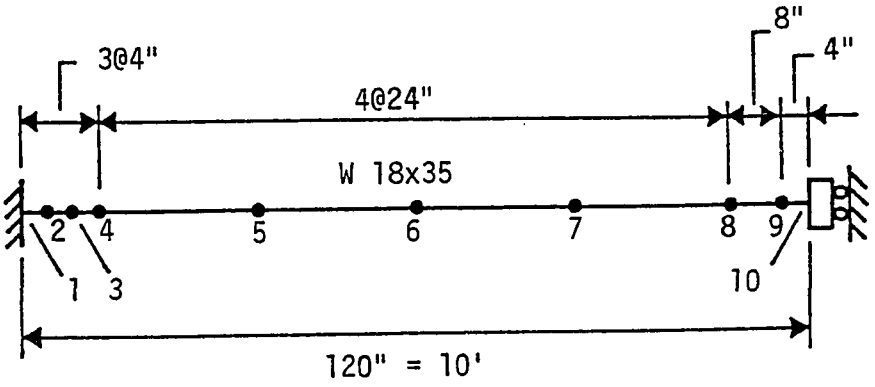

Figure 6.18 Overloaded Beam

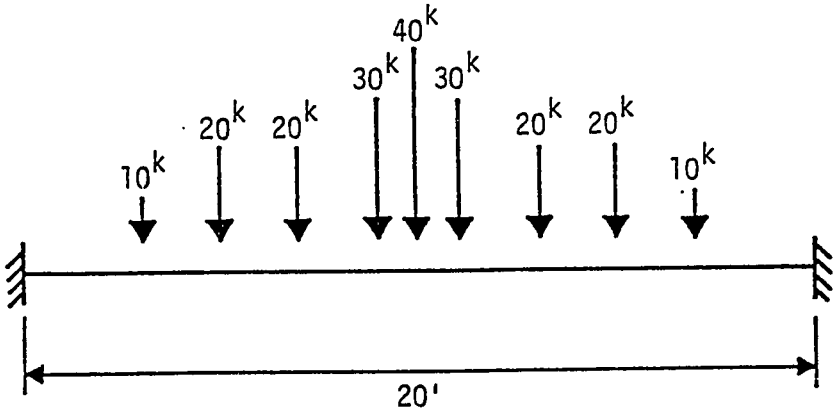

Figure 6.19 Debris Loading on Beam Section

in Figure 6.19 are assumed to include an impact factor since the loads must be applied statically. The loads were applied as two separate load cases; the first case being the design loads and the second case the debris loads.

The design dead plus live load is carried by bending with no plastic hinges forming. As the debris load is applied it is initially carried by bending action. Yielding, however, occurs at the supports and center of the beam. Beyond this point the overload is carried primarily by catenary action; that is by tension in the beam as it deflects. Nonlinear behavior is exhibited as a result of the change of geometry due to elongation of the beam. For a tension structure such as this, the stiffness increases with increasing load. If the axial yield load is reached, the elastic-plastic portion of the beam can carry no additional load and will elongate plastically. The resulting change in geometry, however, will permit the system to remain stable and accommodate additional load.

For the case of no strain-hardening, plastic hinges formed first at the supports and then at the center of the beam. When the center hinge formed, the beam had a total vertical deflection at the mid-span of 0.67 inches. This can be seen in the load-deflection diagram shown in Figure 6.20. Beyond this point the additional load was carried entirely by catenary action. The beam stiffness with respect to the lateral loads was essentially zero since the beam had not as yet deflected significantly. Note the zero-slope portion of the load-deflection curve in Figure 6.20. With increasing deflection, however, the beam stiffness increased. In this particular case the member axial yield load was reached when the vertical deflection was about 5.8 inches.

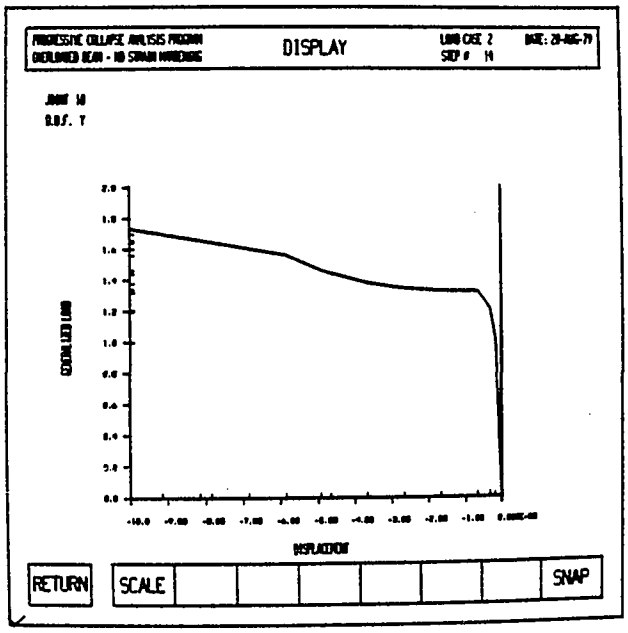

Figure 6.20 Load-Deflection Diagram for 0% Strain-Hardening

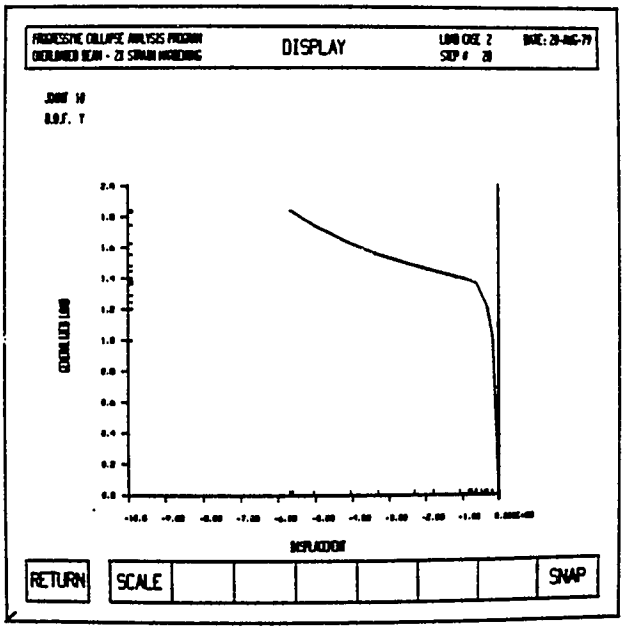

Figure 6.21 Load-Deflection Diagram for 2% Strain-Hardening

Note that the program feature described in Section 4.1.7 permitted a stable solution after axial yielding had occurred. As can be seen, additional load was carried with additional beam elongation. The loading was terminated when the maximum deflection reached 10.0 inches.

Consider next the cases of 2% and 5% strain-hardening. In both cases, once plastic hinges had formed at both the mid-span and the supports, the beam continued to support the overload in part by bending. This was due, of course, to the non-zero strain-hardening modulus. A display of the generalized load versus mid-span deflection is shown in Figures 6.21 and 6.22 for 2% and 5% strain-hardening, respectively. Note the absence of the zero-slope portion of the load-deflection curves. The 5% strain-hardening case exhibited a stiffer behavior and more gradual transitions in the load-deflection characteristics as the hinges formed. Laboratory tests would be necessary to determine the appropriate value of strain-hardening to use. Figures 6.23 and 6.24 show the moment-axial load history for member 6-7 for the cases of 2% and 5% strain-hardening, respectively. It can be seen that axial yielding has occurred in the case of 2% strain-hardening but not in the case of 5%. Again, a stable solution is achieved when a section reaches its axial yield load. A color display of the 2% strain-hardening case is shown in Figure 6.25. The blue areas indicate regions where yielding has occurred. Note the gradual curvature of the beam at both the support and mid-span and the spread of plasticity.

The severe requirements on structural joints and members may be seen from the above analysis. The joint tie force in the above analyses, for example, is approximately equal to the yield force of

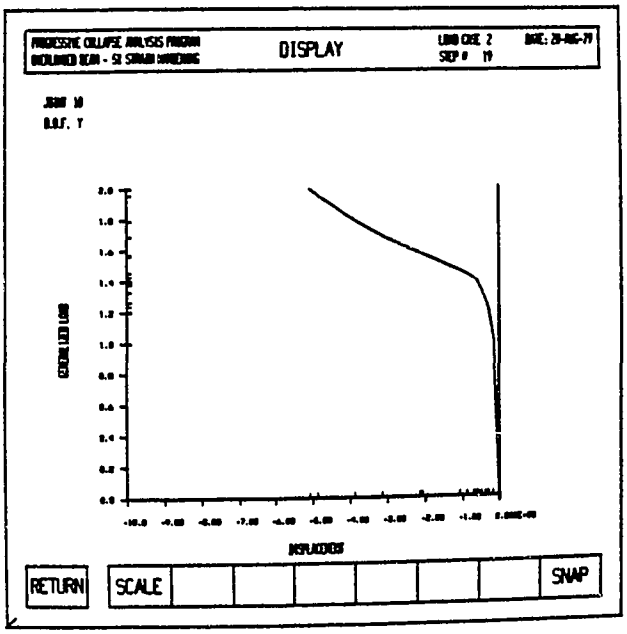

Figure 6.22 Load-Deflection Diagram for 5% Strain-Hardening

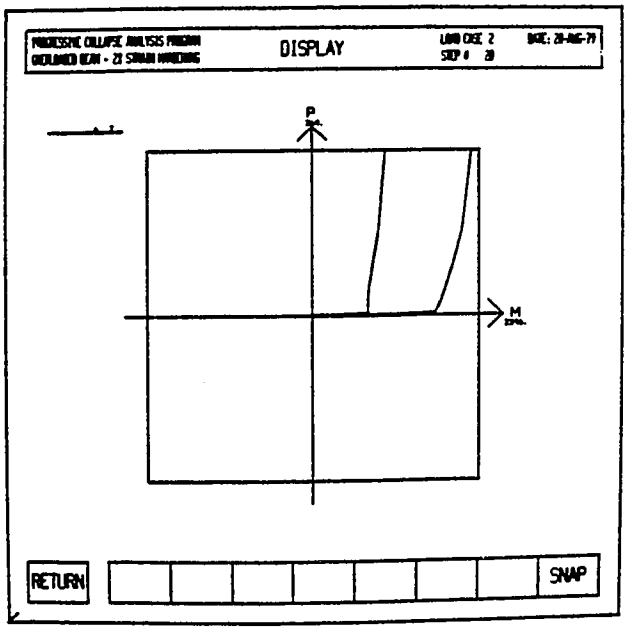

Figure 6.23 Moment-Axial Load History for 2% Strain-Hardening

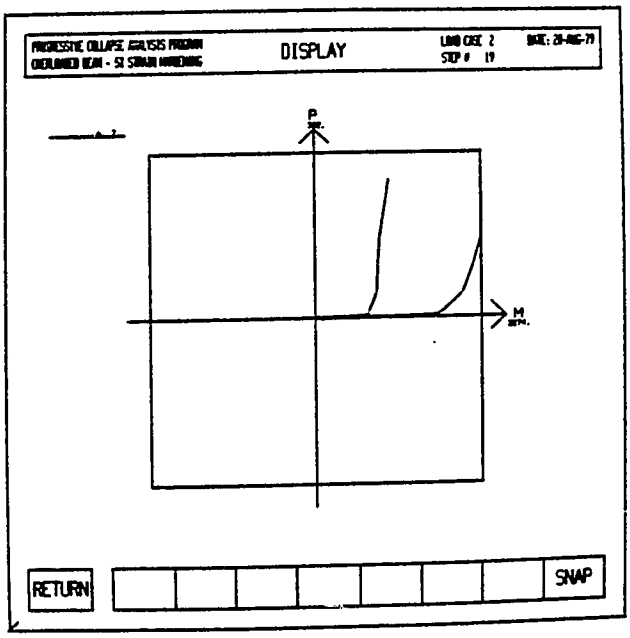

Figure 6.24 Moment-Axial Load History for 5% Strain-Hardening

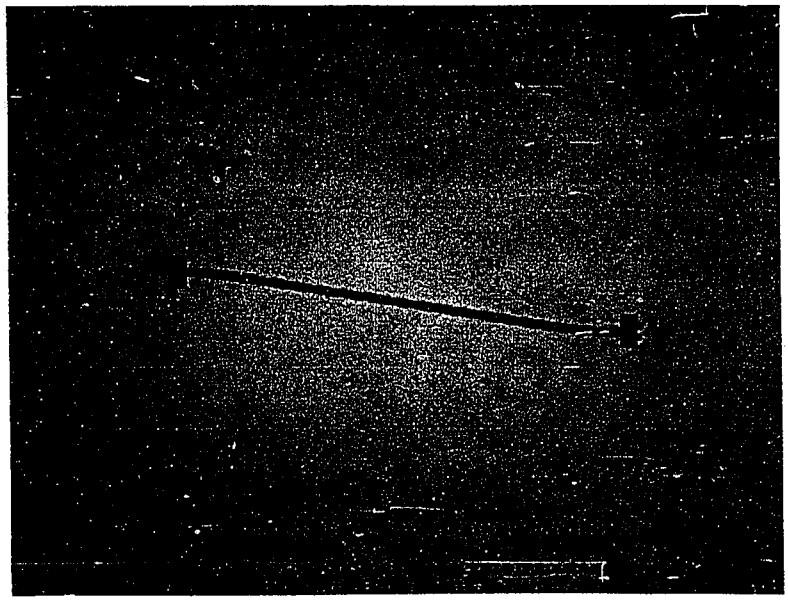

Figure 6.25 Color Display of Yielding Beam for 2% Strain-Hardening

the beam (371 kips). This is an extremely severe requirement for a joint; most standard steel framing joints would not be capable of carrying such a load. It is this type of data, however, which is necessary to determine if a structure will survive an abnormal load as well as possible debris load resulting from partial collapse.

6.5 Lehigh Frame B

This last example illustrates an application of the progressive collapse analysis program to a ten story, three bay steel frame. This frame was presented in the Lehigh lecture notes from the summer course on plastic design in structural steel [90]. A diagram of the frame and loading is shown in Figure 6.26. The members were selected on the basis of the plastic design method. The member sizes are given in Figure 6.27. Each beam is divided into five segments to approximate the uniformly distributed load as a series of concentrated loads. This results in a problem size of 220 members and 194 joints.

The structure was loaded with the service load defined by 1.0 Dead load + 0.45 Live load + 0.2 Wind load. After application of the service load, the exterior column on the third level was removed using the member removal feature. The reverse forces were then applied incrementally. The load step tolerance was specified to be 0.02. This guaranteed that no load step would be smaller than 2% of the reverse forces. Although this feature permits a member to yield at a value below its specified yield, the total number of incremental steps is greatly reduced. For this particular example, the reverse forces were applied in eight steps while plastic hinges formed in a total of 27 joints.

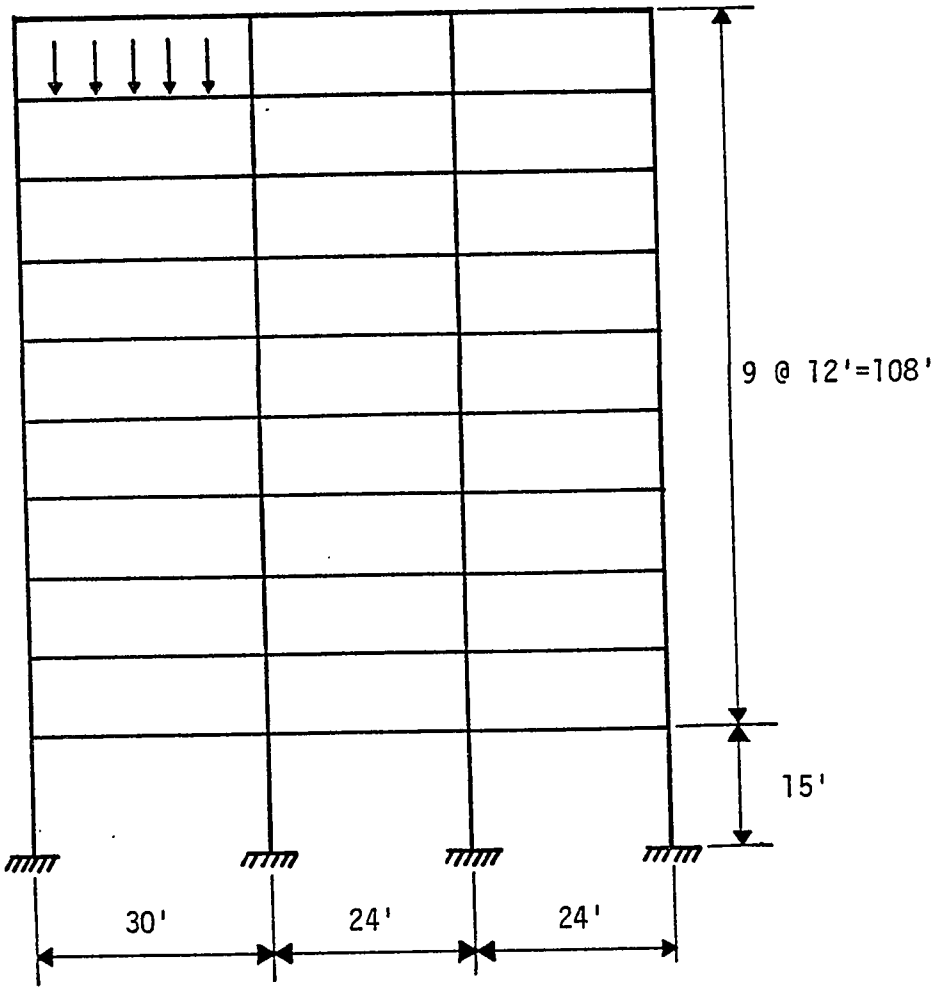

ROOF: D = 60 psf
L = 30 psf

FLOORS: D = 80 psf
L = 80 psf

EXTERIOR WALL: D = 45 psf

WIND: W = 20 psf

BENT SPACING = 24 ft.

Figure 6.26 Lehigh Frame B

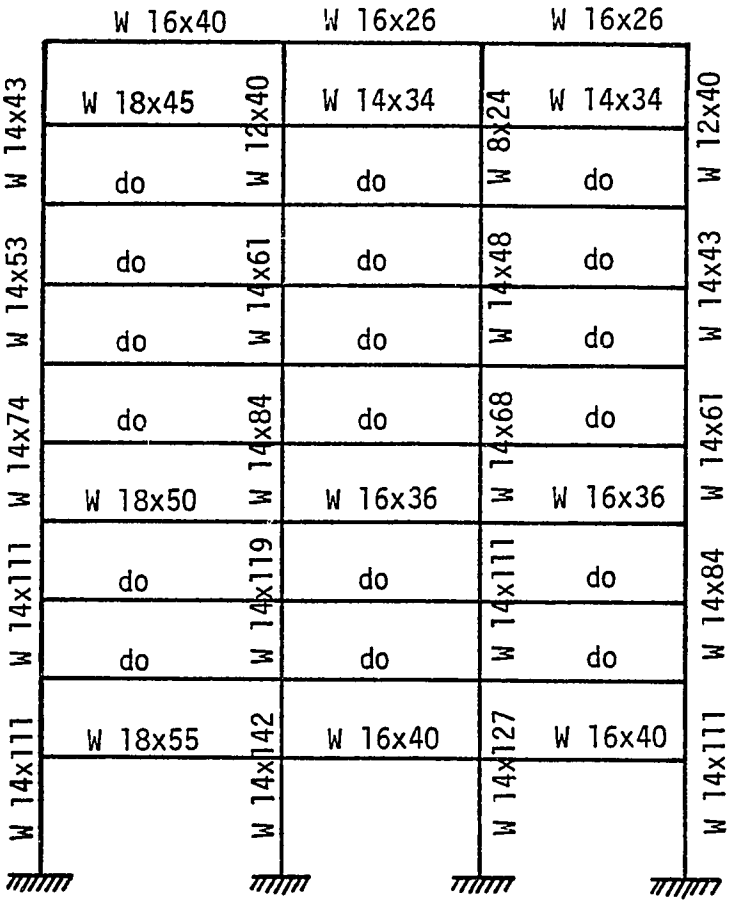

Figure 6.27 Beam and Column Sections
for Lehigh Frame B

It was found that the collapse load was reached when only 36% of the reverse forces were applied. A color display of the structure at collapse is shown in Figure 6.28. A mechanism has formed in the portion of the structure which is cantilevered due to the removal of the exterior column. Since there was very low axial force in the beam members, yielding occurred at the plastic moment capacity and there was no post-yield interaction. In this particular case no strain hardening was specified. Thus, with the formation of sufficient hinges in the beams, a true mechanism occurred. The structure was unable to take additional load beyond this point.

This example is perhaps somewhat unrealistic since the contribution from adjacent frames was neglected. It is likely that a steel frame such as this would have sufficient continuity between bents to assist in bridging the damaged area. Nevertheless, the example points out the use of several program features and illustrates the application of the progressive collapse analysis system to a large, well designed, and realistic frame.

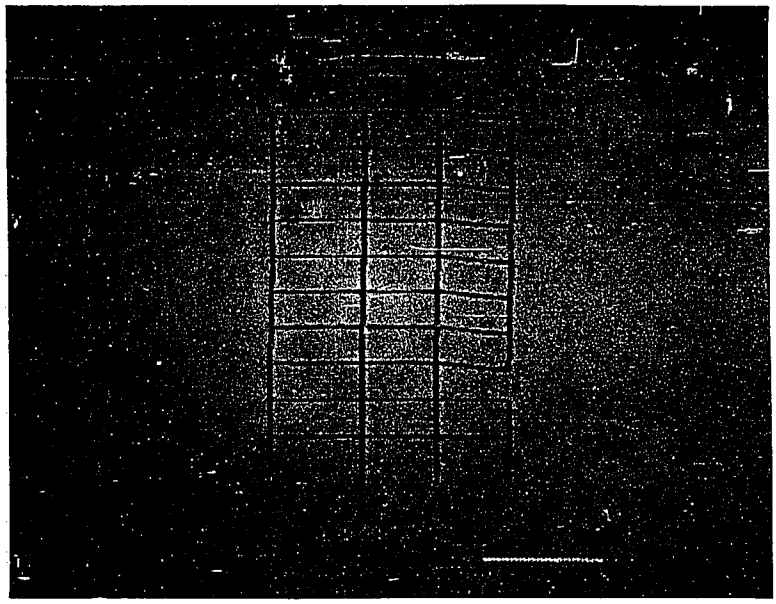

Figure 6.28 Structure Response at Collapse Load

7. SUMMARY AND CONCLUSIONS

The work presented in the previous chapters is summarized here and several conclusions are drawn from the results of the study. In addition, a few suggestions for future work are presented.

7.1 Summary of Work Presented

Progressive collapse is a situation in which a localized failure in a structure, caused by an abnormal load, triggers a cascade of failure affecting a major portion of the structure. Several buildings have collapsed in this fashion in recent years and the possibility of progressive collapse is a source of continuing concern. The incidence of progressive collapse is significant; approximately 15-20% of the total number of collapses which occur may be classified as progressive collapse. More importantly, the trend in the number of collapses of this type is increasing. This is due, in part, to recent developments in the efficient use of building materials and refinements in analysis techniques which have resulted in structures with a considerably smaller true margin of safety.

To investigate whether or not a local failure will spread, the analyst needs procedures that account for the sequential nature of the phenomenon wherein progressive failure of portions of the structure continually modifies the structural system under analysis. The procedures must be capable of tracing the behavior of the structure not only to the point of incipient damage, but beyond the initial damage stage into a true limit state in which the badly damaged structure is called

upon to resist imposed loadings. The research reported herein is concerned with the development of a highly accurate and general computer program for the analysis of structures for their resistance to progressive collapse.

Several alternative methods to deal with the problem of design for the prevention of progressive collapse were discussed in Chapter 2. Among them were event control, indirect design, and direct design. Event control refers to reducing the risk of progressive collapse by either eliminating the abnormal load event which may trigger a collapse or by reducing the effect of the abnormal load. Indirect design refers to consideration of resistance to progressive collapse by specifying minimum levels of strength and ductility so that a structure is able to bridge over a damaged area irrespective of the cause of the initial failure. The direct design approach explicitly considers resistance to progressive collapse and the ability of a structure to absorb localized damage. Direct design has been further divided into the alternate load path method and the specific local resistance method. The computer program described herein has been shown to contribute to the implementation of each of these design strategies.

Chapter 3 dealt with the analysis of structures to account for both material and geometric nonlinearity. Several nonlinear solution techniques including incremental, iterative, and mixed procedures were discussed. It was concluded that, among the various methods described, the incremental procedure offered the most versatility for the class of problems being studied. The Updated Lagrangian formulation was described and the nonlinear incremental stiffness matrix for the beam-column

element was developed from the principle of stationary potential energy. Two incremental solution techniques were described next; the simple-step procedure and the predictor-corrector procedure. The predictor-corrector method has proven to be considerably more efficient than the simple-step method, but either of these procedures may be selected in the analysis program. Finally, several program features such as the incremental step termination criteria, load-step tolerance, and post-collapse behavior were described.

In Chapter 4 the various structural elements which constitute the present capability were described. These elements include the beam-column, shear infill panel, and semi-rigid connection. The beam column element is used to model frame members which may yield through the formation of generalized plastic hinges. The member yield criterion is defined by a two-dimensional yield surface which accounts for the interaction between the member axial force and bending moment. The shear infill panel is included to represent the stiffness imparted to a framed structure by a wall of masonry or other similar construction. The element has shear resistance only and is represented by a bi-linear stress-strain relation. The connection element models both the linear elastic and the nonlinear inelastic behavior of steel beam-to-column building connections. Either a linear segmented model or a continuous Ramberg-Osgood model may be used to represent the nonlinear moment-rotation relation.

Chapter 5 described the computer programs developed for the interactive analysis of building structures for progressive collapse. A definition of interactive computer graphics, as it relates to the

immediate problem of adaptive structural analysis, was given. Next, the four basic program modules which constitute the Progressive Collapse Analysis System were described. They are: problem definition, analysis control, member removal, and result interpretation. The role of both interactive computing and computer graphics in each of these functional areas was stressed. Finally, the data base and the associated data flow between the independent program modules was described.

Several examples which illustrate the use of the Progressive Collapse Analysis System were presented in Chapter 6. The examples included verification of analysis results by comparison with test data and with known solutions. In addition, several applications were presented which demonstrated the member removal capability and the subsequent analysis to determine the collapse resistance of the structure under consideration. The use of graphic displays to assist in both the definition of a structure and its properties and the interpretation of analysis results was illustrated.

7.2 Conclusions

Although the probability of occurrence of an abnormal load is quite small, the consequences of a progressive collapse type of failure are high both in the loss of property and in the potential for injury and loss of life. The collapse of the Ronan Point apartment building bore this out in a tragic way. Thus, the possibility of progressive collapse in residential buildings may be considered to pose a serious threat.

Considerable research needs to be conducted in the area of progressive collapse as there are many questions which remain to be answered.

What types of building construction are most prone to be a progressive collapse type of failure? What joint details contribute most to the overall lack of ductility and continuity in a structure? How can these joint details be improved upon so as to assure good structural integrity? How does one establish whether or not alternate load paths exist in the event of the loss of load carrying capacity of one or more members? And, what would be the extent of damage to a structure if a localized failure were to occur? It is clear that there exists a need for the development of highly accurate analytical models which are capable of predicting behavior of structures in the event that one or more elements or joints becomes ineffective.

Such an analysis system can be employed in a variety of ways to implement the various design strategies. Specifically three alternative ways in which the analysis capability developed herein can be used are:

(1) To determine if alternate paths may be developed upon the removal of one or more load carrying members.

(2) To identify those members which, if removed, would precipitate a collapse.

(3) To assist in evaluating requirements for general structural integrity such as ductility, tie forces, joint resistance, and continuity.

Examples of progressive collapse have occurred in virtually every type of construction. The present study has addressed only the analysis of steel framed structures. It should be noted that steel structures, as a class, are perhaps the least susceptible to progressive collapse. This is due to the inherent ductility of steel and the significant

continuity provided by typical bolted or welded framing connections. Since failure theories of steel frame members are the most refined, it was felt that this type of structure afforded the best opportunity to explore the philosophy of a progressive collapse analysis system.

The risk of progressive collapse is probably the greatest in large panel and bearing wall structures. The increased susceptibility to progressive collapse is due to a combination of the brittle nature of concrete and the general lack of ductility and continuity in the overall structure as a result of the joint details. However, due to the complexity of the behavior of such construction, little analytical work has been conducted in this area. Analytical procedures for evaluating such structures for resistance to progressive collapse must be developed if a realistic analytical approach to progressive collapse is desired.

In the present study only the case of planar frames is considered. Although the representation of a three dimensional structure as a planar frame is often adequate for design purposes, it is not realistic for collapse analysis. This two-dimensional representation of a three dimensional structure precludes taking into account the contribution of adjacent framing. In general, this additional support would assist in bridging over a damaged area and would improve the collapse resistance of the structure. Therefore, to predict more accurately the resistance of a structure to progressive collapse, a three-dimensional analysis should be performed.

Another significant assumption made in the present study was that loads and reverse forces are applied in a quasi-static fashion. In reality, the dynamic response of a structure subjected to abnormal

loading should be considered. There are several areas in which dynamic effects may be significant. For example, when a member loses its load carrying capacity due to some extreme load, it does so over a finite period of time. The actual time history of the application of the reverse forces may have an important effect on the response of the structure. In addition, falling debris may cause significant impact loading to the remaining structure and therefore should be considered dynamically. Considerable research remains to be conducted on the dynamic behavior of structures undergoing collapse. It may be found that approximate methods using static loads are sufficient for the degree of accuracy required. However, the question of the importance of including dynamic effects in analysis for progressive collapse is, as yet, unanswered.

The complex nature of nonlinear analysis of structures in the damaged state has rendered such studies extremely difficult in comparison with linear elastic analysis. This is due, in part, to the time required to generate the structure geometry and properties as well as the difficulty in interpreting the vast amount of data which results from an analysis. This is especially true if three-dimensional and dynamic effects are considered. The incorporation of interactive computer graphics techniques to assist in the definition of a structure and interpretation of the results has aleviated many of these difficulties. With the aid of interactive graphics devices the data defining a structure can be generated in far less time than it can be using conventional methods. Also, the speed with which analysis results may be reviewed is significantly improved with the use of both black and white and color

displays. Graphics has also been shown here to greatly expedite multiple analyses of the same structure with various elements removed.

Many areas of research in progressive collapse remain. The present study has been concerned only with the development of analytical techniques for evaluating building structures for resistance to progressive collapse. Equally important, however, is the area of laboratory tests to both confirm analytical results and provide data for analytical models. Particular emphasis should be given to the study of joint behavior. Tests should be conducted through collapse and should account for the gross deformations characteristic of heavily damaged structures.

7.3 Future Work

The computer program developed in the course of the present research, though limited in scope, has proven to be successful for the particular class of structures it was designed to analyze. The need exists to develop comparable analytical models for a broader class of structures including cast-in-place concrete structures and panel and bearing wall structures. In addition, as was noted in the previous section, these capabilities should be extended to include three-dimensional structures. This is not, in all cases, a simple extension of two-dimensional analysis techniques since increasingly complex stress states are more difficult to model accurately. In many cases the analytical models for predicting such behavior have yet to be developed.

Also noted in the previous section was the need to investigate the dynamic response of structures subjected to abnormal load events. The reverse forces should be applied as a time varying load, possibly with

a linear variation. Also, debris loading should be accounted for including the impact effects. It remains to be determined if such dynamic analyses are justified or whether quasi-static solutions will provide the required accuracy. Whether or not dynamic analyses are routinely conducted in progressive collapse analysis, the time dependent nature of this phenomenon must be studied.

Nonlinear analyses are currently extremely time consuming and expensive to conduct. Extension to the three-dimensional case and inclusion of dynamic behavior will significantly increase the solution time for an analysis and the results will be even more voluminous. The case for computer graphics to assist in the interpretation of analysis results will therefore be even stronger. Color displays could be used to depict some measure of structure response as a function of time. Thus, the analyst could view a real time or slow motion display of the structure and observe the evolving regions of distress; the formation of cracking patterns in concrete and masonry and yielding in steel.

APPENDIX A

Elastic and Geometric Stiffness Matrices for the Beam-Column Element

The six degrees of freedom and corresponding forces for the beam-column element are given in Figures 4.6 and 4.7. The elastic stiffness matrix is

$$[k_e] = \begin{bmatrix} \frac{AE}{L} & 0 & 0 & \frac{-AE}{L} & 0 & 0 \\ & \frac{12EI}{L^3} & \frac{6EI}{L^2} & 0 & \frac{-12EI}{L^3} & \frac{6EI}{L^2} \\ & & \frac{4EI}{L} & 0 & \frac{-6EI}{L^2} & \frac{2EI}{L} \\ & & & \frac{AE}{L} & 0 & 0 \\ & \text{(symmetric)} & & & \frac{12EI}{L^3} & \frac{-6EI}{L^2} \\ & & & & & \frac{4EI}{L} \end{bmatrix}$$

where A is the member cross sectional area, E is the modulus of elasticity, L is the member length, and I is the moment of inertia of the cross section.

The geometric stiffness matrix is

$$[k_g] = \begin{bmatrix} \frac{P}{L} & 0 & 0 & -\frac{P}{L} & 0 & 0 \\ & \frac{6P}{5L} & \frac{P}{10} & 0 & \frac{-6P}{5L} & \frac{P}{10} \\ & & \frac{2PL}{15} & 0 & \frac{-P}{10} & \frac{-PL}{30} \\ & & & \frac{P}{L} & 0 & 0 \\ & \text{(symmetric)} & & & \frac{6P}{5L} & \frac{-P}{10} \\ & & & & & \frac{2PL}{15} \end{bmatrix}$$

where P is the axial force in the member with tension positive ($P = F_{x1}$).

APPENDIX B

Derivation of the Elasto-Plastic Material Stiffness Matrix

The following derivation follows closely the derivation for the tangent stiffness of an elasto-plastic beam-column member presented by Porter and Powell [33].

The element strain increments can be expressed as the sum of the elastic and plastic parts.

$$\{\Delta\varepsilon\} = \{\Delta\varepsilon_e\} + \{\Delta\varepsilon_p\}. \tag{B.1}$$

The stress increments are related to the strain increments by

$$\{\Delta\sigma\} = [E]\ \{\Delta\varepsilon_e\}\ . \tag{B.2}$$

The normality criterion states that the increment in element stresses is orthogonal to the increment in plastic strains

$$\{\Delta\varepsilon_p\}^T\ \{\Delta\sigma\} = 0\ . \tag{B.3}$$

If the yield criterion is given by a series of linear relations of the form

$$\phi_i(\sigma_1,\sigma_2) = 1.0 \tag{B.4}$$

then the plastic strain vector, in accordance with Equation (B.3) may be written as

$$\{\Delta\varepsilon_p\} = \{\phi_{i,\sigma}\}\,\lambda \tag{B.5}$$

in which $\{\phi_{i,\sigma}\}$ is a vector of partial derivatives of ϕ_i with respect to the principle stresses, and λ is the plastic strain magnitude. Since $\{\phi_{i,\sigma}\}$ defines the components of the outward normal to the linear yield criterion, λ must be positive is plastic strain is to occur.

When the stress point lies on more than one linear yield criterion, Equation (B.5) must hold for each. Hence, the total plastic deformation increment is the sum of the contributions from each criterion. In matrix form

$$\{\Delta\varepsilon_p\} = [\phi_{,\sigma}]\ \{\lambda\} \tag{B.6}$$

in which $[\phi_{,\sigma}]$ is a matrix having a column for each of the active yield criteria such that each column is $\{\phi_{i,}\sigma\}$, and $\{\lambda\}$ is a vector having a row for each of the active criteria.

Now, substituting Equation (B.6) into Equation (B.3), the following is obtained:

$$\{\lambda\}^T\ [\phi_{,\sigma}]^T\ \{\Delta\sigma\} = \{0\}. \tag{B.7}$$

Since Equation (B.7) holds regardless of the magnitude of the plastic deformations, it follows that $\{\lambda\}$ is arbitrary and may be eliminated, giving

$$[\phi_{,\sigma}]^T\ \{\Delta\sigma\} = \{0\}\ . \tag{B.8}$$

From Equations (B.1), (B.2), (B.6) and (B.8)

$$\{0\} = [\phi_{,\sigma}]^T [E] \{\Delta\varepsilon_e\} \tag{B.9}$$

$$= [\phi_{,\sigma}]^T [E] \{\{\Delta\varepsilon\} - \{\Delta\varepsilon_p\}\} \tag{B.10}$$

$$= [\phi_{,\sigma}]^T [E] \{\{\Delta\varepsilon\} - [\phi_{,\sigma}] \{\lambda\} \tag{B.11}$$

$$= [\phi_{,\sigma}]^T [E] \{\Delta\varepsilon\} - [\phi_{,\sigma}]^T [E] [\phi_{,\sigma}] \{\lambda\} \ . \tag{B.12}$$

Solving for the plastic strain magnitudes, $\{\lambda\}$

$$\{\lambda\} = \left[[\phi_{,\sigma}]^T [E] [\phi_{,\sigma}]\right]^{-1} [\phi_{,\sigma}]^T [E] \{\Delta\varepsilon\} \ . \tag{B.13}$$

The elasto-plastic material stiffness matrix may be obtained from Equations (B.1), (B.2), (B.6) and (B.13) as follows:

$$\{\Delta\sigma\} = [E] \{\Delta\varepsilon_e\} \tag{B.14}$$

$$= [E] \{\{\Delta\varepsilon\} - \{\Delta\varepsilon_p\}\} \tag{B.15}$$

$$= [E] \{\{\Delta\varepsilon\} - [\phi_{,\sigma}] \{\lambda\}\} \tag{B.16}$$

$$= [E] \{\{\Delta\varepsilon\} - [\phi_{,\sigma}] \left[[\phi_{,\sigma}]^T [E] [\phi_{,\sigma}]\right]^{-1} [\phi_{,\sigma}]^T [E] \{\Delta\varepsilon\}\} \tag{B.17}$$

$$= \left[[E] - [E] [\phi_{,\sigma}] \left[[\phi_{,\sigma}]^T [E] [\phi_{,\sigma}]\right]^{-1} [\phi_{,\sigma}]^T [E]\right] \{\Delta\varepsilon\} \tag{B.18}$$

$$= [E_{ep}] \{\Delta\varepsilon\} \ .$$

LIST OF REFERENCES

1. "The Structural Behavior of Ronan Point," Concrete, Vol. 2, No. 12, December, 1968.

2. Allen, D.E., and Schriever, W.R., "Progressive Collapse, Abnormal Loads, and Building Codes," Structural Failures: Modes, Causes, Responsibilities, ASCE, New York, 1973.

3. McGuire, W., and Leyendecker, E.V., "Analysis of Non-Reinforced Masonry Building Response to Abnormal Loading and Resistance to Progressive Collapse," Report No. NBSIR 74-526, National Bureau of Standards, Washington, D.C., 1974.

4. Clough, R.W., and Peterson, H., "Application of the Finite Element Method," The Mathematics of Finite Elements and Applications II, (J.R. Whiteman, editor), Academic Press, Inc., London, 1975.

5. Rodin, J., "Statistical Design Against Progressive Collapse," The Consulting Engineer, London, August, 1969.

6. Burnett, E.F.P., "The Avoidance of Progressive Collapse: Regulatory Approaches to the Problem," NBS-GCR 75-48, National Bureau of Standards, Washington, D.C., 1975.

7. Taylor, D.A., "Progressive Collapse," Canadian Journal of Civil Engineering, Vol. 2, No. 4, December, 1975.

8. Somes, N.F., "Abnormal Loading on Buildings and Progressive Collapse," Report No. NBSIR 73-221, National Bureau of Standards, Washington, D.C., May, 1973.

9. Leyendecker, E.V., and Ellingwood, B.R., "Design Methods for Reducing the Risk of Progressive Collapse in Buildings," NBS Building Science Series 98, National Bureau of Standards, Washington, D.C., 1977.

10. Leyendecker, E.V., and Burnett, E.F.P., "The Incidence of Abnormal Loading in Residential Buildings," NBS Building Science Series 89, National Bureau of Standards, Washington, D.C., 1976.

11. Ellingwood, B., and Leyendecker, E.V., "Approaches for Design Against Progressive Collapse," Journal of the Structural Division, ASCE, Vol. 104, No. ST3, March, 1978.

12. McGuire, W, "Prevention of Progressive Collapse," ASCE-IABSE Regional Conference on Tall Buildings, Bangkok, January, 1974.

13. "Building Code Requirements for Minimum Design Loads in Buildings and Other Structures," A58.1-1972, American National Standards Institute, Inc., New York, N.Y., 1972.

14. Breen, J. (editor), "Summary Report: Research Workshop on Progressive Collapse of Building Structures," The University of Texas at Austin, November, 1975.

15. Desai, C.S., and Abel, J.F., Introduction to the Finite Element Method, Van Nostrand Reinhold Company, New York, 1972.

16. Gallagher, R.H., Finite Element Analysis Fundamentals, Prentice-Hall, Englewood Cliffs, 1975.

17. McGuire, W., and Gallagher, R.H., Matrix Structural Analysis, John Wiley and Sons, Inc., New York, 1979.

18. Turner, M.J., Dill, E.H., Martin, H.C., and Melosh, R.J., "Large Deflections of Structures Subjected to External Loads," Journal of the Aerospace Sciences, Vol. 27, No. 2, February, 1960.

19. Martin, H.C., "Large Deflection and Stability Analysis by the Direct Stiffness Method," Report No. 32-931, Jet Propulsion Laboratory, California Institute of Technology, 1966.

20. Argyris, J.H., "Recent Advances in Matrix Methods of Structural Analysis," Progress in the Aeronautical Sciences, Vol. 4, (D. Kuchemann and L.H. G. Sterne, editors), Pergamon Press Limited, Oxford, 1964.

21. Felippa, C.A., "Refined Finite Element Analysis of Linear and Nonlinear Two-Dimensional Structures," Ph.D. Thesis, University of California, Berkeley, 1966.

22. Martin, H.C., "Finite Elements and the Analysis of Geometrically Nonlinear Problems," Paper presented at the Japan - U.S. Seminar on Matrix Methods of Structural Analysis and Design, Tokyo, 1969.

23. Oden, J.T., "Finite Element Applications in Nonlinear Structural Analysis," Proceedings of the Symposium on Applications of Finite Element Methods in Civil Engineering, ASCE, 1969.

24. Haisler, W.E., Stricklin, J.A., and Stebbins, F.J., "Development and Evaluation of Solution Procedures for Geometrically Nonlinear Structural Analysis," AIAA Journal, Vol. 10, No. 3, March, 1972.

25. Stricklin, J.A., Von Riesmann, W.A., Tillerson, J.R., and Haisler, W.E., "Static Geometric and Material Nonlinear Analysis," Advances in Computational Methods in Structural Mechanics and Design, UAH Press, Huntsville, 1972.

26. Gallagher, R.H., "Finite Element Analysis of Geometrically Nonlinear Problems," Proceedings of the 1973 Tokyo Seminar on Finite Element Analysis, University of Tokyo Press, Tokyo, 1973.

27. Bathe, K.-J., Ramm, E., and Wilson, E.L., "Finite Element Formulations for Large Deformation Dynamic Analysis," International Journal for Numerical Methods in Engineering, Vol. 9, No. 2, 1975.

28. Tillerson, J.R., Stricklin, J.A., and Haisler, W.E., "Numerical Methods for the Solution of Nonlinear Problems in Structural Analysis," Numerical Solution of Nonlinear Structural Problems, ASME, New York, 1973.

29. Yamada, Y., "Incremental Formulation for Problems with Geometric and Material Nonlinearities," Advances in Computational Methods in Structural Mechanics and Design, UAH Press, Huntsville, 1972.

30. Bathe, K.-J., and Bolourchi, S., "Large Displacement Analysis of Three-Dimensional Beam Structures," International Journal for Numerical Methods in Engineering, Vol. 14, 1979.

31. Novozhilov, V.V., Foundations of the Nonlinear Theory of Elasticity, Graylock Press, Rochester, 1953.

32. Timoshenko, S., Strength of Materials, Part I: Elementary Theory and Problems, D.Van Nostrand Company, New York, 1958.

33. Porter, F.L., and Powell, G.H., "Static and Dynamic Analysis of Inelastic Frame Structures," Report No. EERC 71-3, Earthquake Engineering Research Center, University of California, Berkeley, California, 1971.

34. Sharifi, P., and Popov, E.P., "Nonlinear Buckling Analysis of Sandwich Arches," Journal of the Engineering Mechanics Division, ASCE, Vol. 97, No. EM5, October, 1971.

35. Wright, E.W., and Gaylord, E.H., "Analysis of Unbraced Multistory Steel Rigid Frames," Journal of the Structural Division, ASCE, Vol. 94, No. ST5, May, 1968.

36. Martin, H.C., "On the Derivation of Stiffness Matrices for the Analysis of Large Deflection and Stability Problems," Proceedings of the Conference on Matrix Methods in Structural Mechanics (AFFDL-TR-66-80), Wright-Patterson Air Force Base, Dayton, Ohio, 1965.

37. Connor, J.J., Logcher, R.D., and Chan, S.-C., "Nonlinear Analysis of Elastic Framed Structures," Journal of the Structural Division, ASCE, Vol. 94, No. ST6, June, 1968.

38. Jennings, A., "Frame Analysis Including Change of Geometry," Journal of the Structural Division, ASCE, Vol. 94, No. ST3, March, 1968.

39. Tezcan, S.S., and Mahapatra, B.C., "Tangent Stiffness Matrix for Space Frame Members," Journal of the Structural Division, ASCE, Vol. 95, No. ST6, June, 1969.

40. Tebedge, N., and Tall, L., "Linear Stability Analysis of Beam-Columns," Journal of the Structural Division, ASCE, Vol. 99, No. ST12, December, 1973.

41. Wang, C.-K., "General Computer Program for Limit Analysis," Journal of the Structural Division,, ASCE, Vol. 89, No. ST6, December, 1963.

42. Jennings, A., and Majid, K., "An Elastic-Plastic Analysis by Computer for Framed Structures Loaded up to Collapse," The Structural Engineer, Vol. 43, No. 12, December, 1965.

43. Clough, R.W., Benuska, K.L., and Wilson, E.L., "Inelastic Earthquake Response of Tall Buildings," Proceedings of the Third World Conference on Earthquake Engineering, New Zealand, Vol. II, Session II, 1965.

44. Davies, J.M., "The Response of Plane Frameworks to Static and Variable Repeated Loading in the Elastic-Plastic Range," The Structural Engineer, Vol. 44, No. 8, August, 1966.

45. Korn, A., and Galambos, T.V., "Behavior of Elastic-Plastic Frames," Journal of the Structural Division, ASCE, Vol. 94, ST5, May, 1968.

46. Vijakkhana, C., Nishino, F., and Lee, S.-L., "Inelastic Stability of Unbraced Building Frames," Journal of the Structural Division, ASCE, Vol. 100, No. ST3, March, 1974.

47. Hodge, P.G., Plastic Analysis of Structures, McGraw-Hill Book Company, Inc., New York, N.Y., 1959.

48. Morris, G.A., and Fenves, S.J., "Elastic-Plastic Analysis of Frameworks," Journal of the Structural Division, ASCE, Vol. 96, No. ST5, May, 1970.

49. Nigam, N., "Yielding in Framed Structures Under Dynamic Loads," Journal of the Engineering Mechanics Division, Vol. 96, No. EM5, October, 1970.

50. Wen, R.K., and Farhoomand, F., "Dynamic Analysis of Inelastic Space Frames," Journal of the Engineering Mechanics Division, ASCE, Vol. 96, No. EM5, October, 1970.

51. Gupta, S.D., and Hollmeier, R.J., "Elasto-Plastic Analysis of Space Frames," ASME Paper No. 74-PVP-49, Pressure Vessels and Piping Conference, Miami Beach, Florida, 1974.

52. Gupta, S.D., "Plastic Analysis of Three-Dimensional Frames Considering Finite Length of Yielded Regions," ASME Paper No. 75-PVP-65, Second National Congress on Pressure Vessels and Piping, San Francisco, California, 1975.

53. Morris, G.A., and Fenves, S.J., "Approximate Yield Surface Equations," Journal of the Engineering Mechanics Division, ASCE, Vol. 95, No. EM4, August, 1969.

54. Drucker, D.C., "A More Fundamental Approach to Plastic Stress-Strain Relations," Proceedings of the First U.S. National Congress of Applied Mechanics, Chicago, Illinois, 1951.

55. Manual of Steel Construction, 7th ed., American Institute of Steel Construction, New York, 1970.

56. Anderson, J.C., and Bertero, V.V., "Seismic Behavior of Multistory Frames Designed by Different Philosophies," Report No. EERC 69-11, Earthquake Engineering Research Center, Berkeley, California, 1969.

57. El-Hafez, M.B., and Powell, G.H., "Computer Aided Ultimate Load Design of Unbraced Multistory Steel Frames," EERC Report No. 73-3, Earthquake Engineering Research Center, Berkeley, California, 1973.

58. Mahin, S.A., and Bertero, V.V., "Prediction of Nonlinear Seismic Building Behavior," Journal of the Technical Councils, ASCE, Vol. 104, No. TC1, November, 1978.

59. Harung, H.S., and Millar, M.A., "General Failure Analysis of Skeletal Plane Frames," Journal of the Structural Division, ASCE, Vol. 99, No. ST6, June, 1973.

60. Mytryn, T.A., "Nonlinear, Inelastic Building Connections," M.S. Thesis, Cornell University, Ithaca, New York, 1979.

61. Buyukozturk, O., "Nonlinear Analysis of Reinforced Concrete Structures," Computers and Structures, Vol. 7, Pergamon Press, 1977.

62. Cervenka, V., "Inelastic Finite Element Analysis of Reinforced Concrete Panels Under In-plane Loads," Ph.D. Thesis, University of Colorado, Boulder, Colorado, 1970.

63. Franklin, H.A., "Nonlinear Analysis of Reinforced Concrete Frames and Panels," Report No. SESM-60-5, University of California, Berkeley, California, 1970.

64. Kanaan, A.E., and Powell, G.H., "Drain-2D: A General Purpose Computer Program for Dynamic Analysis of Inelastic Plane Structures," Report Nos. EERC 73-6 and EERC 73-22, Earthquake Engineering Research Center, University of California, Berkeley, California, 1973.

65. Krishnamoorthy, C., and Panneerselvam, A., "A Finite Element Model for Nonlinear Analysis of Reinforced Concrete Framed Structures," The Structural Engineer, Vol. 55, No. 8, August, 1977.

66. McLeod, J.A., "New Rectangular Finite Element for Shear Wall Analysis," Journal of the Structural Division, ASCE, Vol. 95, No. ST3, March, 1969.

67. Moss, P.J., and Carr, A.J., "Aspects of the Analysis of Frame-Panel Interaction," The Bulletin of the New Zealand Society for Earthquake Engineering, Vol. 4, No. 1, March, 1971.

68. Ngo, D., and Scordelis, A.C., "Finite Element Analysis of Reinforced Concrete Beams," American Concrete Institute Journal, Vol. 64, No. 3, March, 1967.

69. Nilson, A.H., "Nonlinear Analysis of Reinforced Concrete by the Finite Element Method," American Concrete Institute Journal, Vol. 66, No. 8, August, 1969.

70. Schnorbrich, W.C., "Behavior of Reinforced Concrete Structures Predicted by the Finite Element Method," Computers and Structures, Vol. 7, 1977.

71. Suidan, M., and Schnobrich, W.C., "Finite Element Analysis of Reinforced Concrete," Journal of the Structural Division, ASCE, Vol. 99, No. ST10, October, 1973.

72. Liu, T.C.Y., Nilson, A.H., and Slate, F.O., "Biaxial Stress-Strain Relations for Concrete," Journal of the Structural Division, ASCE, Vol. 98, No. ST5, May, 1972.

73. Kupfer, H.B., Hilsdorf, H.K., and Rusch, H., "Behavior of Concrete Under Biaxial Stresses," American Concrete Institute Journal, Vol. 66, No. 8, August, 1969.

74. McGuire, W., Steel Structures, Prentice Hall, Englewood Cliffs, N.J., 1968.

75. Popov, E.P., and Pinkney, R.B., "Cyclic Yield Reversal in Steel Building Connections," Journal of the Structural Division, ASCE, Vol. 95, No. ST3, March, 1969.

76. Ramberg, W., and Osgood, W., "Description of Stress-Strain Curves by Three Parameters," NACA Technical Note No. 902. July, 1943.

77. Krishnamurthy, N., Huang, H.-T., and Jeffrey, P.K., "Analytical M-θ Curves for End-Plate Connections," Journal of the Structural Division, ASCE, Vol. 105, No. ST1, January, 1979.

78. Romstad, K.M., and Subramanian, C.V., "Analysis of Frames with Partial Connection Rigidity," Journal of the Structural Division, ASCE, Vol. 96, No. ST11, November, 1970.

79. Gallagher, R.H., "Computerized Structural Analysis and Design - the Next Twenty Years," Computers and Structures, Vol. 7, No. 4, August, 1977.

80. Gallagher, R.H., and Greenberg, D.P., "Computer Graphics in Structural Engineering Research," Interactive Computer Graphics in Engineering, (L.E. Hulbert, editor), ASME, New York, 1977.

81. Gross, J.L., Mutryn, T.A., and McGuire, W., "Computer Graphics in Nonlinear Design Problems," Proceedings of the Conference on Computers in Structural Engineering Practice, McGill University, Montreal, October, 1977.

82. Gross, J.L., Mutryn, T.A., and McGuire, W., "Computer Graphics and Nonlinear Frame Analysis," Proceedings of the ASCE Conference on Electronic Computation, St. Louis, 1979.

83. McGuire, W., "Interactive Computer Graphics and the Design of Steel Frames," paper presented at First Symposium on Metal Structures, Queretaro, Mexico, 1978.

84. Greenberg, D.P., "An Interdisciplinary Laboratory for Graphics Research and Applications," Proceedings of the Fourth Annual Conference on Computer Graphics, Interactive Techniques, and Image Processing, July, 1977.

85. Horne, M.R., and Merchant, W., The Stability of Frames, Pergamon Press, London, 1965.

86. Yarimci, E., "Incremental Inelastic Analysis of Framed Structures and Some Experimental Verifications," Fritz Engineering Laboratory Report No. 273.45, Lehigh University, Bethlehem, Pennsylvania, 1966.

87. Williams, F.W., "An Approach to the Nonlinear Behavior of the Members of a Rigid Jointed Plane Framework with Finite Deflections," Quarterly Journal of Mechanics and Applied Mathematics, Vol. 17, 1964.

88. Ebner, A.M., and Ucciferro, J.J., "A Theoretical and Numerical Comparison of Elastic Nonlinear Finite Element Methods," Computers and Structures, Vol. 2, Nos. 5 and 6, December, 1972.

89. Powell, G.H., "Theory of Nonlinear Elastic Structures," Journal of the Structural Division, ASCE, Vol. 95, No. ST12, December, 1969.

90. Plastic Design of Multi-Story Frames, Lecture Notes, Lehigh University, 1965.